UNIVERSIDADE ESTADUAL DE PONTA GROSSA
PRÓ-REITORIA DE PESQUISA E PÓS-GRADUAÇÃO
PROGRAMA DE PÓS-GRADUAÇÃO EM ODONTOLOGIA – DOUTORADO
ÁREA DE CONCENTRAÇÃO: CLÍNICA INTEGRADA

CRISTIANE MAUCOSKI

ANÁLISE *IN VITRO* DO AUMENTO DE TEMPERATURA PULPAR E EM RESINAS COMPOSTAS BULKFILL DURANTE A UTILIZAÇÃO DE FOTOPOLIMERIZADORES LED CONTEMPORÂNEOS E LASER

PONTA GROSSA
2023

CRISTIANE MAUCOSKI

ANÁLISE *IN VITRO* DO AUMENTO DE TEMPERATURA PULPAR E EM RESINAS COMPOSTAS BULKFILL DURANTE A UTILIZAÇÃO DE FOTOPOLIMERIZADORES LED CONTEMPORÂNEOS E LASER

Tese apresentada para obtenção do título de Doutora em Odontologia na Universidade Estadual de Ponta Grossa, Área de Clínica Integrada.

Orientador: Prof. Dr. Cesar Augusto Galvão Arrais.

PONTA GROSSA
2023

Maucoski, Cristiane

M447 Análise *in vitro* do aumento de temperatura pulpar e em resinas compostas *bulk-fill* durante a utilização de fotopolimerizadores LED contemporâneos e laser / Cristiane Maucoski. Ponta Grossa, 2023.

114 f.

Tese (Doutorado em Odontologia - Área de Concentração: Clínica Integrada), Universidade Estadual de Ponta Grossa.

Orientador: Prof. Dr. César Augusto Galvão Arrais.

1. Temperatura. 2. Polpa dentária. 3. Lasers. 4. Resina composta. I. Arrais, César Augusto Galvão. II. Universidade Estadual de Ponta Grossa. Clínica Integrada. III.T.

CDD: 617.6

Ficha catalográfica elaborada por Maria Luzia Fernandes Bertholino dos Santos- CRB9/986

CRISTIANE MAUCOSKI

Análise in vitro do aumento de temperatura pulpar e em resinas compostas bulk-fill durante a utilização de fotopolimerizadores LED contemporâneos e laser

Tese apresentada ao Programa de Pós-graduação Stricto sensu em Odontologia da Universidade Estadual de Ponta Grossa, como requisito parcial à obtenção do título de Doutor em Odontologia, área de concentração em Clínica Integrada, linha de pesquisa de Propriedades Físico-Químicas e Biológicas de Materiais.

Ponta Grossa, 04 de agosto de 2023.

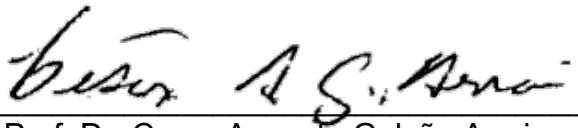

Prof. Dr. Cesar Augusto Galvão Arrais
Universidade Estadual de Ponta Grossa

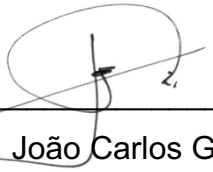

Prof. Dr. João Carlos Gomes
Universidade Estadual de Ponta Grossa

Profª. Drª. Alessandra Reis Silva Loguercio
Universidade Estadual de Ponta Grossa

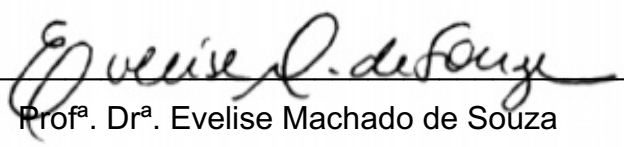

Profª. Drª. Evelise Machado de Souza
Pontifícia Universidade Católica do Paraná

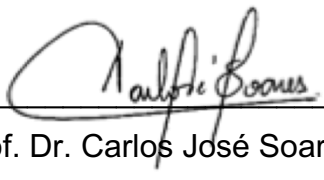

Prof. Dr. Carlos José Soares
Universidade Federal de Uberlândia

AGRADECIMENTOS

Agradeço, primeiramente, a Deus, por me presentear com a vida.

Aos meus pais, Juracir Maucoski e Adriane Stremel Maucoski, e ao meu irmão, Eduardo Henrique Maucoski, pelo incentivo, paciência, apoio e amor incondicional.

À Universidade Estadual de Ponta Grossa pela oportunidade de realização do meu curso de Doutorado em Odontologia.

Ao Programa de Pós-graduação em Odontologia da Universidade Estadual de Ponta Grossa, na pessoa de sua coordenadora Profª Drª Nara Hellen Bombarda.

À Coordenação de Aperfeiçoamento de Pessoal de Nível Superior - CAPES, pela bolsa de estudos concedida no decorrer do curso e pela oportunidade de realização de meu Doutorado Sanduíche (O presente trabalho foi realizado com apoio da Coordenação de Aperfeiçoamento de Pessoal de Nível Superior - Brasil (CAPES) - Código de Financiamento 001).

Ao meu orientador Prof. Dr. Cesar Augusto Galvão Arrais pela contribuição de seus conhecimentos, amizade, orientação, correções e dedicação. Agradeço a orientação ao longo dos anos e por me dar toda a ajuda, mesmo a distância.

A Dalhousie University pela oportunidade de realização de parte do meu Doutorado na cidade de Halifax, Nova Scotia, Canadá.

A Faculdade de Odontologia, da Dalhousie University, na pessoa de seu reitor Prof. Dr. Ben Davis.

Ao meu orientador no exterior Prof. Dr. Richard Bengt Price por me receber em Halifax e por me dar a oportunidade de fazer parte do meu Doutorado. Agradeço por todo o aprendizado, amizade, correções e orientação.

Ao MITACS pelo estágio que realizei durante meu período em Halifax e por dar a oportunidade de aprender mais com pesquisa.

A Ultradent Products Inc., na pessoa do Vice-Presidente de Pesquisa e Desenvolvimento Neil Jessoup pelo estágio.

Aos meus amigos, pela amizade e apoio em todos os momentos.

Aos professores, funcionários e colegas de pesquisa pela convivência, conhecimento e amizade.

A todos que direta ou indiretamente contribuíram para a conclusão de mais uma etapa em minha vida.

RESUMO

MAUCOSKI C. **Análise in vitro do aumento de temperatura pulpar e em resinas compostas *bulk-fill* durante a utilização de fotopolimerizadores LED contemporâneos e laser.** [Tese] Doutorado em Clínica Integrada. Ponta Grossa: Universidade Estadual de Ponta Grossa; 2023.

Objetivo: Avaliar in vitro os efeitos de fotopolimerizador laser e de novos fotopolimerizadores LED na alteração da temperatura pulpar (TP) e de resinas compostas (RC) em tempo real e em condições intraorais simuladas. **Materiais e Métodos:** O estudo foi dividido em três experimentos. Experimento 01: A temperatura produzida pelos fotopolimerizadores Monet (1 e 3s, AMD Lasers), Valo Grand (3 e 10s, Ultradent), DeepCure (10s, 3M), PowerCure, (3 e 10s, Ivoclar) e PinkWave (10s, Vista Dental Products) foram medidas na base de amostras cilíndricas de 2 mm de profundidade × 6 mm largura feitas com Filtek Universal (3M), Tetric Evoceram (Ivoclar) e Transcend (Ultradent). Os valores de ΔT foram submetidos à ANOVA dois fatores e os valores de dureza (VH) foram avaliados no topo e base usando ANOVA e teste post hoc de Scheffe ($p < 0.05$). Experimento 02: Após aprovação do Comitê de Ética (#2021-5703), o aumento de TP em preparos Classe I e V não retentivos vazios em molar superior foi avaliado quando os preparos foram expostos ao laser emitido pelo Monet (1 e 3s, AMD Lasers), ou à luz emitida pelos fotopolimerizadores PinkWave (3 e 10s, Vista Dental Products), Valo Grand (3 e 10s, Ultradent), PowerCure (3 e 10s, Ivoclar) e SmartLite Pro (10s, Dentsply Sirona). A temperatura basal foi mantida a 32°C. Dois termopares (tipo T) foram inseridos no interior da câmara pulpar através das raízes, sendo posicionados próximos ao corno pulpar e na parede vestibular próximo ao preparo Classe V. O fluxo de água foi ajustado para 0,026 mL/min e os dados de temperatura em tempo real foram coletados (cada 0,5s). As medições de TP foram feitas com a ponteira do LCU a 0 e 6 mm de distância da superfície do dente. O efeito do fluxo pulpar foi comparado usando ANOVA um fator seguido pelo teste post hoc de Scheffe. Os valores de ΔT foram submetidos a ANOVA dois fatores. Experimento 03: Os mesmos preparos do experimento 02 foram restaurados com Filtek One Bulk Fill (3M), Filtek Bulk Fill Flow (3M), Tetric PowerFill (Ivoclar) ou Tetric Power Flow (Ivoclar). As RCs foram expostas à luz emitida pelos fotopolimerizadores Monet (1 e 3s, AMD Lasers), PowerCure (3 e 20s, Ivoclar), PinkWave (3 e 20s, Vista Dental Products), Valo X (5 e 20s, Ultradent) e SmartLite Pro (20 s, Dentsply Sirona). Os dados de ΔT foram submetidos a ANOVA um fator seguido por teste post hoc de Scheffe. **Resultados**: Experimento 01: Os maiores aumentos de temperatura ocorreram para Transcend sem diferenças significativas entre os valores observados na Filtek Universal e Tetric Evoceram ($p = 0,9756$). A Transcend alcançou os maiores valores de VH. O PinkWave 10s produziu o maior aumento de temperatura e Monet 1s produziu o menor aumento e a menor relação base:topo VH. Experimento 02: Monet 3s e PinkWave 10s produziram o maior aumento na TP no preparo Classe I. O fluxo pulpar simulado não influenciou a elevação de TP. No geral, as cavidades expostas na distância de 0 mm tiveram valores de ΔT mais altos do que na distância de 6 mm. Experimento 03: Monet 1s e PinkWave 20s forneceram a menor e a maior quantidade de energia, respectivamente. Valo X e PinkWave usados por 20s produziram os maiores valores de ΔT. Monet 1s, PinkWave 3s, PowerCure 3s e Monet 3 s produziram os valores de ΔT mais baixos. Não foram encontradas diferenças significativas entre as RCs. **Conclusão**: o aumento da temperatura é relacionado à

quantidade de energia entregue ao dente e à habilidade do fotopolimerizador de ser posicionado diretamente sobre a restauração; a translucidez das RCs afeta o aumento de temperatura e dureza (VH); o fluxo pulpar simulado de 0.026 mL/min não tem efeito significante no aumento de PT; o aumento da distância entre ponta de fotopolimerizador e superfície do dente reduziu o aumento de temperatura para a maioria dos fotopolimerizadores; e a fotopolimerização com modos de exposição curtos e alta irradiância não produzem aumentos de TP devido à menor quantidade de energia liberada.

Palavras-chave: Temperatura, Polpa Dentária, Lasers, Resinas Compostas

ABSTRACT

MAUCOSKI C. **In vitro analysis of the increase in pulp temperature and in bulk-fill composite resins during the use of contemporary LED light curing units and laser.** [Thesis] Doctorate in Integrated Clinic. Ponta Grossa: State University of Ponta Grossa; 2023.

Objective: To evaluate in vitro the effects of laser and contemporary LED light curing units on real-time pulp temperature (PT) change under simulated intraoral conditions. **Materials and Methods:** The study was divided into three experiments. Experiment 01: The temperature produced by Monet laser (1 and 3s, AMD Lasers), Valo Grand (3 and 10s, Ultradent), DeepCure (10s, 3M), PowerCure, (3 and 10s, Ivoclar) and PinkWave (10s, Vista Dental Products) were measured at the bottom of 2 mm deep × 6 mm wide cylindrical specimens made with Filtek Universal (3M), Tetric Evoceram (Ivoclar) and Transcend (Ultradent). ΔT values were subjected to two-way ANOVA and hardness values (VH) were evaluated at the top and bottom using ANOVA and Scheffe's post hoc test ($p < 0.05$). Experiment 02: After the Ethics Committee approval (#2021-5703), the PT increase in non-retentive Class I and V preparations in maxillary molars was evaluated when the preparations were exposed to the laser emitted by the Monet (1 and 3s, AMD Lasers), or to light emitted by PinkWave (3 and 10s, Vista Dental Products), Valo Grand (3 and 10s, Ultradent), PowerCure (3 and 10s, Ivoclar) and SmartLite Pro (10s, Dentsply Sirona). The baseline was kept at 32°C. Two thermocouples (type T) were inserted inside the pulp chamber through the roots, being positioned close to the pulp horn and on the buccal wall near the Class V cavity. The water flow was adjusted to 0.026 mL/min and real-time temperature data was collected (every 0.5s). PT measurements were obtained with the LCU tip 0 and 6 mm away from the tooth surface. The effect of pulp flow was compared using one-way ANOVA followed by Scheffe's post hoc test and ΔT values were submitted to two-way ANOVA. Experiment 03: The cavities were filled with Filtek One Bulk Fill (3M), Filtek Bulk Fill Flow (3M), Tetric PowerFill (Ivoclar) or Tetric Power Flow (Ivoclar). The tooth was exposed to Monet (1 and 3s, AMD Lasers), PowerCure (3 and 20s, Ivoclar), PinkWave (3 and 20s, Vista Dental Products), Valo X (5 and 20s, Ultradent) and SmartLite Pro (20s, Dentsply Sirona). ΔT data was subjected to one-way ANOVA followed by Scheffe's post hoc test. **Results:** Experiment 01: The greatest temperature increases occurred for Transcend without significant differences between Filtek Universal and Tetric Evoceram ($p = 0.9756$). Transcend achieved the highest VH values. PinkWave 10s produced the highest temperature rise and Monet 1s produced the lowest rise and lowest VH bottom:top ratio. Experiment 02: Monet 3s and PinkWave 10s produced the highest PT rise in the Class I cavity. Simulated pulp flow did not influence the PT rise. Overall, cavities exposed at the 0 mm distance had higher ΔT values than at the 6 mm distance. Experiment 03: Monet 1s and PinkWave 20s provided the lowest and highest amount of energy, respectively. Valo X and PinkWave used for 20s produced the highest ΔT values. Monet 1s, PinkWave 3s, PowerCure 3s and Monet 3s produced the lowest ΔT values. No significant differences were found between the RBCs. **Conclusion:** the temperature increase is related to the amount of energy delivered to the tooth and the curing light's ability to be positioned directly over the restoration; the translucency of RBCs affects the increase in temperature and hardness (VH); simulated pulpal flow of 0.026 mL/min has no significant effect on PT changes; increasing the distance between curing light tip and tooth surface reduced the

temperature rise for most curing lights; and short exposure modes do not produce increases in PT due to the lower amount of energy released.

Keywords: Temperature, Dental Pulp, Lasers, Composite Resins

LISTA DE FIGURAS

LISTA DE TABELAS

SUMÁRIO

1 INTRODUÇÃO

A resina composta (RC) utilizada nas restaurações deve ser fotopolimerizada adequadamente a fim de se obter uma restauração com maior longevidade e com adequadas propriedades mecânicas (RUEGGEBERG, F. A., 2011; PRICE; FERRACANE; SHORTALL, 2015). Portanto, bons fotopolimerizadores se tornaram indispensáveis no dia a dia do consultório. O fotopolimerizador a base de diodos emissores de luz (LED) é considerado a fonte de luz mais popular para fotopolimerização de RCs (JANDT; MILLS, 2013; ERNST et al., 2018). Quando comparado aos fotopolimerizadores de luz halógena (QTH – quartzo-tungstênio-halogênio), possui vantagens como maior vida útil do aparelho, não necessidade de filtros, são energeticamente eficientes, podem ser utilizados com baterias, emitem uma estreita faixa de comprimentos de onda e podem emitir uma alta irradiância na ponta do aparelho (JANDT; MILLS, 2013; MILLY; BANERJEE, 2018). Estão disponíveis para a aquisição pelo clínico fotopolimerizadores LED capazes de emitir uma banda de comprimentos de onda (*single-peak)* e aparelhos capazes de emitir várias bandas de comprimentos de onda (*multi-peak*). Os fotopolimerizadores LED *monowave* foram designados para ativar o fotoiniciador mais comumente utilizado nas RCs: a canforoquinona (RUEGGEBERG, F. A. et al., 2017). Para ativar uma gama mais ampla de fotoiniciadores, alguns fotopolimerizadores LED emitem bandas de comprimento de onda na faixa violeta e azul (RUEGGEBERG, F. A. et al., 2017). Outra recente tecnologia de fotopolimerizadores LED é um novo aparelho com tecnologia que o fabricante afirma ser *Quadwave*, capaz de emitir quatro bandas distintas de comprimentos de onda: violeta, azul, vermelho e infravermelho (MAUCOSKI et al., 2022b).

Os primeiros fotopolimerizadores LED eram considerados aparelhos que geravam menos calor, visto que emitiam uma menor irradiância (aproximadamente 240 mW/cm^2) do que fotopolimerizadores QTH (aproximadamente 450 a 1.200 mW/cm^2) (RUEGGEBERG, F. A. et al., 2017). Entretanto, com objetivo de reduzir o tempo gasto dentro do consultório e aumentar as propriedades mecânicas das RCs, fotopolimerizadores que emitem irradiâncias maiores que 2.000 mW/cm^2 e com tempo de exposição menores que 5 s estão disponíveis no mercado odontológico (ALMEIDA et al., 2021). Tamanha irradiância se tornou uma preocupação durante procedimentos restauradores (WAHBI et al., 2012; MOUHAT et al., 2017; OLIVEIRA; ROCHA, 2022)

devido ao risco potencial de danos ao tecido gengival (SPRANLEY et al., 2012; MAUCOSKI et al., 2017) e aos tecidos pulpares (ZACH; COHEN, 1965; RUNNACLES et al., 2015; ZARPELLON et al., 2018; ZARPELLON et al., 2019; GROSS et al., 2020; NILSEN et al., 2020; ZARPELLON et al., 2021). O aumento de temperatura dentro da câmara pulpar está relacionado à quantidade de energia (Joules) depositada durante a fotoativação da resina e à liberação de calor da RC enquanto polimeriza, pela natureza exotérmica da reação de polimerização (ARMELLIN et al., 2016; ZARPELLON et al., 2018; MOUHAT et al., 2021). Deste modo, o aumento de temperatura dependerá do tipo de RC, da taxa de polimerização, da potência, da irradiância recebida (mW/cm^2), dos comprimentos de onda emitidos, do tempo de exposição e da quantidade de energia emitida (PRICE; FERRACANE; SHORTALL, 2015; BALESTRINO et al., 2016; MOUHAT et al., 2017; RUEGGEBERG, F. A. et al., 2017; AKARSU; AKTUG KARADEMIR, 2019; PAR et al., 2019; MOUHAT et al., 2021; WANG et al., 2021). Além disso, outros fatores podem influenciar o aumento de temperatura pulpar (TP), como a espessura de dentina remanescente e o fluxo pulpar (SAVAS et al., 2014; AKARSU; AKTUG KARADEMIR, 2019; BRAGA et al., 2019; PRICE et al., 2020).

Novos fotopolimerizadores com potência e diferentes espectros estão disponíveis comercialmente. Recentemente, lasers de diodo azul com emissão de luz com comprimento de onda entre 445-455 nm têm sido sugeridos como uma fonte de luz alternativa (DROST et al., 2019; KOUROS et al., 2020). Um fotopolimerizador laser compacto, portátil e sem fio que emite uma alta potência e irradiância (ROCHA et al., 2022) sobre uma faixa muito estreita de comprimentos de onda foi introduzida no mercado (Monet Laser, AMD Lasers, West Jordan, UT, EUA). O fabricante afirma que este novo fotopolimerizador laser emite uma irradiância de 2.000 a 2.400 mW/cm^2 e possui um feixe colimado que permite a luz penetrar profundamente na RBC e polimerizá-la a uma espessura de 2 mm em 1 s de exposição (AMD, 2021). Por ser um laser, este tem a capacidade de emitir uma faixa estreita de comprimento de onda com uma alta densidade de fótons (DROST et al., 2019). Além disso, ele pode emitir uma alta irradiância mesmo com o aumento da distância da ponta do fotopolimerizador em relação ao substrato (DROST et al., 2019). Mesmo com a alta potência e irradiância, um estudo recente mostrou que utilizando este fotopolimerizador por 1 s, menor profundidade de polimerização foi observada nas dez RCs testadas. Isso foi

atribuído a baixa exposição radiante (J/cm^2) entregue por esse fotopolimerizador em 1 s (ROCHA et al., 2022).

Outros dois novos fotopolimerizadores LED estão disponíveis no mercado. Um possui uma tecnologia que o fabricante afirma ser *Quadwave* (*PinkWave*, Vista Dental Products, Racine, WI, EUA), por ser capaz de emitir quatro bandas diferentes de comprimento de onda (VISTA APEX, 2022): luz azul, violeta, vermelha e infravermelha (MAUCOSKI et al., 2022b). O fabricante também afirma que este fotopolimerizador produz uma irradiância de 1.720 mW/cm^2 em 3 s de exposição (VISTA APEX, 2022). O outro consiste na terceira geração de um fotopolimerizador da linha Valo (Valo X, Ultradent Products, South Jordan, UT, EUA). Este fotopolimerizador LED *multi-peak* possui um maior diâmetro de ponta que as suas gerações anteriores (12,5 mm), com capacidade de emitir três bandas de comprimentos de onda, entre 380 nm e 515 nm, e o fabricante afirma que emite uma irradiância de 1.100 mW/cm^2 no modo de exposição *Standard* e 2.200 mW/cm^2 no modo *Xtra* (ULTRADENT, 2022). Levando em conta que uma saída de alta irradiância e fotopolimerizadores com amplo espectro de emissão pode influenciar o aumento de TP (MOUHAT et al., 2017; MOUHAT et al., 2021), algumas preocupações tem sido levantadas em relação ao aumento de temperatura dentro da câmara pulpar quando os dentes são expostos à luz destes fotopolimerizadores de alta potência (MOUHAT et al., 2017). As características dos fotopolimerizadores desempenham um papel importante no aumento da TP (OBERHOLZER et al., 2012) e tem sido sugerido que um aumento da TP maior que 5,5 °C pode ser prejudicial e levar à um dano irreversível do tecido pulpar (ZACH; COHEN, 1965). Alguns estudos avaliaram o aumento de temperatura nos tecidos ao redor do dente (SPRANLEY et al., 2012; MAUCOSKI et al., 2017), *in vitro* (OBERHOLZER et al., 2012; VINALL et al., 2017; AKARSU; AKTUG KARADEMIR, 2019; BRAGA et al., 2019; LEE; LEE, 2021; LEMPEL et al., 2021) e *in vivo (RUNNACLES et al., 2019; ZARPELLON et al., 2019; GROSS et al., 2020; ZARPELLON et al., 2021)* no interior do dente.

Alguns estudos *in vitro* simularam o fluxo pulpar para melhor representar um ambiente *in vivo* (AKARSU; AKTUG KARADEMIR, 2019; BRAGA et al., 2019; RUNNACLES et al., 2019). Porém o fluxo pulpar pode ser afetado pelo preparo cavitário (SUKAPATTEE et al., 2016) e uso de anestesia local (ODOR; PITT FORD; MCDONALD, 1994; VONGSAVAN et al., 2019). Portanto, o fluxo pulpar é altamente variável. Alguns estudos *in vitro* também avaliaram o calor gerado em amostras

cilíndricas à temperatura ambiente usando sondas termopares do tipo T e K (SPANOVIC et al., 2018; PAR et al., 2019; KOUROS et al., 2020; WANG et al., 2021). Porém, nestes estudos, o volume de RC usado não foi bem definido, os comprimentos de onda emitidos pelos fotopolimerizadores não foram relatados, a energia emitida não foi relatada, nem uma temperatura basal similar com a temperatura intrapulpar observada em estudos prévios *in vivo* (ZARPELLON et al., 2021) foi utilizada.

O aumento da TP é também influenciado pela reação exotérmica (BALESTRINO et al., 2016) e pelo volume de RC (LEMPEL et al., 2021). A exotermia pode gerar preocupação quando utilizadas resinas do tipo *bulk-fill,* visto que um maior volume de resina é fotopolimerizado (LEMPEL et al., 2021). Uma nova abordagem que combina fotopolimerização com alta irradiância com modificação do mecanismo de polimerização da RC tem sido proposta (ILIE; WATTS, 2020). Esta nova geração de RCs *bulk-fill* utiliza um mecanismo reversível de polimerização de transferência de cadeia de fragmentação (RAFT), e alguns fabricantes afirmam que essas RCs podem ser adequadamente fotopolimerizadas em apenas 3s. Embora tempos de exposição tão curtos tenham produzido comportamento viscoelástico e propriedades mecânicas semelhantes aos obtidos quando tempos de exposição mais longos foram usados (ILIE; WATTS, 2020; ILIE; DIEGELMANN, 2021), não há informações até o momento sobre o efeito da utilização de RCs RAFT do tipo *bulk-fill* são fotopolimerizadas. Além disso, mesmo com informação presente na literatura do aumento de temperatura quando lasers de diodo azul (445 nm) foram utilizados (DROST et al., 2019; KOUROS et al., 2020), não há informação em relação ao aumento de TP que ocorre quando fotopolimerizadores laser ou fotopolimerizadores LED *quadwave* são utilizados.

2 PROPOSIÇÃO

2.1 PROPOSIÇÃO GERAL

Avaliar os efeitos de fotopolimerizador laser e de novos fotopolimerizadores LED na alteração da temperatura pulpar *in vitro* em tempo real em condições intraorais simuladas.

2.2 PROPOSIÇÃO ESPECÍFICA

(1) Avaliar o aumento de temperatura em tempo real produzido na base de RCs, a transmissão de luz e a dureza Vickers na base e topo de RCs quando utilizados fotopolimerizadores laser e fotopolimerizadores contemporâneos.

(2) Avaliar *in vitro* o aumento da TP em molar superior com preparos cavitários Classe I e Classe V quando expostos à luz emitida por fotopolimerizadores laser e fotopolimerizadores contemporâneos.

(3) Avaliar *in vitro* o aumento da TP quando RCs do tipo *bulk-fill* são fotopolimerizadas em preparos cavitários Classe I e Classe V por fotopolimerizadores laser e fotopolimerizadores contemporâneos.

3 MATERIAL E MÉTODOS

3.1 DESCRIÇÃO DOS EXPERIMENTOS REALIZADOS

Os experimentos realizados neste estudo são parte de uma sequência de avaliações *in vitro* realizadas para avaliar os efeitos de fotopolimerizador laser e de novos fotopolimerizadores LED na alteração da temperatura em tempo real em condições intraorais simuladas.

Para a realização do estudo, os experimentos foram divididos em três etapas:

Experimento 01: Alterações de temperatura e dureza de compósitos à base de resina fotoativados com fotopolimerizadores laser ou LED.

Experimento 02: Alterações *in vitro* de temperatura na câmara pulpar causadas por unidades de fotopolimerização laser e LED *Quadwave.*

Experimento 03: Aumento *in vitro* da temperatura pulpar durante a fotopolimerização de compósitos à base de resina do tipo *bulk-fill* usando unidades de fotopolimerização laser ou LED.

3.2 EXPERIMENTO 01

3.2.1 RCs e Fotopolimerizadores

Três RCs de alta viscosidade, cujo fabricantes recomendam um incremento máximo de 2 mm, foram utilizadas no estudo. São elas: Tetric Evoceram (Cor A2, Ivoclar Vivadent, Schaan, Liechtenstein), Filtek Universal (Cor A2, 3M Oral Care, St. Paul, MN, EUA) e uma RC experimental chamada Transcend (Cor UB, Ultradent, South Jordan, Utah, EUA). Os números dos lotes e os fabricantes podem ser encontrados na Tabela 1.

Cinco fotopolimerizadores de alta potência foram utilizados: DeepCure S(DC, 3M Oral Care, St. Paul, MN, EUA), PinkWave (PW, Vista Dental Products, Racine, WI, EUA), PowerCure (PC, Ivoclar Vivadent, Schaan, Liechtenstein), Valo Grand (VG, Ultradent Products Inc., South Jordan, UT, EUA), and Monet Laser (ML, AMD Lasers, West Jordan, UT, EUA). A marca, número de série, fabricante, tipo, espectro de emissão (nm), os modos de exposição recomendados pelo fabricante para fotopolimerizar 2 mm de incremento e a irradiância podem ser encontrados na Tabela 2.

Tabela 1 – Informação dos fabricantes para as RCs para o Experimento 01.

RC	Lote	Fabricante	Cor	Composição da matriz resinosa	Composição de conteúdo inorgânico	Conteúdo inorgânico (%)
Filtek Universal	NE15442	3M, St Paul, MN, EUA	A2	AUDMA, AFM, diuretano-DMA e 1,12-dodecano-DMA.	Sílica nanométrica não-aglomerada/não-agregada, zircônia nanométrica não-aglomerada/não-agregada, aglomerados de zircônia e sílica (compostos de partículas de sílica e de zircônia nanométricas) e aglomerados de partículas nanométricas de trifluoreto de itérbio.	76,5 % por peso (58,4% por volume)
Tetric Evoceram	X22319	Ivoclar Vivadent, Schaan, Liechtenstein	A2	Dimetacrilatos (17–18% peso).	Vidro de bário, trifluoreto de itérbio, óxido misto e pré-polímero. Tamanho de partícula entre 40 nm e 3.000 nm com um tamanho médio de partícula de 550 nm.	75 - 76% por peso (53 – 55 % por volume)
Transcend	RN776	Ultradent Products Inc., South Jordan, UT, EUA	UB	Cinco diferentes monômeros de resina descritos como metacrilatos funcionais.	Cinco tipos diferentes de cargas que são composições de silicato variando de 5 nm a 3 um.	77.5% por peso

Tabela 2 - Informações fornecidas pelos fabricantes sobre os fotopolimerizadores e modos de exposição para o Experimento 01.

Fotopolimerizador	Abreviação	Número de Série	Fabricante	Tipo	Comprimento de onda (nm)	Modo de exposição	Irradiância (mW/cm²)
Deep Cure	DC	939112012777	3M Oral Care, St. Paul, MN, EUA	LED *Monowave*	430 - 480	1 x 10 s (*Standard*)	1.470 (-10 % / + 20 %)
PinkWave	PW	00380H	Vista Dental Products, Racine, WI, EUA	LED *Polywave*	395 - 900	1 x 10 s (*Standard*)	> 1.515
PowerCure	PC	1428005297	Ivoclar Vivadent, Schaan, Liechtenstein	LED *Polywave*	385 - 515	1 x 10 s (*High*)	1.200
						1 x 3 s (*3s Cure)*	3.000
Valo Grand	VG	S011264	Ultradent, South Jordan, UT, EUA	LED *Polywave*	395 - 480	1 x 10 s (*Standard*)	1.000
						1 x 3 s (*Xtra Power*)	3.200
Monet Laser	ML	00249	AMD Lasers, West Jordan, UT, EUA	Laser	450 ± 5	1 x 1 s	2.000 – 2.400
						3 x 1 s	2.000 – 2.400

3.2.2 Análise da Luz Emitida pelos Fotopolimerizadores e Transmitida pelas RCs

Uma matriz de Delrin semi-transpante (polioximetileno) de 2 mm de espessura com uma abertura circular de 6 mm de diâmetro foi utilizado no estudo para avaliar as mudanças de temperatura, a luz recebida do fotopolimerizador, e a quantidade de luz transmitida pela RC. Primeiro, a irradiância foi medida através da matriz de Delrin vazia posicionada entre a ponta do fotopolimerizador e a entrada da esfera de 6 polegadas (Labsphere, North Sutton, NH, EUA). Esta esfera estava acoplada a um espectrômetro de fibra óptica (Flame, Ocean Insight, Logan, FL, EUA). Todo este sistema de medição foi previamente calibrado usando uma lâmpada de calibração interna SCL-600 (Labsphere). Em seguida, a ponteira do fotopolimerizador foi posicionada centralmente sob a entrada de 6 mm do molde, e a saída de luz de cada fotopolimerizador através da abertura para dentro da esfera foi medida. Importante salientar que esta não foi a irradiância emitida na ponteira do fotopolimerizador, e sim foi a mesma irradiância recebida pelas amostras de 6 mm. Após isso, moldes Delrin adicionais foram preenchidos com as RCs utilizadas no estudo e fotopolimerizadas com o fotopolimerizador PowerCure por 20 s. Esses moldes foram então colocados na entrada da esfera integradora e a luz que passou através da RC polimerizada e alcançou a esfera foi mensurada. Três repetições foram feitas para cada grupo para obter as médias de potência (mW), exposição radiante (J/cm^2), e valores de potência atenuada da luz que atingiu a base de cada RC.

3.2.3 Análise de Temperatura

A mesma matriz Delrin semi-transparente de 2 mm de espessura com uma abertura circular de 6 mm de diâmetro (volume de 56,5 mm^3 ($V = \pi r^2 h$) para cada amostra) foi posicionado em um bloco de 31 mm de largura e 57 mm de comprimento feito de resina composta polimerizada Filtek Supreme Ultra Shade (Cor A2, 3M Oral Care, St. Paul, EUA). Uma sonda termopar de rápida resposta tipo T (Physitemp Instruments, Clifton, EUA) foi posicionada no bloco, centralmente na base da amostra, e a temperatura foi registrada em tempo real (cada 0,5 s) com a sonda termopar conectada a um sistema de aquisição de temperatura (T.C. Chart 1.03, Nomadics Inc., EUA). O blobo foi colocado no topo de uma placa de aquecimento (Cimarec, Thermo Fisher Scientifc, Waltham, EUA) programada para 32 ºC e a temperatura foi

monitorada em tempo real até estar estabilizada. Uma fina camada de pasta térmica de óxido de zinco (Corsair Memory, Almere, Holanda) foi aplicada sob a sonda termopar para melhorar a transferência de temperatura da resina para a sonda termopar. Uma vez que a temperatura alcançou 32 ºC (ZARPELLON et al., 2021), abertura de 6 mm de diâmetro na matriz Delrin foi preenchida com resina, que se encontrava a temperatura ambiente. Isso levou a uma queda da temperatura, mas a partir do momento que a temperatura retornou a 32 ºC, as resinas de cada grupo foram expostas com a luz da ponteira do fotopolimerizador posicionada a 0 mm da superfície da resina. Um exemplo de como as três medições foram realizadas é mostrada na Figura 1. Depois que as amostras de RC foram expostas à luz, a ponteira do fotopolimerizador foi tirada de contato com a superfície da resina para evitar que a ponteira agisse como um dissipador térmico. A temperatura foi monitorada em tempo real até que retornasse para 32 ºC, momento em que uma exposição adicional foi realizada. As amostras receberam esta segunda exposição à luz como uma tentativa de fotopolimerizar completamente a resina. Isso foi seguido de uma terceira exposição. O aumento de temperatura resultante foi usado para calcular a contribuição da reação exotérmica das RCs subtraindo esse aumento de temperatura (ΔT3) do primeiro (ΔT1) aumento de temperatura. O tempo para alcançar a temperatura máxima (pico T1) e retornar para 32 ºC foi de aproximadamente 6 minutos. Um total de cinco repetições (n=5) foram realizadas para cada grupo.

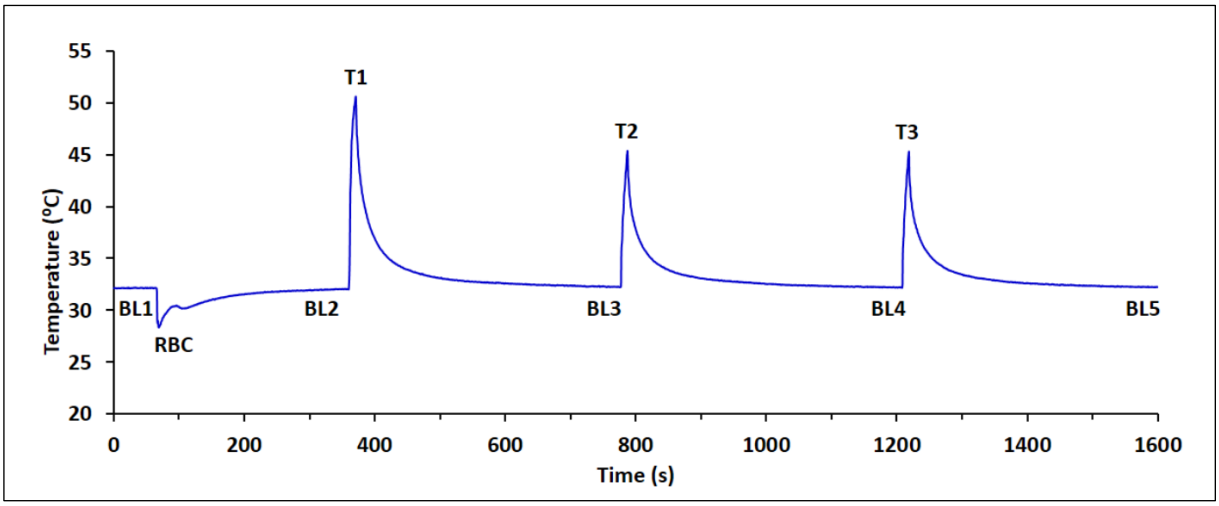

Figura 1 - Exemplo de uma das medições de temperatura (Tetric Evoceram + PW 10 s). BL: *baseline*. RBC: Inserção do compósito no molde; e T: aumento de temperatura para cada exposição. Note que os valores de BL retornaram a 32 ºC após cada exposição.

3.2.4 Micro-Dureza Vickers (VH)

Após as avaliações de temperatura serem realizadas, as amostras (n=5) foram removidas do molde Delrin e armazenadas em condições escuras e secas por 24 h. As resinas foram pesadas utilizando uma balança digital (Mettler AE 160, Mettler Toledo Instruments, Canadá) para confirmar que as amostras eram similares. A dureza Vickers (VH) foi então medida utilizando um microdurômetro (HM 123, Mitutoyo, Kawasaki, Japão) onde foi aplicada uma carga de 300 g por 8 s (KAISER; PRICE, 2020). Três edentações equidistantes foram realizadas próximo ao centro das superfícies não polidas de base e topo das amostras.

3.2.5 Análise Estatística

O presente estudo consistiu de 2 variáveis independentes (“RC” e “fotopolimerizador”), com o fator “RC” contendo 3 subníveis e “fotopolimerizador” com 8 subníveis. O esquema fatorial resultou em 24 grupos experimentais, com 5 repetições para cada grupo (n = 5). Os valores de ΔT foram submetidos à ANOVA dois fatores com “RC” e “modos de exposição” sendo as variáveis independentes, seguidas de teste post hoc de Scheffe. O peso das amostras, o tempo para atingir. A temperatura máxima, a contribuição da reação exotérmica e valores de VH entre os produtos foram comparados utilizando ANOVA um fator seguida do teste post hoc de Scheffe. Todos os testes estatísticos foram conduzidos usando um α predefinido de 0,05. As análises de regressão logarítmica foram realizadas (Excel, Microsoft, Redmond, WA, EUA) para cada aumento de temperatura de cada RC nos diferentes modos de exposição usando a Potência (Watts) ou a Energia (Joules) liberadas pelo fotopolimerizador para as RCs.

3.3 EXPERIMENTO 02

3.3.1 Análise Espectral da Luz Emitida pelos Fotopolimerizadores

O estudo utilizou um fotopolimerizador a base de diodo laser, um fotopolimerizador LED monowave, e três fotopolimerizadores LED multi-peak. As marcas, fabricantes, números de série e informações do fabricante podem ser encontrados na Tabela 3. A potência espectral radiante dos fotopolimerizadores foram

Tabela 3 - Marcas dos fotopolimerizadores, números de série e informações do fabricante para o Experimento 02.

Fotopolimerizador	Número de Série	Fabricante	Tipo	Comprimento de onda (nm)	Modo de exposição	Irradiância (mW/cm²)
SmartLite Pro	H00466	DentsplySirona, Charlotte, NC, EUA	LED *Monowave*	450 - 480	10 s (*Standard)*	1.200
Pinkwave	00380H	Vista Dental Products, Racine, WI, EUA	LED *Quadwave*	395 - 900	10 s (*Standard*)	> 1.515
					3 s (*Boost*)	> 1.720
PowerCure	1428005297	Ivoclar, Schaan, Liechtenstein	LED *Multi-peak*	385 - 515	10 s (*High*)	1.200
					3 s (*3s Cure*)	3.000
Valo Grand	S011264	Ultradent, South Jordan, UT, EUA	LED *Multi-peak*	395 - 480	10 s (*Standard*)	1.000
					3 s (*Xtra Power*)	3.200
Monet Versão 1s	00249	AMD Lasers, West Jordan, UT, EUA	Laser	450 ± 5	1 s	2.000 – 2.400
Monet Versão 3s	Not Present	AMD Lasers, West Jordan, UT, EUA	Laser	450 ± 5	3 s	2.000 – 2.400

medidas utilizando um espectroradiômetro óptico (Flame-T, Ocean Insight, Orlando, FL, EUA) conectado a uma esfera integradora de 6 polegadas de diâmetro (Labsphere, North Sutton, NH, EUA) que foi previamente calibrada utilizando uma lâmpada de calibração interna do mesmo fabricante. Cada ponteira de cada fotopolimerizador foi posicionada na entrada da esfera a fim de capturar toda a luz emitida do fotopolimerizador. As potências espectrais radiantes de 350 a 900 nm foram obtidas utilizando o programa OceanView (Ocean Insight). O diâmetro interno da região óptica de cada ponteira foi medida utilizando um paquímetro digital (Mitutoyo, Canada Inc, Mississauga, Canadá). A área da ponteira foi calculada e dividida pela potência para calcular a irradiância (mW/cm^2) dos fotopolimerizadores para cada modo de exposição. A exposição radiante de cada modo de exposição do fotopolimerizador foi calculada (J/cm^2) do produto do tempo de exposição e irradiância.

3.3.2 Medição *in vitro* de Temperatura

Após a aprovação do Conselho de Ética local (#2021-5703), um molar superior saudável extraído do Banco de Dentes da Universidade foi utilizado no estudo. Devido a questões de privacidade do Conselho de Ética da Universidade, nenhum detalhe do paciente foi revelado. Os critérios de inclusão foi dente molar não restaurado. Os critérios de exclusão foi a não alteração no esmalte e/ou dentina, cárie ou presença de quaisquer restaurações. Uma cavidade não retentiva, oclusal, Classe I (4 mm de profundidade, 3 mm de largura e 5 mm de comprimento) e vestibular, Classe V (2 mm de profundidade, 2 mm de largura e 5 mm de comprimento) foi então preparada no mesmo dente usando uma broca carbide (#330, Brasseler, Savannah, GA, EUA) sob refrigeração constante com água, e as dimensões da cavidade foram verificadas usando uma sonda periodontal de Williams. As paredes da cavidade foram polidas usando polidores Enhance (Dentsply Sirona, York, PA, EUA) para produzir uma cavidade lisa e não retentiva. As raízes foram seccionadas 4 mm abaixo da junção cemento-esmalte e ampliadas com brocas Gates Glidden (Dentsply Sirona). Após a preparação da cavidade, o dente foi escaneado (Figura 2) usando um CEREC Primescan (Dentsply Sirona) e uma imagem digital foi criada.

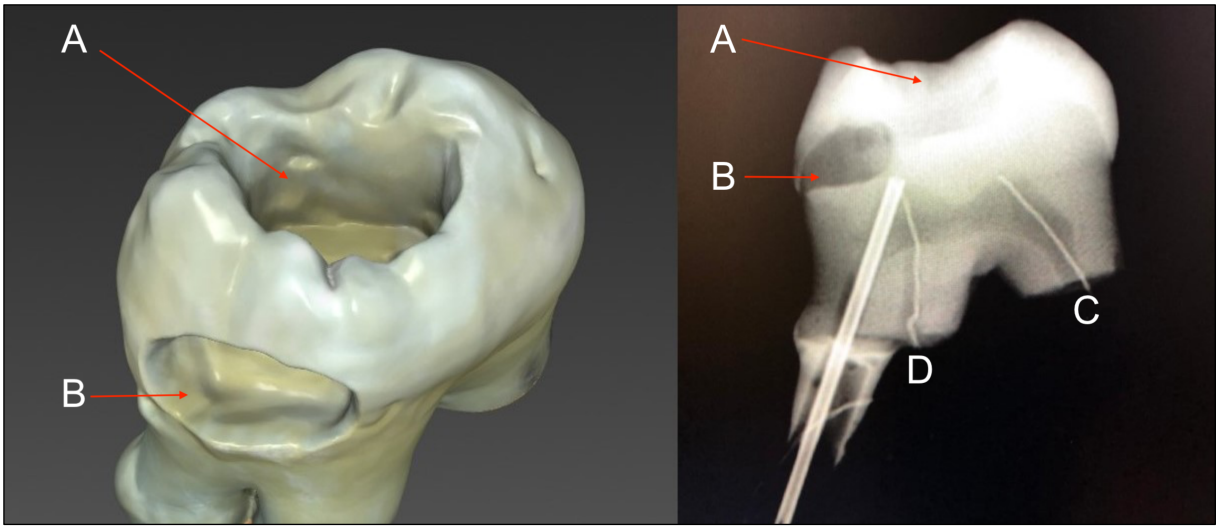

Figura 2 - Imagens 3D dos preparos Classe I e Classe V obtidas com CEREC Primescan (Dentsply Sirona) e imagens radiográficas para verificar a posição dos termopares. A: Preparo Classe I; B: Preparo Classe V; C: Termopares no Preparo Classe I; e D: Termopares no Preparo Classe V.

Foram utilizados duas sondas termopares ultrarrápidas tipo T com 0,011" (0,2794 mm) de diâmetro (IT-23 Physitemp Instruments, Clifton, NJ, EUA). As sondas foram inseridas através das raízes na câmara pulpar em duas posições: próximo ao corno pulpar e à parede bucal e próximo ao preparo Classe V. Um tubo de 1 mm de diâmetro interno foi colocado na raiz mesial para que o fluido pudesse entrar na polpa e simular o fluxo pulpar. Radiografias foram realizadas para verificar a posição das sondas e estimar a espessura da dentina remanescente entre o assoalho da cavidade e a polpa (Figura 2). A espessura de dentina remanescente foi medida usando o software radiográfico sendo de aproximadamente 1 mm. Para simular condições fisiológicas, a medição da temperatura dentro da câmara pulpar foi realizada a partir de uma temperatura basal controlada da polpa de aproximadamente 32 °C (ZARPELLON et al., 2021) em banho com água aquecida (Isotemp 2150 Immersion Circulator, Fisher Scientific Inc., Pittsburgh, PA, EUA). A temperatura basal de 32 °C é o valor aproximado dentro de uma polpa humana de um dente preparado após condicionamento e enxágue, seguido pela fotopolimerização do agente de união (ZARPELLON et al., 2021). Outra sonda termopar foi inserida dentro do banho aquecido para registrar a temperatura da água. Para simular o fluxo da polpa, o tubo de 1 mm de diâmetro foi conectado a uma Bomba Peristáltica P-1 (Pharmacia Fine Chemicals, Uppsala, Suécia). O fluxo de água foi ajustado para uma taxa de fluxo de 0,026 mL/min (SAVAS et al., 2014; AKARSU; AKTUG KARADEMIR, 2019) a 32 °C ±

0,5. O dente foi fixado em uma placa de acrílico com uma perfuração no centro e posicionado em banho de água morna até a junção amelocementária.

Dados de temperatura em tempo real foram coletados das sondas termopar (TCChart software, Nomadics Inc, Still- water, OK, EUA) a cada 0,5 s antes, durante e após a exposição à luz com e sem qualquer fluxo através da câmara pulpar. Após a estabilização da temperatura em 32°C, o preparo Classe I vazia foi exposta à luz do fotopolimerizador a uma distância de 0 mm entre a ponteira do fotopolimerizador e a superfície oclusal. Depois que a medição da temperatura voltou a 32 °C, uma segunda exposição foi feita a uma distância de 6 mm entre a ponteira do fotopolimerizador e a superfície oclusal. O mesmo procedimento foi realizado no preparo Classe V, mas a ponteira do fotopolimerizador foi posicionada sobre a superfície vestibular. A Figura 3 ilustra a posição da ponteira do fotopolimerizador para as avaliações dos preparos de Classe I e V.

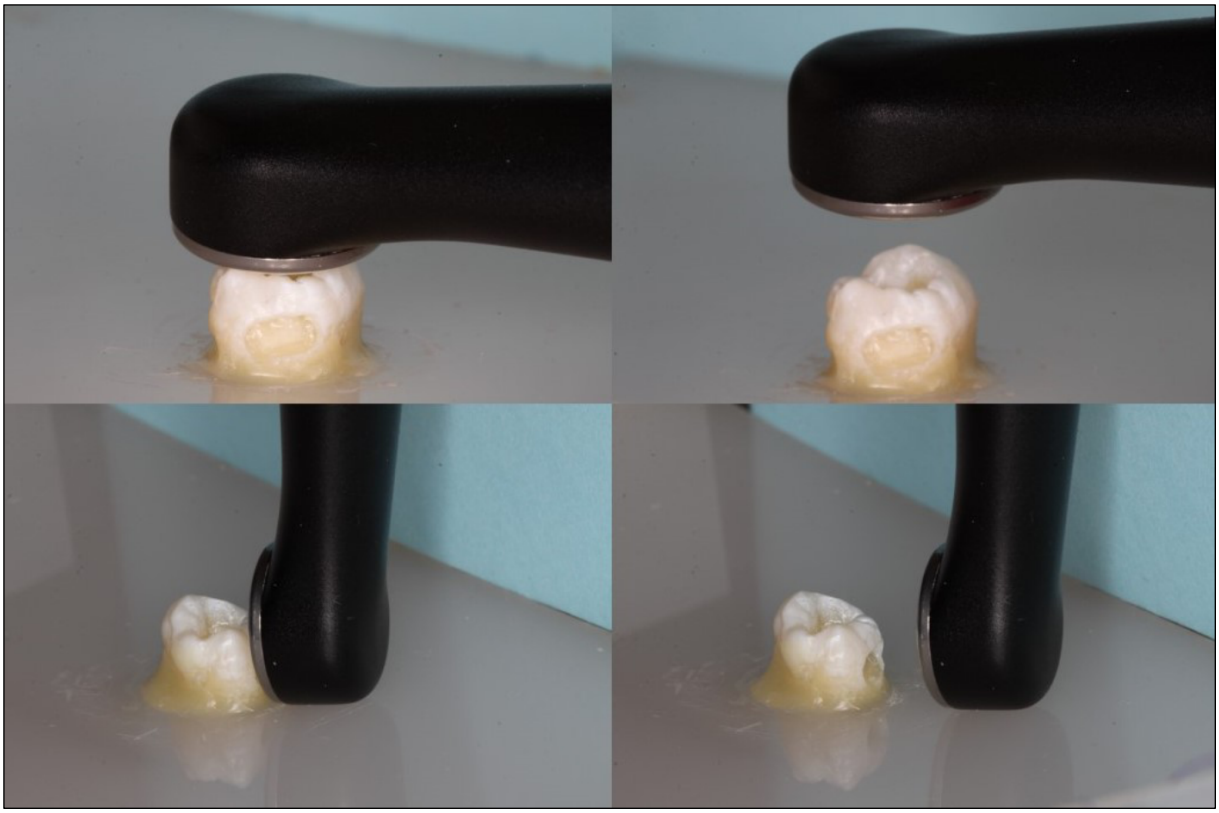

Figura 3 - Distâncias de exposição de 0 mm e 6 mm para cavidades vazias Classe I e Classe V no dente molar.

A Figura 4 mostra como a ponteira foi posicionada para os fotopolimerizadores PowerCure e Monet Laser, respectivamente. Cinco medições de temperatura foram feitas para cada condição com e sem fluxo pulpar.

Figura 4 – Ponteiras dos fotopolimerizadores PowerCure e Monet Laser posicionadas sobre o preparo Classe V. Observe como o centro da ponteira do fotopolimerizador Monet de grande diâmetro está no mesmo nível que a ponteira da cúspide, enquanto o centro da ponteira do fotopolimerizador PowerCure de diâmetro menor está mais centralizado no preparo Classe V.

3.3.3 Análise Estatística

O efeito do fluxo pulpar simulado foi comparado usando ANOVA um fator seguido pelo teste post hoc de Scheffe. Os valores de ΔT foram submetidos a ANOVA dois fatores com "modos de exposição" e "distância" como variáveis independentes, seguidos pelos testes post hoc de Scheffe. Testes estatísticos e análises post hoc foram conduzidos em um α predefinido de 0,05.

3.4 EXPERIMENTO 03

3.4.1 Análise da Luz emitida pelos Fotopolimerizadores

Um diodo laser, um LED monowave e três LEDs *multi-peak* de alta potência (Figura 5) foram utilizados (Tabela 4). A potência espectral radiante dos fotopolimerizadores foi medida utilizando um espectrorradiômetro de fibra óptica (Flame-T, Ocean Insight, Orlando, FL, EUA) conectado à uma esfera integradora de 6” de diâmetro (Labsphere, North Sutton, NH, EUA) previamente calibrada utilizando uma lâmpada interna de calibração NIST (ICS-600, Labsphere). A ponteira de cada fotopolimerizador foi posicionada na entrada da esfera para capturar toda a luz emitida pelo fotopolimerizador na distância de 0 mm. A saída de luz foi gravada utilizando o programa OceanView (Ocean Insight, Orlando, FL, EUA), que forneceu a potência total emitida e a potência espectral radiante. A potência foi multiplicada pelo tempo de exposição para fornecer a energia (J) entregue ao dente oriunda de cada fotopolimerizador. Para determinar a irradiância de cada fotopolimerizador, o diâmetro interno de cada ponteira foi medida com paquímetro digital (Mitutoyo, Canada Inc,

Mississauga, ON, Canadá) e a área de emissão óptica da ponteira de cada fotopolimerizador foi calculada. Este valor foi dividido pela potência (W) para obter a irradiância total (mW/cm^2) do fotopolimerizador para cada modo de exposição.

Tabela 4 – Informação provida pelos fabricantes sobre os fotopolimerizadores utilizados no Experimento 03.

Fotopolimerizador	Número de série	Fabricante	Tipo	Irradiância (mW/cm²)	Modo de Exposição
SmartLite Pro	H00466	Dentsply Sirona, Charlotte, NC, EUA	LED *Monowave*	1.200	2 x 10s (*Standard*)
PinkWave	00380H	Vista Dental Products, Racine, WI, EUA	LED *Polywave*	> 1.515 > 1.720	20s (*Standard*) 3s (*Boost*)
PowerCure	1428005297	Ivoclar Vivadent, Schaan, Liechtenstein	LED *Polywave*	1.200 3.050	20s (*High*) 3s (*3s Cure*)
Monet Laser	00249	AMD Lasers, West Jordan, UT, EUA	Laser	2.000 – 2.400 2.000 – 2.400	1s 3 x 1s
Valo X	00249	Ultradent Jordan, UT, EUA	LED *Polywave*	1.100 2.200	2 x 10s (*Standard*) 5 s (*Xtra*)

Figura 5 – Cinco fotopolimerizadores utilizados no Experimento 03.

3.4.2 Análise *in vitro* de Temperatura

O presente estudo foi aprovado pelo Conselho de Ética local (#2021–5703). Foi utilizado no estudo, para todos os experimentos, um molar superior do Banco de Dentes da Universidade para todos os experimentos. Os critérios de inclusão foram que o dente molar tinha que estar intacto e não restaurado. Um preparo oclusal, não retentivo, Classe I (3 mm de largura, 4 mm de profundidade e 5 mm de comprimento) e um preparo vestibular, não retentivo, Classe V (2 mm de largura, 2 mm de profundidade e 5 mm de comprimento) com paredes divergentes foram realizadas utilizando uma broca carbide (#330, Brasseler, Savannah, GA, EUA) sob refrigeração constante com água. As dimensões da cavidade foram verificadas através de uma sonda periodontal de William. A espessura da parede de fundo dos preparos Classe I e V ficou com aproximadamente 1 mm. Para verificar a espessura do restante dentina e a posição das sondas termopares, foram tiradas radiografias e as medidas foram feitas a partir dessas radiografias (Figura 6). Os preparos cavitários Classe I e V no dente molar são mostrados na Figura 7. As paredes da cavidade foram polidas com Enhance (Dentsply Sirona) para que houvesse mínima retenção mecânica na parede da cavidade e a resina pudesse ser facilmente removida. As raízes dos dentes foram seccionadas 4 mm abaixo da junção cemento-esmalte e foram ampliadas com brocas Gates Glidden (Dentsply Sirona, York, PA, EUA).

Duas sondas termopares tipo T de resposta ultrarrápida de 0,011” de diâmetro (IT-23 Physitemp Instruments, Clifton, NJ, EUA) foram inseridas na câmara pulpar através das raízes alargadas, uma próxima ao corno pulpar e a outra próximo ao preparo Classe V. O molar foi anexado a uma placa de acrílico para simular o efeito do uso de dique borracha e grampo. Para simular as condições da cavidade oral, o dente foi inserido em um banho de água morna (Isotemp 2150 Immersion Circulator, Fisher Scientific Inc., Pittsburgh, PA, EUA) até a junção cemento-esmalte. As medições de temperatura dentro da câmara pulpar foram realizadas sob simulação fisiológica controlada em uma temperatura basal da polpa de aproximadamente 32°C, simulando a temperatura basal do dente após condicionamento adesivo e enxágue (ZARPELLON et al., 2021). Um tubo foi colocado na raiz mesial e conectado a uma bomba peristáltica (Peristaltic Pump P-1, Pharmacia Fine Chemicals, Uppsala, Suécia). A taxa de fluxo de água através do tubo para a câmara pulpar foi ajustada

para 0,026 mL/min (SAVAS et al., 2014; AKARSU; AKTUG KARADEMIR, 2019). Uma terceira sonda termopar foi inserida no banho para medir a temperatura da água.

Figura 6 - Imagem de radiográfica para verificar a posição dos termopares e a espessura da dentina.

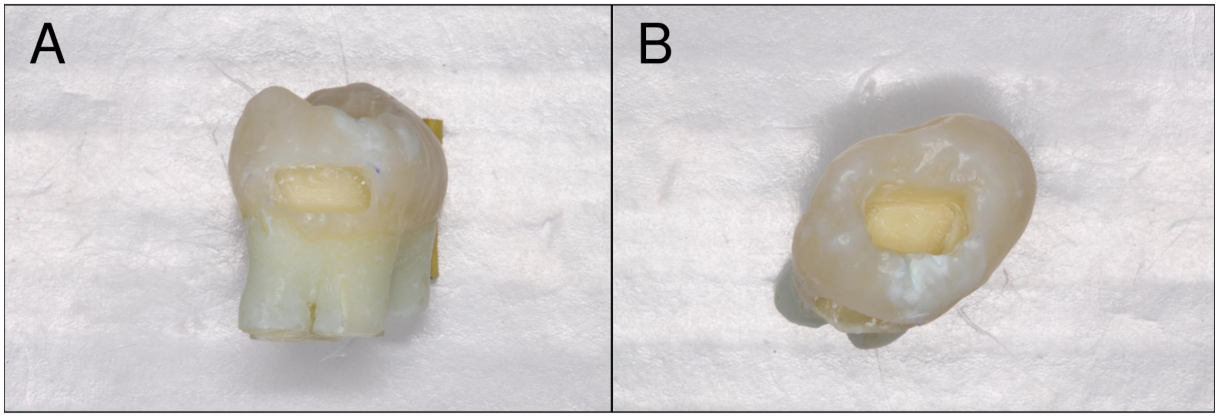

Figura 7 – Preparos Classe V (A) e Classe I (B) do molar utilizado no estudo.

Um sistema de aquisição de temperatura (TCChart, Nomadics Inc., Stillwater, OK, EUA) foi utilizado para registrar a temperatura a cada 0,05 s antes, durante e após os procedimentos de restauração. Um esquema ilustrando como a temperatura foi registrada é mostrado na Figura 8. A fim de que a restauração pudesse ser removida após fotopolimerização, nenhum procedimento adesivo foi realizado. Ao invés disso, uma camada muito fina de vaselina (Covidien, Mansfield, MA, EUA) foi aplicada na cavidade, e uma peça de fio dental foi inserido na RC antes da fotopolimerização. Depois de atingir a temperatura basal de 32°C, o preparo Classe I foi preenchido até uma profundidade de 4 mm usando uma das seguintes RCs (Tabela 5): Filtek One Bulk Fill (FB-One; Cor A2; 3M, St. Paul, MN, EUA), Filtek Bulk Fill Flowable (FB-Flow; Cor A2; 3M), Tetric PowerFill (TP-Fill; Cor IVA; Ivoclar Vivadent, Schaan, Liechtenstein), ou Tetric PowerFlow (TP-Flow; Cor IVA; Ivoclar Vivadent). TP-Fill e TP-

Flow usam o mecanismo de polimerização RAFT. As resinas FB-One e FB-Flow utilizam tecnologia RAFT. A ponteira do fotopolimerizador foi posicionado a 0 mm da ponta da cúspide e as RCs bulk-fill foram expostas às condições de fotopolimerização relatadas na Tabela 4. O mesmo procedimento foi realizado para o preparo Classe V, onde a ponta LCU foi colocada na superfície bucal, exceto que o preparo Classe V tinha apenas 2 mm de profundidade. A Figura 9 descreve o delineamento experimental.

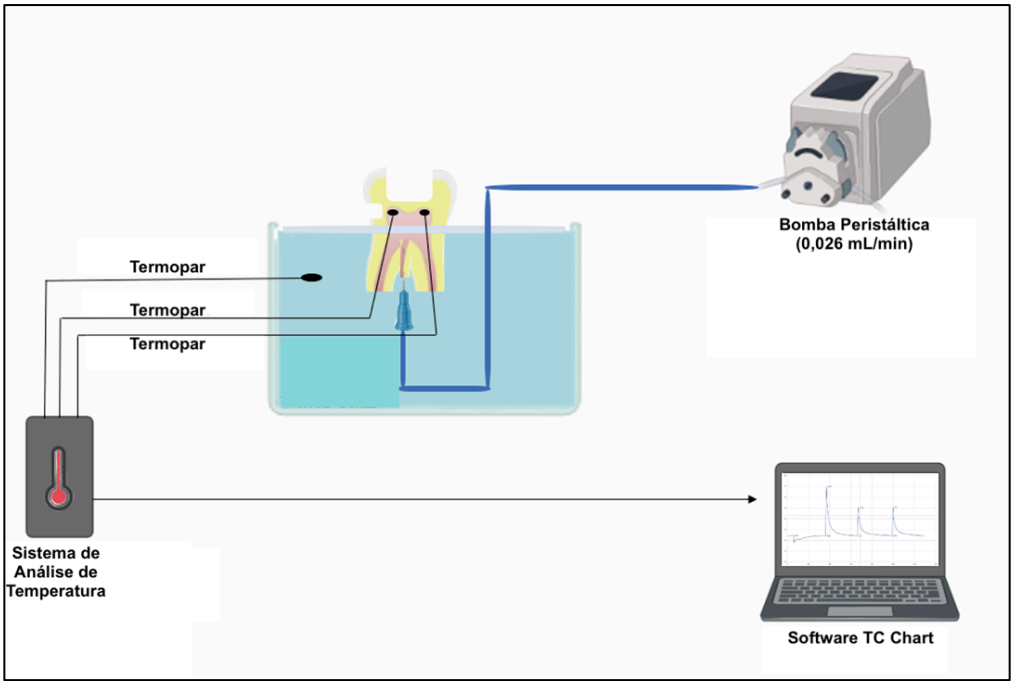

Figura 8 – Ilustração esquemática de como a temperatura foi mensurada no Experimento 03.

Tabela 5 – RCs utilizadas no Experimento 03.

RC	Lote	Tipo	Fabricante	Cor
Filtek Bulk Fill Flowable	NF23205	Baixa Viscosidade	3M Oral Care, St Paul, MN, EUA	A2
Filtek One Bulk Fill	NC44145 NE63556	Alta Viscosidade	3M Oral Care, St Paul, MN, EUA	A2
Tetric PowerFlow	Z02X2L Z010KV	Baixa Viscosidade	Ivoclar Vivadent, Schaan, Liechtenstein	IVA
Tetric PowerFill	Z02PCM Z033N3	Alta Viscosidade	Ivoclar Vivadent, Schaan, Liechtenstein	IVA

3.4.3 Análise Estatística

Uma vez que alguns fabricantes comercializam a RC *bulk-fill* e o fotopolimerizador (Ivoclar Vivadent) como um sistema restaurador, o desenho fatorial do estudo consistiu em uma variável independente (RBC bulk-fill/fotopolimerizador) e uma variável dependente (temperatura). O esquema fatorial resultou em 72 grupos experimentais, com cinco repetições para cada (n = 5). Os valores de ΔT para Classe I e Classe V foram primeiro submetidas a uma análise de variância (ANOVA) um fator seguido pelos testes post-hoc de Scheffe. Testes estatísticos e análises post hoc foram conduzidas em um α predefinido de 0,05. Análises de regressão logarítmica foram realizadas (Excel, Microsoft, Redmond, WA, EUA) para cada aumento da temperatura da RC nos diferentes modos de exposição usando a Energia (Joules) liberada dos fotopolimerizadores para as RCs.

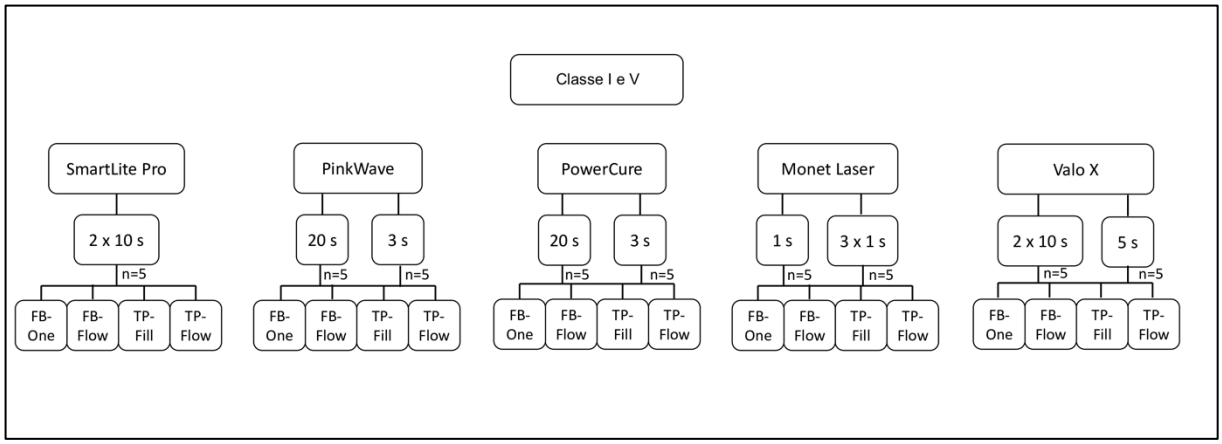

Figura 9 – Delineamento experimental do Experimento 03.

4 RESULTADOS

4.1 ARTIGO 1: TEMPERATURE CHANGES AND HARDNESS OF RESIN-BASED COMPOSITES LIGHT-CURED WITH LASER DIODE OR LIGHT-EMITTING DIODE CURING LIGHTS

Cristiane Maucoski[a,b]
Richard Bengt Price[a]
Cesar Augusto Galvão Arrais[b]

[a] Department of Dental Clinical Sciences, Dalhousie University, Halifax, Nova Scotia, B3H 4R2, Canada.
[b] Department of Restorative Dentistry, State University of Ponta Grossa, Ponta Grossa, Parana, Brazil.

Revista: Odontology
Aceito: 13 de setembro de 2022
Publicado: 03 de outubro de 2022
DOI: 10.1007/s10266-022-00745-1

4.1.1 Abstract

The temperature and Vickers Hardness (VH) at the top and bottom surfaces of three resin-based composites (RBCs) were measured when light-cured using five light-curing units (LCUs). The spectrum, power, and energy delivered to the top of the RBCs and transmitted through the RBCs were measured. Starting at 32℃, the temperature rise produced by the Monet Laser (ML—1 s and 3 s), Valo Grand (VG—3 s and 10 s), DeepCure (DC—10 s), PowerCure, (PC—3 s and 10 s) and PinkWave (PW—10 s) were measured at the bottom of specimens 2 mm deep × 6 mm wide made of Filtek Universal A2, Tetric Evoceram A2 and an experimental RBC codenamed Transcend UB. The VH values measured at the top and bottom of these RBCs were analyzed using ANOVA and Scheffe's post hoc test ($p < 0.05$) to determine the effects of the LCUs on the RBCs. The transmitted power from the ML was reduced by 77.4% through 2 mm of Filtek Universal, whereas light from PW decreased by only 36.8% through Transcend. The highest temperature increases from the LCU combined with the

exothermic reaction occurred for Transcend, and overall, no significant differences were detected between Filtek Universal and Tetric Evoceram (p = 0.9756). Transcend achieved the highest VH values at the top and bottom surfaces. The PinkWave used for 10 s produced the largest temperature increase (20.2°C) in Transcend. The Monet used for 1 s produced the smallest increase (7.8°C) and the lowest bottom:top VH ratios.

Keywords: Dental curing lights, Light-emitting diode, Laser, Temperature, Vickers hardness, Hardness ratio

4.1.2 Introduction

The resin used in light-activated resin-based composite restorations (RBCs) must be adequately photo-cured for the restoration to be clinically successful; otherwise, the RBC remains a liquid or soft paste. Therefore, good light-curing units (LCUs) have become indispensable in the dental office. Light-emitting diode (LED) LCUs are now the most popular (JANDT; MILLS, 2013; ERNST et al., 2018). They deliver a narrow emission range of wavelengths, they do not require any filters, they are energy efficient, and they can be battery operated (JANDT; MILLS, 2013). Clinicians may choose to use single-peak LED LCUs that deliver only a narrow band of wavelengths, or they may use multi-peak LED LCUs, also called polywave, that use several LEDs to emit multiple emission peaks that cover a broader range of wavelengths. Consequently, compared to single-peak LCUs, these multi-peak LED LCUs can activate a wider range of photoinitiators, as well as the commonly used camphorquinone initiator (RUEGGEBERG, F. A. et al., 2017).

To achieve improved mechanical properties and reduce chair time, manufacturers make and promote LCUs that deliver irradiances greater than 2,000 mW/cm2 and offer short exposure times, some as short as 1 s (CMS, 2016; AMD, 2021). However, when using LCUs that deliver a high irradiance, there is a potential risk for heat-induced pulpal injury as the RBC polymerizes (WAHBI et al., 2012) because the LCU can deliver a considerable amount of energy (RUEGGEBERG, F. A., 2011) to the gingivae (SPRANLEY et al., 2012; MAUCOSKI et al., 2017) and the pulpal tissues (ZACH; COHEN, 1965; RUNNACLES et al., 2015; ZARPELLON et al., 2018; ZARPELLON et al., 2019; GROSS et al., 2020; NILSEN et al., 2020;

ZARPELLON et al., 2021). In addition, the exothermic polymerization reaction produces additional heat that increases the magnitude of the temperature rise. Thus, the temperature rise in the tooth depends on the RBC, power (Watts), irradiance (mW/cm^2), exposure time, amount of energy delivered (Joules), the rate at which the RBC polymerizes, and the wavelengths of light delivered from the LCU (PRICE; FERRACANE; SHORTALL, 2015; BALESTRINO et al., 2016; MOUHAT et al., 2017; RUEGGEBERG, F. A. et al., 2017; AKARSU; AKTUG KARADEMIR, 2019; PAR et al., 2019; WANG et al., 2021). It has been suggested that temperature increases greater than 5.5 °C inside the pulp chamber might be dangerous to the pulp (ZACH; COHEN, 1965). For this reason, the heat generated when using LCUs that deliver an irradiance greater than 1,200 mW/cm^2 has become a concern (MOUHAT et al., 2017).

A new approach to the photo-activation of composites uses a fast, 1–3-s light exposure at a high irradiance (ILIE; WATTS, 2020; ALGAMAIAH; SILIKAS; WATTS, 2021; GAROUSHI; LASSILA; VALLITTU, 2021). A recent development uses a laser diode LCU to deliver such a high irradiance at 450 nm in a 1-s exposure (Monet, AMD). The manufacturer claims that this laser diode LCU has a collimated beam that allows the light to penetrate deeply into the RBC and photo-cure the RBC to a depth of 2 mm in only 1 s. Some blue diode lasers using 445 nm have already been tested as an alternative light source to photo-cure dental RBCs (DROST et al., 2019; KOUROS et al., 2020). Since they are a laser, they deliver a high photon density and a high irradiance even as the distance from the light tip increases, but their output is over a very narrow range of wavelengths (DROST et al., 2019). A previous study reported that using one laser diode LCU for 1 s produced the shallowest depth of cure in all ten RBCs tested. This was attributed to the low radiant exposure delivered by this LCU in 1 s (ROCHA et al., 2022). Another new LCU is the PinkWave. This LCU has what the manufacturer describes as Quadwave technology to deliver four distinct bands of wavelengths over a wider range of wavelengths than conventional LCUs. In addition to blue and violet light, the PinkWave delivers nearinfrared (NIR) and red light. However, there is currently no information regarding the temperature rise that occurs when using the Monet or the PinkWave LCUs.

Some previous laboratory studies have evaluated the heat generated on cylindrical RBC specimens made in Teflon molds at room temperature using both K- and T-type thermocouples (SPANOVIC et al., 2018; PAR et al., 2019; KOUROS et al., 2020; WANG et al., 2021). Alternatively, high-definition digital infrared imagery has

been used to monitor the temperature (MOUHAT et al., 2017; YANG; ALGAMAIAH; WATTS, 2021). However, in these studies, the volume of RBCs used was often not well defined, the energy or the wavelengths delivered by the LCU were not reported, nor was a baseline temperature used that was similar to the intraoral temperature found in a tooth (YANG; ALGAMAIAH; WATTS, 2021; ZARPELLON et al., 2021). Therefore, this study recorded the real-time temperature rise produced at the bottom of standardized volumes of three RBCs using a fast response T-type thermocouple starting at a simulated intraoral temperature of 32°C (ZARPELLON et al., 2021) when light-cured using five different LCUs. In addition, the light transmission through the RBCs and the Vickers micro-hardness (VH) at the top and bottom surfaces were measured.

The null research hypotheses are that:

(1) The five LCUs would not deliver the same amount of energy (Joules);

(2) The combined effect of the light from the LCUs and the exothermic reaction would not produce the same temperature increase at the bottom of the three RBCs;

(3) There would be no differences in the exothermic temperature rise produced by different RBCs;

(4) The exothermic heat contribution to the temperature increase would not be greater than 5.5°C (ZACH; COHEN, 1965); and

(5) There would be no differences in hardness values at the top and bottom of the RBCs when the different LCUs were used.

4.1.3 Materials and Methods

4.1.3.1 Resin-based composites (RBCs) and light-curing units (LCUs)

Three conventional paste consistency RBCs whose manufacturers recommend a 2 mm maximum increment thickness were used in the study: Tetric Evoceram A2 (Ivoclar Vivadent, Schaan, Liechtenstein); Filtek Universal A2 (3 M Oral Care, St. Paul, MN, USA) and one experimental RBC codenamed Transcend UB (Ultradent, South Jordan, Utah, USA). The lot numbers and manufacturers are reported in Table 1.

Five contemporary high-output LCUs were used: Deep- Cure (DC, 3M Oral Care, St. Paul, MN, USA), PinkWave (PW, Vista Dental Products, Racine, WI, USA), Power-Cure (PC, Ivoclar Vivadent, Schaan, Liechtenstein), Valo Grand (VG, Ultradent Products Inc., South Jordan, UT, USA), and Monet Laser (ML, AMD Lasers, West

Jordan, UT, USA). The brand, serial number, manufacturer, type, emission spectrum (nm), the exposure modes recommended by the manufacturer to light cure 2 mm of RBC (APEX; 3M, 2015; ULTRADENT PRODUCTS, 2017; IVOCLAR VIVADENT, 2019; AMD, 2021) and their claimed irradiance outputs are reported in Table 2.

4.1.3.2 Analysis of the light emitted by the LCUs and transmitted through the RBCs

A 2 mm thick semi-transparent Delrin (polyoxymethylene homopolymer) mold with a 6 mm diameter hole was used in the study to measure the temperature changes, the light received by the specimens from the LCU, and the amount of light transmitted through the RBCs. First, the irradiance was measured through the unfilled Delrin mold placed between the LCU tip and the entrance into a 6″ integrating sphere (Labsphere, North Sutton, NH, USA). This sphere was attached to a fiber-optic Flame spectrometer (Ocean Insight, Logan, FL, USA). This entire measurement system had been previously calibrated using an internal calibration lamp SCL-600 (Labsphere). Next, the tip of each LCU was centrally positioned at the entrance to the 6 mm diameter hole, and the light output from each LCU through the hole in the mold and into the sphere was measured. Of note, this was not the irradiance emitted at the tip of the LCU; instead, it was the same irradiance received by the 6 mm diameter specimens. Then, additional Delrin molds were filled with the RBCs used in the study and photo-activated with the PowerCure for 20 s. These molds were then placed at the entrance of the integrating sphere, and the light that passed through the cured RBC and into the sphere was measured for each LCU condition (Supplemental Table 1). Three measurements were made for each group to obtain the mean powers (mW), radiant exposures (J/cm^2), and the attenuated powers of the light that reached the bottom of each RBC.

4.1.3.3 Temperature analysis

The same 2 mm thick semi-transparent Delrin mold with a 6 mm diameter hole (volume of 56.5 mm^3 ($V = \pi r^2 h$) for each specimen) was placed on a block of cured Filtek Supreme Ultra Shade A2 RBC (3 M Oral Care, St.mPaul, USA) that was 31 mm wide by 57 mm long. A fastresponse thermocouple T-type (Physitemp Instruments, Clifton, USA) was placed on the block, centrally at the bottom of the specimen, and the

temperature was recorded in real-time (every 0.5 s) with the T-type thermocouple connected to a temperature acquisition software (T.C. Chart 1.03, Nomadics Inc., USA). The block was placed on top of a warming plate (Cimarec, Thermo Fisher Scientific, Waltham, USA) set at 32°C and the temperature was monitored in real-time until it stabilized. A thin layer of zinc oxide thermal paste (Corsair Memory, Almere, Netherlands) was placed over the thermocouple to improve the temperature transfer from the RBC to the thermocouple. Once the baseline temperature had reached 32°C (ZARPELLON et al., 2021), the 6 mm diameter hole in the Delrin ring was filled with RBC. This caused the temperature to fall, but once the baseline temperature had returned to 32°C, the RBCs in each group were exposed to light with the tip of the LCU positioned 0 mm from the surface of the RBC. An example of how the three temperature measurements were made is shown in Figure 1. After the RBC specimens had been exposed to light, the LCU was taken out of contact with the surface of the RBC so that the light tip did not act as a thermal heat sink. The temperature was monitored in realtime until it returned to 32°C, at which time an additional light exposure was performed. The samples received this second light exposure to hopefully fully photo-polymerize the RBC. This was then followed by a third exposure. The resulting temperature rise was used to calculate the exothermic heat contribution from the RBCs by subtracting this temperature rise (ΔT3) from the first (ΔT1) temperature rise. The time to reach the maximum temperature (T1 peak) and then return to 32°C was approximately 6 min. A total of five temperature measurements (n = 5) were made for each group.

4.1.3.4 Vickers micro-hardness (VH)

After temperature measurements had been made, the specimens (n = 5) were removed from the Delrin mold and store in dry and dark conditions for 24 h. The RBCs were weighed using a Mettler AE 160 digital scale (Mettler Toledo Instruments, Ontario, Canada) to confirm that the specimens were similar. The Vickers hardness (VH) was then measured using a micro-hardness testing machine (HM 123, Mitutoyo, Kawasaki, Kanagawa, Japan) that applied a 300 g load for 8 s (KAISER; PRICE, 2020). Three equidistant indentations were made close to the center of the unpolished top and bottom surfaces.

4.1.3.5 Statistical analysis

The present study consisted of 2 independent variables (“RBC” and “LCU”), with the factor “RBC” containing 3 sublevels and “LCU” with 8 sublevels. The factorial scheme resulted in 24 experimental groups, with 5 repetitions for each group (n = 5). The ΔT values were subjected to a two-way, repeated-measures analysis of variance (ANOVA) test with “RBC” and “exposure modes” as the independent variables, followed by Scheffe’s post hoc tests. The specimen weight, time to take the maximum temperature, exothermic heat contribution and VH values among the products were compared using one-way ANOVA followed by Scheffe’s post hoc test. All statistical testing and post hoc analyses were conducted using a preset α of 0.05. Logarithmic regression analyses were performed (Excel, Microsoft, Redmond, WA, USA) for each RBC temperature rise at the different exposure modes using either the Power (Watts) or the Energy (Joules) delivered from the LCUs to the RBCs.

4.1.4 Results

4.1.4.1 Weight

Overall, the specimens made using Tetric Evoceram had the highest mean ± standard deviation weight value of 0.120 ± 0.005 g, followed by Transcend UB at 0.117 ± 0.005 g and Filtek Universal A2 at 0.115 ± 0.004 g. These differences of ± 0.005 g represented, at most, a 4% difference in the weight of the RBCs in each group. No significant differences were found between the Filtek Universal A2 and Transcend UB groups of RBC ($p = 0.2658$), but Scheffe’s post hoc test detected a significant difference for the specimens of Tetric Evoceram ($p < 0.05$).

4.1.4.2 Analysis of the light emitted by the LCUs and transmitted through the RBCs

Figure 10 shows the total power (mW) and emission spectra from the LCUs. The Valo Grand, PowerCure and PinkWave were multi-peak broadband LED lights. The Power-Cure delivered two wavelength peaks, and the Valo Grand had three peaks. One peak was in the violet range (Valo Grand = 393 nm and PowerCure = 408 nm), and the others were in the blue wavelength region (Valo Grand at 448 and 461 nm and PowerCure = 451 nm). The PinkWave LCU emitted four distinct bands of

wavelengths, three were in the range of visible light (λ1 = 410 nm; λ2 = 471 nm, λ3 = 631 nm), and one was in the near-infrared spectral range (thermal radiation) with an emission peak (λ4) at 860 nm. The Monet and DeepCure LCUs delivered only a single emission peak (Figure 10). The DeepCure emitted a broader range of wavelengths with a peak emission at 448 nm. Since the Monet is a laser, it emitted a very narrow band of wavelengths with an emission peak at 451 nm.

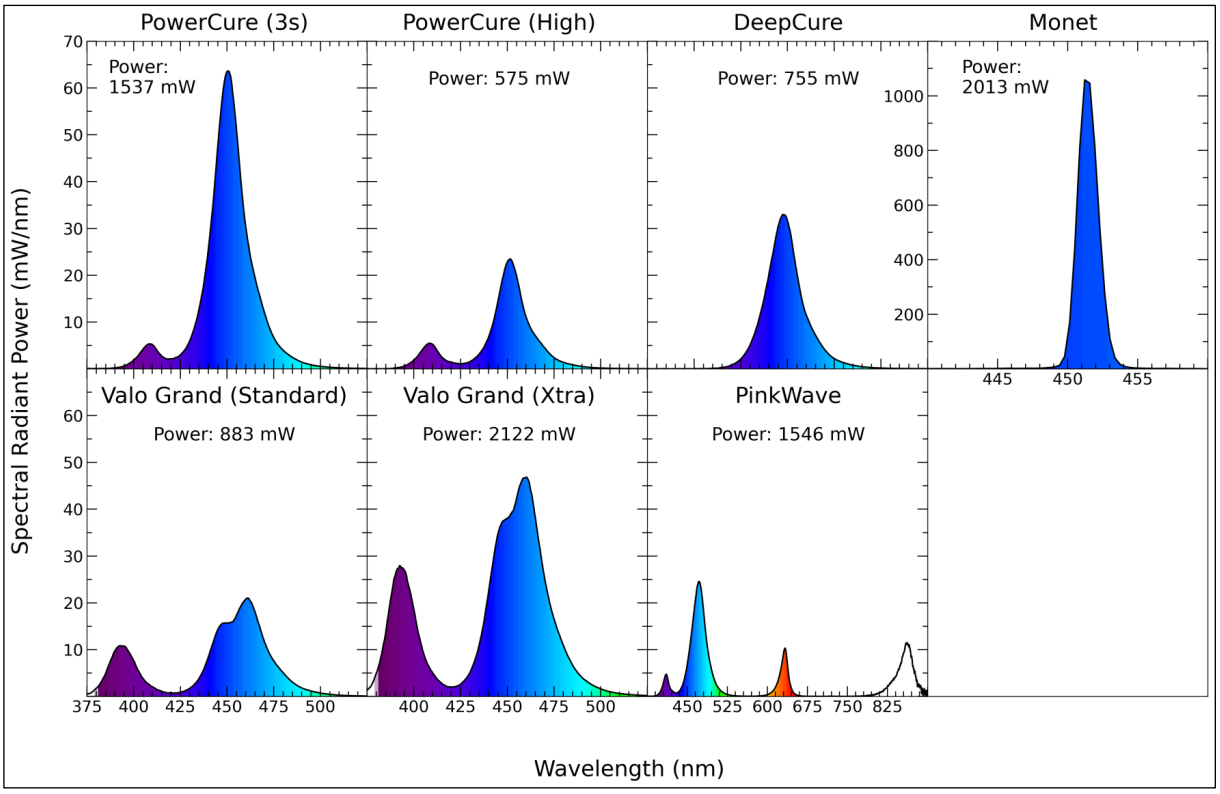

Figura 10 - Power (mW) and emission spectra of LED curing lights and Monet Laser. Note the different power and wavelength ranges of the Monet Laser compared to other LED curing lights.

The power (mW) transmitted through the empty mold and through the molds filled with RBC are reported in Table 6. The transmitted power from the ML was reduced by 77.4% when passing through 2 mm of Filtek Universal A2, whereas the power of the light from the PW decreased by only 36.8% after passing through 2 mm of Transcend UB. Figure 11 shows the emission spectra from PinkWave and Valo Grand through the empty ring and the ring filled with the RBCs. Note the greater reduction of the lower wavelengths of violet light. Table 7 reports the irradiance and radiant exposure received by the RBCs in the 6 mm diameter mold. Note that the radiant exposure delivered in every single exposure ranged from a little as 5.4 J/cm^2 to a high of 31.0 J/cm^2, depending on the LCU and exposure time. This value must be

multiplied by 3 to give the total radiant exposure delivered to the RBCs after they had received 3 light exposures.

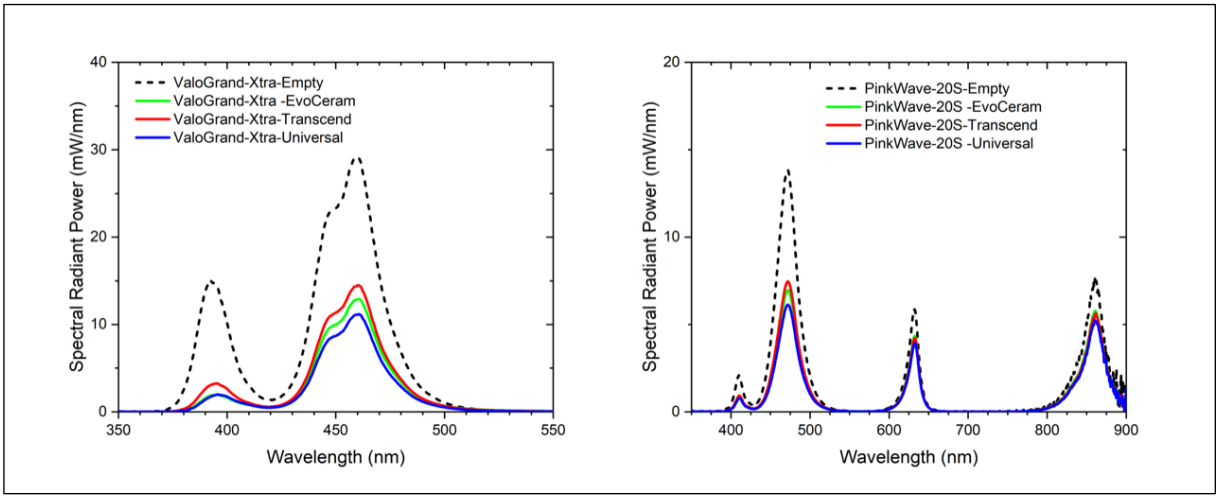

Figura 11 - Emission spectra (mW/nm) of PinkWave and Valo Grand through empty molds and through molds filled with RBC. Note that the x-axis for Pinkwave is on a different scale.

4.1.4.3 Temperature analysis

The greatest mean temperature (± Standard Deviation) increases during the first light exposure of the RBCs, regardless of the exposure mode, occurred at the bottom of Transcend UB (mean ΔT1 = 17.2℃, SD = 4.4), followed by Tetric Evoceram A2 (mean ΔT1 = 13.1℃, SD = 3.1) and Filtek Universal A2 (mean ΔT1 = 13.0°C, SD = 3.1). Scheffe's test detected a significant difference for Transcend ($p < 0.0001$), but there was no significant difference between the temperature increase for Filtek Universal and Tetric Evoceram ($p = 0.9756$).

The greatest temperature increase was found when the PinkWave was used for 10 s (mean ΔT1 = 20.2°C, SD = 2.2), regardless of the RBC used. The smallest temperature increase was from the Monet when used for 1 s (mean ΔT1 = 7.8°C, SD = 0.6). No significant differences were found between PowerCure used for 10 or 3 s, Valo Grand used for 10 or 3 s, DeepCure used for 10 s, and the Monet used for 3 s (Figure 12). Except for Monet used for 1 s, the temperature rises on the two subsequent exposures of the now cured RBC were significantly lower, but again the PinkWave used for 10 s produced the greatest overall temperature increase (Table 8 and Figure 12).

Tabela 6 – Means and standard deviations (SD) of transmitted power (mW) through the empty mold and through the mold filled with cured RBC, difference (mW) and percentage reduction (%). Note the low percentage reduction (%) for PinkWave.

	Potência através do molde vazio (mW)		**Potência através do molde preenchido com RBC (mW)**		**Diferença (mW)**	**Porcentagem da redução (%)**
	Média	DP	Média	DP		
Filtek Universal + ML	1538	45.1	347	2.4	1191 [A]	77 [A]
Tetric Evoceram + ML	1538	45.1	401	3.7	1136 [B]	74 [BC]
Transcend + ML	1538	45.1	542	0.6	995 [C]	65 [H]
Filtek Universal + VG Xtra	1268	5.9	418	1.9	850 [D]	67 [F]
Filtek Universal + PC 3 s Cure	1108	15.0	280	5.4	828 [E]	75 [B]
Tetric Evoceram + PC 3 s Cure	1108	15.0	315	0.7	793 [F]	72 [D]
Tetric Evoceram + VG Xtra	1268	5.9	484	3.1	784 [F]	62 [J]
Transcend + PC 3 s Cure	1108	15.0	393	1.6	715 [G]	65 [H]
Transcend + VG Xtra	1268	5.9	555	2.8	713 [G]	56 [K]
Filtek Universal + DC	535	4.3	143	0.9	392 [H]	73 [C]
Filtek Universal + PW	875	7.8	489	0.8	386 [H]	44 [L]
Tetric Evoceram + DC	535	4.3	160	0.3	375 [I]	70 [E]
Filtek Universal + VG Standard	529	2.6	180	0.6	349 [J]	66 [G]
Transcend + DC	535	4.3	198	0.9	337 [K]	63 [I]
Tetric Evoceram + PW	875	7.8	541	0.7	334 [K]	38 [M]
Tetric Evoceram + VG Standard	529	2.6	206	1.2	323 [L]	61 [J]
Transcend + PW	875	7.8	553	0.9	322 [L]	37 [N]
Filtek Universal + PC High	408	4.5	103	1.1	305 [M]	75 [B]
Transcend + VG Standard	529	2.6	235	0.6	294 [N]	56 [K]

Tetric Evoceram + PC High	408	4.5	115	0.7	293 [N]	72 [D]
Transcend + PC High	408	4.5	144	0.5	264 [O]	65 [H]

Tabela 7 – Exposure time (s), average power (mW) and standard deviation (SD), irradiance (mW/cm²) and radiant exposure (J/cm²) values delivered to the RBCs in the 6 mm diameter Delrin mold..

Fotopolimerizador	**Tempo de Exposição (s)**	**Potência (mW)**		**Irradiância (mW/cm²)**	**Exposição Radiante (J/cm²)**
		Mean	**SD**		
Monet	1	1538	45.1	5441	5.4
PowerCure	3	1108	15.0	3921	11.8
Valo Grand	3	1268	5.9	4485	13.5
PowerCure	10	408	4.5	1445	14.5
Monet	3	1538	45.1	5441	16.3
Valo Grand	10	529	2.6	1873	18.7
DeepCure	10	535	4.3	1894	18.9
PinkWave	10	875	7.8	3096	31.0

Logarithmic regression analyses examined the relationship between the combined exothermic and LCU temperature rises and either the Power (Watts) or the Energy (Joules) delivered by the LCUs to the RBCs. For all the RBCs, Figure 13 shows no correlation between the power output from the LCUs and the temperature rise (R2 = 0.0067 for Filtek Universal, R^2 = 0.0177 for Tetric Evoceram and R^2 = 0.0027 for Transcend). However, there was an excellent positive correlation between the energy delivered from the LCU and the temperature rise at the bottom of the RBC (R^2 = 0.827 for Filtek Universal, R^2 = 0.763 for Tetric Evoceram and R^2 = 0.721 for Transcend).

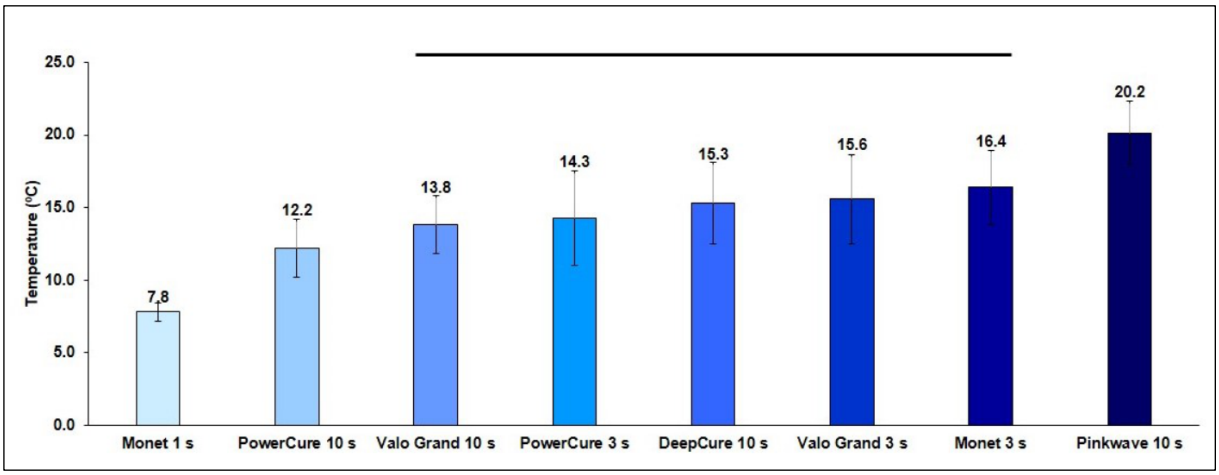

Figure 12 - General ncrease in mean temperature (ΔT) as RBCs were exposed to different exposure modes. The line over the columns shows where there was no significant difference between exposure modes (Scheffe post-hoc test p ≥ 0.05). Note that the greatest increase in temperature occurred using PinkWave for 10 s.

Table 9 reports the mean and standard deviation time (s) the RBCs took to reach their respective maximum temperatures and then return to 37°C. After the initial first exposure, Filtek Universal exposed to the Deep Cure for 10 s (11.8 s ± 1.6) and Transcend exposed to the PinkWave for 10 s (11.0 s ± 0.5) took the longest to reach their maximum temperature. The RBCs exposed to the PinkWave used for 10 s took the longest time to return to 37°C (32.4 s ± 3.5 for Transcend, 29.6 s ± 3.5 for Filtek and 29.0 s ± 3.0 for Tetric Evoceram).

The exothermic heat contribution from each RBC was calculated by subtracting the third temperature rise (ΔT3) from the first temperature rise (ΔT1). Figure 14 shows the exothermic heat contribution for each group. Except for Monet used for 1 s (1.4°C ± 0.3), the highest exothermic heat contributions from the RBC were found at the bottom of Transcend (temperatures ranging between 8.2°C ± 0.7 and 11.2°C ± 1.0).

Tabela 8 – Mean temperature increase and standard deviation (SD) in RBCs caused by different LCUs and exposure times ranked from highest to lowest temperature rise.

RBC	Fotopolimerizador e tempo de exposição	ΔT1			ΔT2			ΔT3		
		Média	DP		Média	DP		Média	DP	
Transcend	**PW 10 s**	22.8	1.1	Aa	14.1	0.6	Ab	14.0	0.6	Ab
Transcend	**VG 3 s**	19.5	1.6	ABa	8.8	0.9	BCDEFb	8.3	0.9	BCDEFb
Transcend	**ML 3 s**	19.5	0.7	ABa	11.2	1.0	ABCDb	11.2	0.8	ABCDb
Tetric Evoceram	**PW 10 s**	19.2	1.0	ABCa	13.6	0.4	ABb	13.5	0.7	ABb
Transcend	**DC 10 s**	18.8	1.4	ABCDa	9.8	0.7	ABCDEb	9.8	0.7	ABCDEb
Filtek Universal	**PW 10 s**	18.5	0.7	ABCDEa	12.1	0.7	ABCb	12.0	0.7	ABCb
Transcend	**PC 3 s**	18.4	1.2	ABCDEFa	8.9	0.8	ABCDEFb	8.8	0.5	BCDEFb
Transcend	**VG 10 s**	16.3	0.9	BCDEFGa	8.1	0.5	CDEFb	8.2	0.6	CDEFb
Tetric Evoceram	**ML 3 s**	15.0	1.6	BCDEFGHa	8.7	1.8	BCDEFb	8.3	1.6	BCDEFb
Filtek Universal	**ML 3 s**	14.7	1.4	BCDEFGHa	7.9	1.0	CDEFb	7.6	0.8	CDEFb
Transcend	**PC 10 s**	14.5	0.8	CDEFGHa	6.2	0.2	DEFb	6.1	0.1	DEFb
Tetric Evoceram	**DC 10 s**	13.9	0.9	DEFGHa	8.4	0.4	CDEFb	8.1	0.4	CDEFb
Filtek Universal	**VG 3 s**	13.6	0.4	DEFGHa	6.0	0.5	EFb	5.8	0.4	EFb
Tetric Evoceram	**VG 3 s**	13.6	0.8	EFGHa	6.4	0.4	DEFb	6.3	0.4	DEFb
Filtek Universal	**DC 10 s**	13.2	1.5	FGHIa	7.2	0.9	CDEFb	6.8	1.1	DEFb
Filtek Universal	**VG 10 s**	12.7	1.1	GHIJa	6.0	0.3	EFb	6.1	0.4	DEFb
Tetric Evoceram	**VG 10 s**	12.4	0.3	GHIJKa	6.6	0.3	DEFb	6.6	0.3	DEFb
Filtek Universal	**PC 3 s**	12.2	1.2	GHIJKa	5.4	0.7	EFb	5.5	0.6	EFb
Tetric Evoceram	**PC 3 s**	12.1	1.3	GHIJKa	6.0	0.3	EFb	6.1	0.5	DEFb
Filtek Universal	**PC 10 s**	11.2	1.6	GHIJKa	5.2	0.7	EFb	5.2	0.7	EFb
Tetric Evoceram	**PC 10 s**	10.9	1.1	HIJKa	5.6	0.5	EFb	5.5	0.3	EFb

Tetric Evoceram	**ML 1 s**	8.2	0.7	IJKa	3.9	0.6	Fa	4.0	0.8	Fa
Transcend	**ML 1 s**	7.7	0.8	JKa	6.2	0.8	DEFa	6.3	0.9	DEFa
Filtek Universal	**ML 1 s**	7.5	0.2	Ka	3.8	0.2	Fa	3.9	0.4	Fa

Means followed by similar superscript letters (lower case: within the row; upper case: within the column) are not significantly different (Scheffe post-hoc test, $p \geq 0.05$).

Tabela 9 – Mean and Standard Deviation (SD) of the time (s) taken for the temperature to reach the maximum temperature (T1 peak) and return to 37 ºC.

RBC	Fotopolimerizador e tempo de exposição	Tempo para atingir a temperature máxima (s)			Tempo para retornar para 37ºC (s)		
		Média	DP		Média	DP	
Filtek Universal	**DC 10 s**	11.8	1.6	A	19.1	3.5	BCDEF
Transcend	**PW 10 s**	11	0.5	A	32.4	3.5	A
Tetric Evoceram	**PC 10 s**	10.8	1.0	A	12.2	2.6	EF
Filtek Universal	**VG 10 s**	10.7	1.3	A	22.3	4.5	ABCDE
Filtek Universal	**PW 10 s**	10.6	1.0	A	29.6	3.5	AB
Tetric Evoceram	**PW 10 s**	10.5	0.4	A	29	3.0	ABC
Tetric Evoceram	**VG 10 s**	10.4	1.0	A	20	3.7	BCDEF
Tetric Evoceram	**DC 10 s**	10.3	0.8	A	16.9	1.5	DEF
Filtek Universal	**PC 10 s**	10.2	0.6	A	12.7	5.0	EF
Transcend	**DC 10 s**	9.7	1.0	A	22.6	2.2	ABCDE
Transcend	**VG 10 s**	9	1.5	A	24.6	4.3	ABCD
Transcend	**PC 10 s**	8.5	1.7	AB	20	3.6	BCDEF
Tetric Evoceram	**ML 3 s**	5.1	0.9	BC	19.9	2.0	BCDEF
Tetric Evoceram	**VG 3 s**	5.1	0.8	BC	22.2	1.2	ABCDE
Filtek Universal	**VG 3 s**	4.9	0.5	C	22	0.9	ABCDE
Filtek Universal	**PC 3 s**	4.7	0.4	C	17.7	4.3	CDEF
Tetric Evoceram	**PC 3 s**	4.7	1.3	C	16.4	2.2	DEF
Transcend	**ML 3 s**	4.6	0.4	C	26.9	2.2	ABCD
Transcend	**ML 1 s**	4.6	0.4	C	10.3	1.5	F

Filtek Universal	**ML 3 s**	4.4	0.4	C	24.5	2.2	ABCD
Transcend	**PC 3 s**	4	0.9	C	23.5	2.3	ABCDE
Tetric Evoceram	**ML 1 s**	3.6	0.4	C	9.4	2.1	F
Filtek Universal	**ML 1 s**	3.4	0.4	C	10.1	1.2	F
Transcend	**VG 3 s**	3.2	0.6	C	26	2.0	ABCD

Means followed by similar superscript letters (lower case: within the row; upper case: within the column) are not significantly different (Scheffe post-hoc test, $p \geq 0.05$).

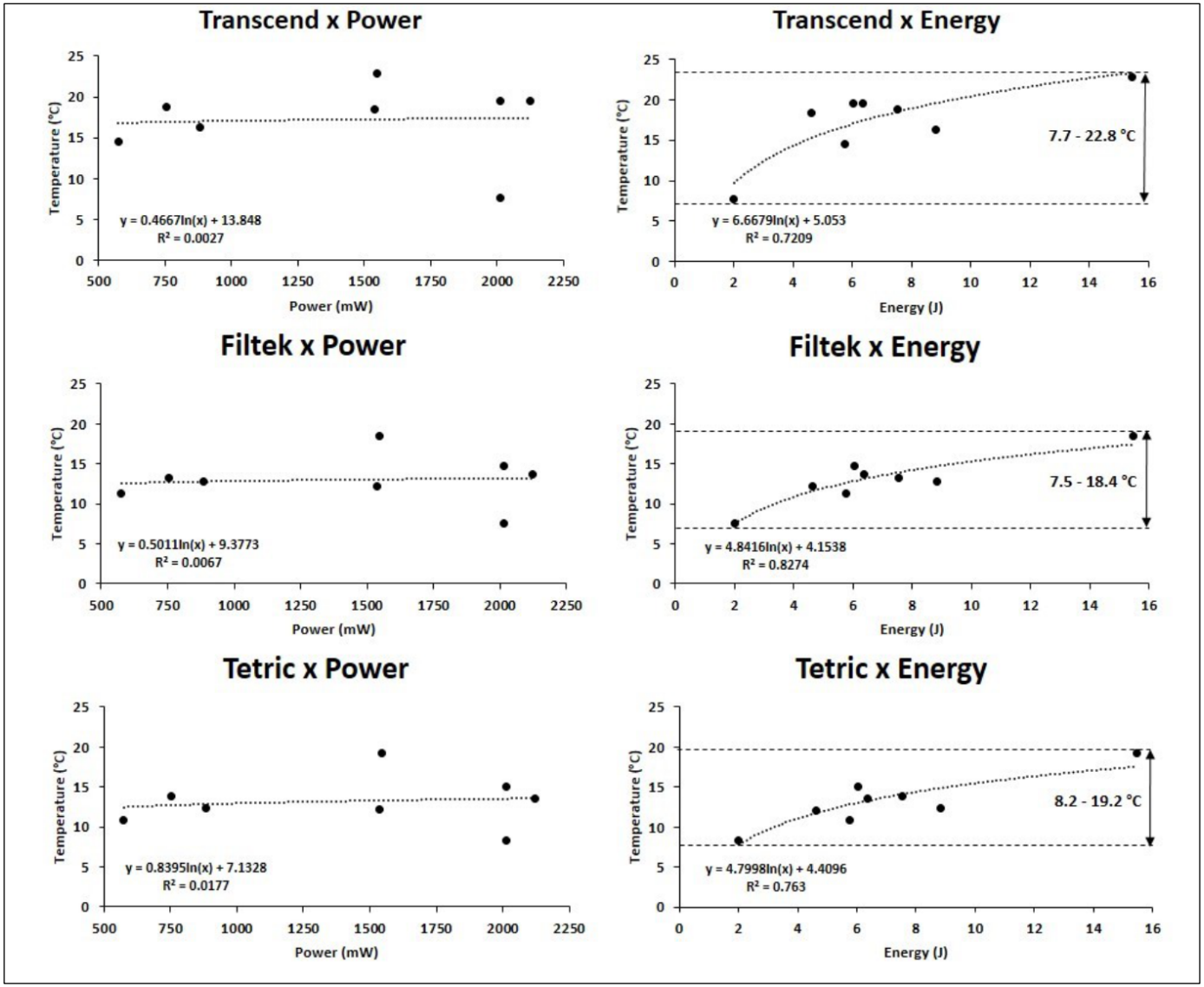

Figura 13 - Semi-logarithmic regression for temperature rise of Transcend, Filtek Universal and Tetric Evoceram RBCs for different exposure modes when analyzing the different effects of power and energy from the LCUs.

Overall, when comparing the RBCs, irrespective of which LCU was used, Transcend produced the greatest ($p < 0.05$) exothermic temperature rise (8.1°C ± 2.8). However, Scheffe's post hoc test found no significant difference ($p = 0.4935$) between the overall exothermic temperature increases of Filtek Universal (6.4°C ± 1.4) and Tetric Evoceram (5.8°C ± 1.0).

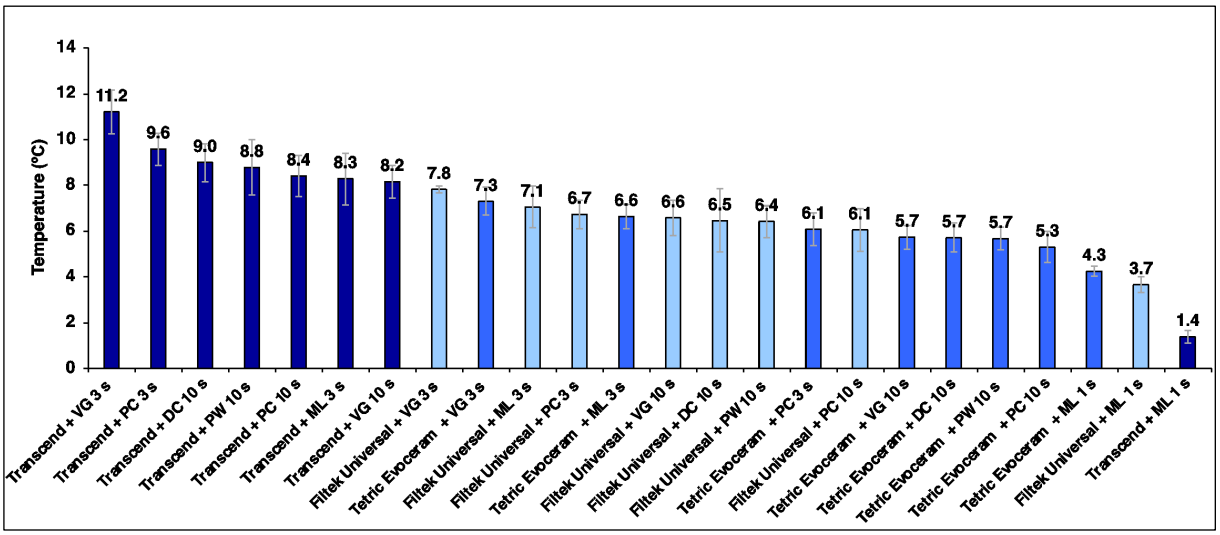

Figura 14 - Contribution of the exothermic reaction to the temperature increase (Mean ± Standard Deviation) caused by different LCUs and exposure times.

4.1.4.4 Vickers micro-hardness (VH)

Table 10 reports the mean and standard deviation VH values at the top and bottom surfaces of the 2 mm thick specimens after they had received three light exposures. The bottom:top ratio for each RBC and LCU was calculated by dividing the bottom to the top values for the same condition of RBC and LCU. In addition, the bottom:top ratio for each RBC was calculated based on the greatest mean VH value at the top achieved using any LCU for that RBC, divided by the bottom VH value. Scheffe's post hoc test detected a significant difference between the surfaces for Filtek Universal and Tetric Evoceram ($p = 0.0015$). No difference between top and bottom was detected for Transcend ($p = 0.3594$). Although a significant difference was detected for Filtek Universal and Tetric Evoceram, the percentage differences between the top and bottom were low (Filtek Universal = 3.3% and Tetric Evoceram = 7.6%).

Figure 15 shows the mean VH values for each exposure mode used in the study, regardless of the RBC used. Overall, the Valo Grand used for 10 s produced the highest VH values, whereas the Monet, used for both 1 s and 3 s, achieved the lowest

VH values. Although the specimens were harder after a 3-s exposure, there were no significant differences between the 1 and 3-s exposure (p = 0.1825).

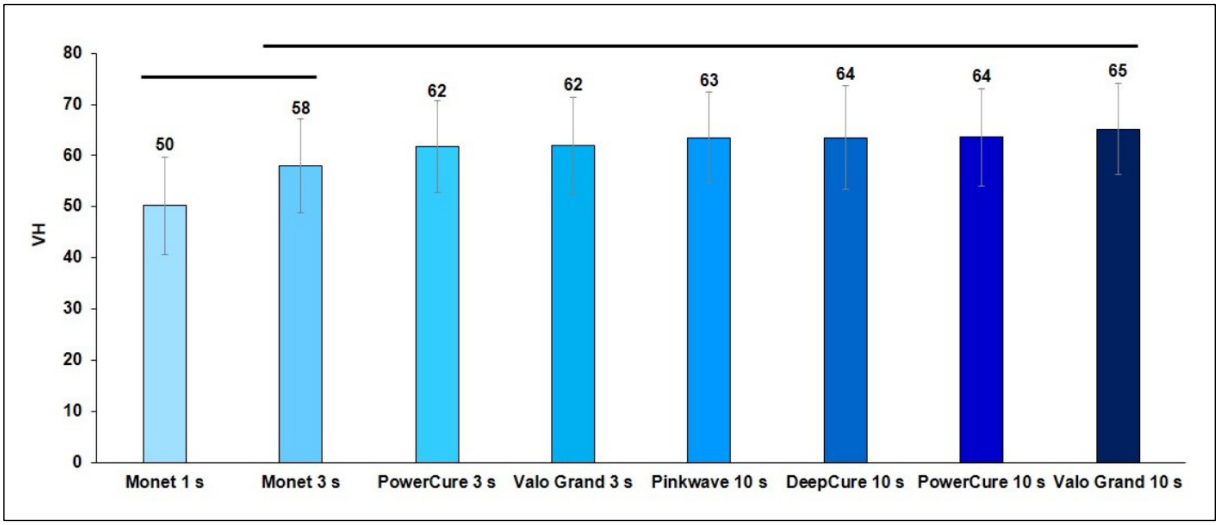

Figura15 - Mean ± standard deviation (error bars) of VH values for all RBCs for each exposure mode. Lines over columns show where there was no significant difference between different exposure modes (Scheffe post-hoc test p ≥ 0.05).

Tabela 10 – Mean ± standard deviation (SD) Vickers hardness (VH) on the top and bottom surfaces of RBCs after three repeated exposures using the different LCUs and exposure times. Top/bottom ratios for each RBC and LCU and top/bottom ratios for each RBC based on the highest average VH achieved at the top.

RBC, fotopolimerizador e tempo de expoisção (s)	**Topo - VH**		**Base -VH**		**Razão Topo/Base para cada RBC e fotopolimerizador**	**Razão Topo/Base para cada RBC baseada na maior VH no topo**
	Mean	**SD**	**Mean**	**SD**		
Transcend + VG 10 s	75.0	2.2	73.5	2.3	0.98	0.98
Transcend + DC 10 s	74.5	0.9	71.7	2.0	0.96	0.96
Transcend + PC 10 s	74.5	1.2	72.3	1.7	0.97	0.96
Transcend + PW 10 s	74.3	0.8	71.9	2.7	0.97	0.96
Transcend + VG 3 s	72.7	1.8	72.7	0.9	1.00	0.97
Transcend + PC 3 s	69.9	1.2	67.5	2.4	0.97	0.90
Filtek Universal + DC 10 s	68.9	1.6	65.4	1.5	0.95	0.95
Filtek Universal+ PC 3 s	68.1	2.0	65.0	1.9	0.96	0.94
Filtek Universal + VG 10 s	68.0	1.2	66.3	2.2	0.97	0.96
Filtek Universal+ PC 10s	67.1	1.0	64.7	1.4	0.96	0.94
Filtek Universal + ML 3 s	65.7	2.1	64.4	2.1	0.98	0.93
Filtek Universal + PW 10 s	64.9	2.4	64.8	1.6	1.00	0.94
Filtek Universal+ VG 3 s	63.8	3.2	60.0	1.6	0.94	0.87
Transcend + ML 3 s	63.1	3.0	63.1	2.0	1.00	0.84
Filtek Universal + ML 1 s	61.1	1.1	59.5	2.3	0.97	0.86
Tetric + VG 10 s	56.7	3.0	51.5	1.9	0.91	0.91
Tetric + PC 10 s	54.3	1.3	48.5	2.0	0.89	0.85
Tetric + VG 3 s	54.3	1.9	47.9	1.7	0.88	0.84
Tetric + PW 10 s	54.0	2.0	51.0	1.1	0.95	0.90
Transcend + ML 1 s	52.7	1.6	51.8	2.3	0.98	0.69

Tetric + PC 3 s	52.6	3.1	47.0	1.0	0.89	0.83
Tetric + DC 10 s	51.9	0.7	48.9	3.4	0.94	0.86
Tetric + ML 3 s	45.4	3.0	45.8	1.5	1.01	0.81
Tetric + ML 1 s	39.4	1.5	37.0	2.3	0.94	0.65

4.1.5 Discussion

This study evaluated different types of LCUs and exposure times: one curing laser, one monowave LED and three polywave LEDs. Thus, it was not unexpected that the five LCUs would not deliver similar irradiances and radiant exposures (Figure 10 and Table 7). However, the magnitude of the differences was unexpected. There was a threefold difference in power (408–1538 mW), and a sixfold range in the radiant exposure delivered (5.4–31.0 J/cm^2). Therefore, the first hypothesis that the five LCUs would not deliver the same amount of energy (Joules) during light-curing was accepted. Unfortunately, many dentists do not recognize how large these differences are, and many use the same exposure time to photo-cure everything (ERNST et al., 2018; WATTS et al., 2019; FRAZIER et al., 2020).

The second hypothesis that the combined effects of the light from the LCUs and the exothermic reaction would not produce the same temperature increase at the bottom of the three RBCs was accepted. In the present study, the PinkWave used for 10 s caused a significant increase in the temperature at the bottom of the RBCs during photo-activation (Figure 12). This can be attributed to the higher amount of energy delivered and the different wavelengths emitted by this LCU. The spectral analysis reported in Figure 10 shows the four wavelength bands from the PinkWave: of note, one wavelength band had an emission peak at 631 nm and another was at 860 nm in the near-infrared region. Light in these regions can cause a heating effect. Figure 11 shows the transmission spectrum (mW/nm) from the PinkWave and Valo Grand through the empty molds and through the molds filled with each RBC. Note that for the PinkWave, there was a significant attenuation of the violet light at 410 nm (λ1) and the blue light at 471 nm (λ2) when light passed through the RBCs, which cannot be seen for the other two bands wavelengths with peaks at 631 nm (λ3) and 860 nm (λ4). Thus, Figure 11 shows that most of the red and near-infrared light penetrated through the RBC. This explains why the reduction (%) in power from the Pinkwave (Table 6) was much less than the other LCUs. This infrared radiation from the PinkWave is likely responsible for the larger increase in temperature observed when this LCU was used (Table 8).

When analyzing the Logarithmic Regression for the RBCs temperature rise recordings for Power and Energy (Fig. 5), only the Energy (Joules) delivered had a significant positive correlation (R2 = 0.827 for Filtek, R2 = 0.763 for Tetric Evoceram

and R2 = 0.721 for Transcend) with the temperature rise in the RBCs. The results from previous studies support that it is the radiant energy that mainly determines temperature rise and not the irradiance (PAR et al., 2019). The greater the amount of energy delivered, the greater the temperature rise. In contrast, no correlation was found between the Power (Watts) and the Temperature (°C). The greater the amount of energy delivered, the greater the temperature rise. Thus, despite delivering the highest power (1,538 mW) and the highest irradiance (5,441 mW/cm^2) to the RBCs (Table 7), using the Monet Laser produced the smallest temperature increase. Since the energy delivered is related to the exposure time, the short, 1-s exposure delivered the lowest low radiant exposure values (5.4 J/cm^2) when the Monet Laser was used. This likely explained why the Monet Laser produced the lowest temperature increase in the RBCs. However, this was likely because the RBCs were not as well photo-activated. Of note, the exothermic temperature rises (Figure 14) when the Monet laser was used were also low probably because there was less polymerization of the RBCs. This is supported by the observation that the Monet Laser used for 1 s produced the lowest hardness values in the RBCs (Table 10). Thus, photo-curing most RBCs for 1 or 3 s does not appear advisable because, in addition to the observation that less energy was delivered when the LCUs were used for shorter times, the polymerization shrinkage forces may develop more rapidly (PAR et al., 2020). This may cause increased debonding between the tooth and the RBC to occur. Therefore, clinicians should only use a fast-curing protocol with RBCs that use high-yielding photoinitiators and that have been specifically designed to be photo-cured in 1 to 3 s (GAROUSHI; LASSILA; VALLITTU, 2021; ROCHA et al., 2022).

The samples were made in identical 2 mm thick Delrin rings, and this thickness did not exceed the manufacturer's instructions for the RBCs. The specimens were weighed to verify that the RBCs in each group were almost identical, and there was only ± 0.005 g (4%) difference in the weight of the RBCs in each group. Thus, any differences in the temperature could only be attributed to the light or to the RBC, and not to any differences in the amount of RBC in the specimens. The decision to use a block of cured RBC was made to provide reflective and thermal backgrounds similar to the cavity floor instead of using white filter paper or a glass slab. Table 8 shows that the choice of RBC affected the temperature rise. Thus, the third hypothesis that there would be no differences in the exothermic temperature rise produced by different RBCs was rejected. Due to the COVID pandemic, the experimental RBC codenamed

Transcend has not yet been released to the public, and this is the first report about this experimental RBC from Ultradent. Although some studies show that fillers are chemically inert and do not affect the temperature rise (AKARSU; AKTUG KARADEMIR, 2019) and that there is a high correlation between matrix ratio and temperature rise (HORI et al., 2020), the highest temperature rise occurred in Transcend UB, regardless of the exposure mode used, even though the manufacturer claims that Transcend had the highest filler content (77.5% per weight – Table 1 among the RBCs tested. This can be explained by the greater translucency (Table 6) of the experimental RBC, Transcend, which allows more light to pass through the RBC. This results in a greater temperature rise (LEMPEL et al., 2021) at the bottom and better photo-activation at the bottom (Table 10) of this RBC, but this also produces more exothermic heat from the more complete polymerization reaction (Table 8 and Figure 14).

If the same exposure time is used, the LCU that delivers a high irradiance can cause a high thermal transfer and increase the risk of pulpal damage (KIM et al., 2017). When the irradiance is the same, the longer the exposure time, the greater radiant exposure delivered Consequently, there is also a greater the risk of pulpal damage. Thus, it is important to know the exposure time and the radiant exposure received by the specimens. Unfortunately, most contemporary research publications lack an adequate description of the light received by the RBC specimens (WATTS et al., 2019). Despite these limitations, previous studies have reported that temperature increases of 5.5°C or more in the pulp can lead to irreversible pulp damage (ZACH; COHEN, 1965; LYNCH et al., 2018). The present study found that the combination of the light and the exothermic reaction produced an increase in the temperature at the bottom of all three RBCs as they photocured that was greater than 5.5°C. Thus, all the RBCs could potentially cause some thermal damage to the pulp when they were photo-cured. However, hopefully, pulpal damage should not happen because the dentin between the RBC and the pulp is an excellent thermal insulator (LIPSKI et al., 2020). Reducing the exposure time or the irradiance may reduce the risk of tissue damage, since less energy is delivered. However, Tables 6 and 10 show this can adversely affect the mechanical properties of the RBC (MOUHAT et al., 2017). Therefore, it seems preferable to use a 10-s exposure time from a conventional LCU to deliver an adequate amount of energy, produce an adequately cured RBC, and an acceptable temperature rise (PAR et al., 2019).

Figure 1 and Table 8 show that the photo-curing reaction is exothermic, and this exothermic component is RBC dependent (NILSEN et al., 2020). Thus, the temperature increase is a cumulative result of this exothermic reaction and the exposure to light from the LCU. In contrast, for the post-cured RBCs (T3 in Fig. 1 and Table 8), the temperature increase was only a result of the effect of the light from the LCU (NILSEN et al., 2020). Therefore, the fourth hypothesis that this exothermic heat contribution to the temperature increase would be less than 5.5°C (ZACH; COHEN, 1965) was rejected. Except for these groups: Transcend UB + Monet used for 1 s, Filtek Universal A2 + Monet used for 1 s, Tetric Evoceram A2 + Monet used for 1 s Tetric Evoceram A2 + PC 10 s, all the other combinations of LCU and RBC produced temperature increases that were greater than the 5.5°C threshold (Figure 14). Transcend generated the highest temperature values using the other 4 LCUs (Table 8) and consistently had the greatest exothermic temperature rise (Figure 14). The reader can easily test the results by placing some RBC on the back of the hand and then light-curing the RBC. The RBC gets hot. When this is repeated using the cured RBC, the temperature rise is less.

According to all the manufacturers' instructions, all the exposure times used in the study should have adequately photo-activated the 2 mm thick specimens of all the RBCs tested. Transcend was the most transparent RBC (Table 6), and there were no significant differences in the VH between the top and bottom surfaces (Table 10). After the RBCs had received three repeated exposures, the bottom:top hardness ratios of Transcend were 0.90 or greater using four of the five LCUs. However, even when the Monet was used three times, for a total of 9 s, the bottom:top ratio was only 0.84, and it was only 0.65 when three 1-s exposures were used with the Monet. This may occur because the extent of polymerization has an exponential relationship with the amount of transmitted light received by the RBC (PAR et al., 2018). Since there was so much more light at the bottom of the RBC, the RBC was well photo-activated at the bottom. Finally, when analyzing the LCUs, regardless of the RBC used and even after three repeated exposures, the Monet Laser produced the lowest VH values in the RBCs (Figure 15 and Table 10). Although the Monet Laser delivered a high irradiance of 5,441 mW/cm^2 at 451 nm, the radiant exposure delivered to the RBCs in the 1-s exposures was only 5.4 J/cm^2. This was less than from the other LCUs (Table 7). This 2 mm increment of RBC should receive approximately 16 J/cm^2 of radiant exposure (ANUSAVICE et al., 2013). Thus, it is not surprising that when the Monet was used for

1 s, the Vickers Hardness values were low. When comparing the bottom:top VH values from the top and bottom of the RBCs, there were significant differences between the surfaces for Filtek Universal and Tetric Evoceram ($p = 0.0015$) despite the low difference between
the bottom and bottom values (Table 7). When the VH values at the bottom for each RBC were compared against the LCU that produced the highest value at the top for that specific RBC, the differences in the bottom:top ratios became even more apparent (Table 10). Thus, because not all of the LCUs tested produced the same hardness values at the top and bottom of the RBCs, the fifth hypothesis of the study was rejected. Table 10 also highlights the importance of using the highest value reached at the top surface under any condition for that RBC when determining the overall bottom:top ratios.

The clinicians should be aware that the choice of the LCU or RBC can affect the temperature rise of the bottom of RBCs by the energy delivered from the LCU (Figure 13) and that there can be a significant exothermic contribution from the RBC itself (Figure 14). This becomes more important when placing restorations in children with deep cavities because the amount of thermal transfer to the pulp is affected by the remaining dentin thickness (ARMELLIN et al., 2016); the thinner the thickness of dentin remaining, the greater the thermal transfer. Therefore, to prevent irreversible pulpal damage (ZACH; COHEN, 1965), it is recommended to blow a stream of air over the tooth during exposure (ZARPELLON et al., 2019) and to use a cavity liner (LAKHANI et al., 2018).

Although this was a well-controlled study using known volumes of RBC exposed to well-defined amounts of light, it is important to note that the study did not consider other factors that could affect the temperature rise. Future in vitro or in vivo studies should examine the temperature rise in teeth, the effect of dentin thickness (AKARSU; AKTUG KARADEMIR, 2019) and the consequences of different. pulpal fluid flow rates (BRAGA et al., 2019).

4.1.6 Conclusion

Dentists should be aware that the choice of LCU, the exposure time, and the exothermic contribution from the RBC will affect the temperature rise and hardness values. Within the limitations of this in vitro study, it was concluded that: (1) the

energies delivered (J) from the five LCUs were not the same, and different LCUs produced different changes in the temperature as the RBC is photoactivated; (2) the temperature rise is related to the amount of energy delivered and not to the power or the irradiance from the LCU; (3) the combined effect of the light from the LCU and the exothermic reaction of the RBC produced an increase in the temperature that was greater than 5.5℃. The PinkWave caused a significant increase in the temperature of the RBC due to the amount of energy delivered and the energy delivered in the near-infrared region. The Monet Laser used for 1 s delivered the lowest radiant exposure and produced the smallest temperature rise and lowest Vickers hardness values; (4) the translucency of RBCs affects the temperature rise and hardness.

4.2 ARTIGO 2: *IN VITRO* TEMPERATURE CHANGES IN THE PULP CHAMBER CAUSED BY LASER AND QUADWAVE LED-LIGHT CURING UNITS

Cristiane Maucoski[1,2]
Richard Bengt Price[1]
Cesar Augusto Galvão Arrais[2]
Braden Sullivan[1]

[1] Department of Dental Clinical Sciences, Dalhousie University, Halifax, Nova Scotia, B3H 4R2, Canada.
[2] Department of Restorative Dentistry, State University of Ponta Grossa, Ponta Grossa, Parana, Brazil.

Revista: Odontology
Aceito: 06 de dezembro de 2022
Publ: 19 de dezembro de 2022
DOI: 10.1007/s10266-022-00780-y

4.2.1 Abstract

The study evaluated the pulp temperature (PT) increase in Class I and V preparations when exposed to the Monet Laser (for 1 and 3 s), the PinkWave (for 3 and 10 s), the Valo Grand (for 3 and 10 s), the PowerCure, (for 3 and 10 s) and the

SmartLite Pro (for 10 s). Non-retentive Class I and Class V cavities were prepared in one molar fixed in an acrylic plate and positioned in a warm water bath. The PT baseline was kept at 32 °C to simulate physiological conditions. Two T-type thermocouples were inserted through the roots into the pulp chamber in two positions: close to the pulp horn and the buccal wall close to the Class V cavity. The water flow was adjusted to 0.026 mL/min, and real-time temperature data were collected every 0.5 s. PT measurements were made with the tip of the LCU 0 and 6 mm away from the tooth surface. The radiant exitance (mW/cm^2) and radiant exposure (J/cm^2) were calculated. One-way ANOVA compared the effect of the pulpal flow, and ΔT values were subjected to two-way ANOVA, followed by Scheffe's post hoc tests. The Monet Laser used for 3 s and the PinkWave used for 10 s produced the greatest PT rise in the Class I cavity. The simulated pulpal flow did not influence the PT rise. Overall, cavities exposed at the 0 mm distance had higher ΔT values than groups at 6 mm distance. The placement of a rubber dam for Class V restorations may prevent positioning LCUs directly over the cavity, which may affect the rise in PT.

4.2.2 Introduction

Using Light-Emitting Diodes (LEDs) as the light source in Light Curing Units (LCUs) has become the most popular method to photocure resin-based composites (RBCs) (JANDT; MILLS, 2013). These LCUs have a long lifespan, can be battery-operated, and can deliver a high radiant exitance (irradiance) at the light tip (MILLY; BANERJEE, 2018). Some LED units produce one well-defined band of wavelengths (monowave) in the blue range and are designed to activate the camphorquinone photoinitiator used in most dental RBCs. To activate a broader range of photoinitiators (RUEGGEBERG, F. A. et al., 2017), some brands of LCU emit several sharply defined emission bands that are usually in the violet and blue range (multi-peak or polywave). A new LED LCU has what the manufacturer calls Quadwave technology. This unit delivers four distinct bands of wavelengths: violet, blue, and also in the infrared and near-infrared (NIR) (APEX).

Lasers have also been used to photocure dental resins, but their high cost, larger size, and technique sensitivity have limited their use (KNEZEVIC et al., 2007). However, recently blue diode lasers that deliver light in the 445-455 nm region have been suggested as an alternative light source (DROST et al., 2019; KOUROS et al.,

2020). One portable, compact, and battery-operated blue laser diode LCU (Monet, AMD Lasers) delivers a sharply defined spectral emission with a high irradiance at 450 nm. The manufacturer claims that dental RBCs up to 2 mm thick can be adequately photocured in a short 1-s exposure using this laser-based LCU (AMD, 2021). In addition, since it is a laser, it can deliver a high irradiance even as the distance from the LCU tip increases [6]. A recent study showed that this laser based LCU emitted the highest power, radiant emittance and delivered the greatest irradiance among the LCUs tested. However, although this laser could photocure the top surface of all 10 of the RBCs tested (ROCHA et al., 2022), it produced the shallowest depth of cure compared to conventional LED units used for 10s.

Using an LCU that delivers irradiance values greater than 2,000 mW/cm² may reduce the chair time spent light curing and increase patient comfort (ALMEIDA et al., 2021). However, such high radiant exitance values have become a concern, since they may also increase the risk of damaging the soft tissues and pulp (MOUHAT et al., 2017). The temperature rise inside the pulp chamber is related to the amount of energy (Joules) delivered from the LCU and the exothermic reaction from the RBC as it polymerizes (ARMELLIN et al., 2016). Thus, this temperature rise depends on the brand of RBC, the rate at which it polymerizes, the power (W), the irradiance received (mW/cm²), the wavelengths of light delivered, the exposure time, and amount of energy delivered (PRICE; FERRACANE; SHORTALL, 2015; BALESTRINO et al., 2016; MOUHAT et al., 2017; RUEGGEBERG, F. A. et al., 2017; AKARSU; AKTUG KARADEMIR, 2019; PAR et al., 2019; MOUHAT et al., 2021; WANG et al., 2021). In addition, the thickness of the dentin floor, the distance from the LCU tip to the tooth, and the blood flow through the pulp can influence the change in PT (PRICE et al., 2000; SAVAS et al., 2014; AKARSU; AKTUG KARADEMIR, 2019; BRAGA et al., 2019; PRICE et al., 2020).

The characteristics of LCUs play an important role in the increase in pulpal temperature (PT) (OBERHOLZER et al., 2012), and a PT rise of more than 5.5 ºC is thought to be harmful to the pulpal tissues (ZACH; COHEN, 1965). Some studies have investigated the temperature rise in soft tissues (SPRANLEY et al., 2012; MAUCOSKI et al., 2017) and inside the pulp *in vitro* (OBERHOLZER et al., 2012; VINALL et al., 2017; AKARSU; AKTUG KARADEMIR, 2019; BRAGA et al., 2019; LEE; LEE, 2021; LEMPEL et al., 2021) and some *in vivo* (RUNNACLES et al., 2019; ZARPELLON et al., 2019; GROSS et al., 2020; ZARPELLON et al., 2021). Some *in vitro* studies have

tried to simulate the blood flow through the tooth to better simulate an *in vivo* environment (AKARSU; AKTUG KARADEMIR, 2019; BRAGA et al., 2019; RUNNACLES et al., 2019). However, the blood flow through the tooth is affected by the presence of pulpal inflammation (BERGGREEN; BLETSA; HEYERAAS, 2007), tooth preparation (SUKAPATTEE et al., 2016), by the use of local anesthesia (ODOR; PITT FORD; MCDONALD, 1994; VONGSAVAN et al., 2019), and also where the local anesthetic injection has been deposited (ZHENG et al., 2018). Thus, the actual flow rate inside the pulp is highly variable.

Although there is some information in the literature about the temperature rise of an RBC when a blue diode laser (445 nm) was used 'off label' (DROST et al., 2019; KOUROS et al., 2020), currently, there is no information regarding the PT rise that occurs when using a blue diode laser, or the new Quadwave LCU which emits infra-red and near infra-red wavelengths of light. Therefore, this study evaluates the *in vitro* PT rise in one molar tooth with Class I and V preparations when exposed to a blue diode laser, a Quadwave LCU, and conventional LCUs under different light exposure conditions and exposure times. The null research hypotheses are: (1) there would be no differences in the rise in the PT produced by different LCUs; (2) a simulated pulpal fluid flow would not influence the rise in the PT; and (3) increasing the distance between the LCU tip and the tooth surface to 6 mm will not affect the PT.

4.2.3 Materials and Methods

4.2.3.1 Spectral analysis of the light emitted by the LCUs

The study used one laser diode, one monowave, and three multi-peak LED LCUs. The brand names, manufacturers, serial numbers and manufacturer's information are reported in Table 3. The spectral radiant powers from the LCUs were measured using a fiberoptic spectroradiometer (Flame-T, Ocean Insight, Orlando, FL, USA) connected to a 6-inch diameter integrating sphere (Labsphere, North Sutton, NH, USA) that had been previously calibrated using an internal calibration lamp from the same manufacturer. Each LCU tip was positioned at the sphere entrance to capture all the light emitted from the LCU. The spectral radiant powers from 350 nm to 900 nm were recorded using OceanView software (Ocean Insight). The internal optical tip diameter of each light-curing tip was measured using a digital caliper (Mitutoyo, Canada Inc, Mississauga, ON, Canada). The tip area was calculated and divided into

the power to calculate the radiant exitance (mW/cm²) from the LCUs for each exposure mode. The radiant exposure delivered during each exposure mode from the LCUs was calculated (J/cm²) from the product of the exposure time and the irradiance.

4.2.3.2 In vitro temperature measurements

After approval from the local Ethics Board (#2021-5703), one healthy extracted maxillary molar from the University Tooth Bank was used in the study. Due to privacy concerns by the University Ethics Board, no patient details were known. The inclusion criteria were that this was an unrestored molar tooth. The exclusion criteria were that there could be no alteration to the enamel and/or dentin, decay, or the presence of any restorations. A non-retentive, occlusal, Class I (4 mm deep, 3 mm wide, and 5 mm long) and a buccal, Class V cavity (2 mm deep, 2 mm wide, and 5 mm long) were then prepared on the same tooth using a carbide bur (#330, Brasseler, Savannah, GA, USA) under constant water cooling, and the cavity dimensions were verified using a Williams periodontal probe. The cavity walls were polished using Enhance polishers (Dentsply Sirona, York, PA, USA) to produce a smooth, non-retentive cavity. The roots were sectioned 4 mm below the cement–enamel junction and were enlarged with Gates Glidden drills (Dentsply Sirona). After the cavity preparation, the tooth was scanned (Figure 2) using a CEREC Primescan (Dentsply Sirona), and a digital image was created.

Two ultra-fast tissue implantable T-type thermocouples 0.011″ in diameter (IT-23 Physitemp Instruments, Clifton, NJ, USA) were used. They were inserted through the roots into the pulp chamber in two positions: close to the pulp horn and the buccal wall and close to the Class V cavity. A 1-mm internal diameter tube was placed into the mesial root so that fluid could enter the pulp and simulate pulpal fluid flow. Radiographs were taken from two directions to verify the position of the probes and to estimate the thickness of the remaining dentin between the cavity floor and the pulp (Figure 2). The thickness of the remaining dentin floor was measured using the radiographic software to be approximately 2 mm. To simulate physiological conditions, the temperature measurement inside the pulp chamber was carried out starting at a controlled baseline pulp temperature of approximately 32 °C (ZARPELLON et al., 2021) in a warm water bath (Isotemp 2150 Immersion Circulator, Fisher Scientific Inc., Pittsburgh, PA, USA). The baseline temperature of 32º C is the approximate value

inside a human pulp of a prepared tooth after etching and rinsing, followed by photocuring of the bonding agent (ZARPELLON et al., 2021). Another thermocouple was inserted inside the water bath to register the water temperature. To simulate pulp flow, the 1 mm diameter tube was connected to a Peristaltic Pump P-1 (Pharmacia Fine Chemicals, Uppsala, Sweden). The water flow was adjusted for a flow rate of 0.026 mL/min [18, 20] at 32°C ± 0.5. To simulate the conditions in the oral cavity where a rubber dam is used, the tooth was fixed in an acrylic plate with a perforation at the center and positioned in the warm water bath up to the cementoenamel junction.

Real-time temperature data was collected from the thermocouple probes (TCChart software, Nomadics Inc, Stillwater, OK, USA) every 0.5 seconds before, during, and after light exposure. After the temperature had stabilized at 32ºC, the empty Class I cavity was exposed to light from the LCU at a 0 mm distance between the LCU tip and the occlusal surface. After the temperature measurement had returned to 32ºC, a second exposure was made at a 6 mm distance between the LCU tip and occlusal surface. The same procedure was performed on the Class V cavity, but the LCU tip was positioned over the buccal surface. Figure 3 illustrates the position of the LCU light tip for the Class I and V cavity measurements.

Similar to when a rubber dam is used in a clinical situation to protect the gingiva, the plastic plate that held the tooth also served as a barrier so that light from the LCU did not reach the root. Figure 4 shows how the tip was positioned for PowerCure and Monet Laser LCUs, respectively. The temperature was recorded using two conditions: with and without pulpal fluid flow. Five measurements were made for each condition.

4.2.3.3 Statistical analysis

The effect of the simulated flow was compared using one-way ANOVA followed by Scheffe’s post-hoc test. The ΔT values were subjected to a two-way, repeated-measures analysis of variance (ANOVA) test with “exposure modes" and "distance” as the independent variables, followed by Scheffe’s post-hoc tests. Statistical testing and post hoc analyses were conducted at a preset α of 0.05.

4.2.4 Results

4.2.4.1 Spectral analysis

Table 11 reports the power (mW), energy, tip irradiance (radiant exitance) and radiant exposure emitted by each LCU and for each exposure time used in the study. The values correspond to the power emitted in the wavelength range between 350 and 900 nm. The LCU and setting that delivered the highest power was Valo Grand on the Xtra Power mode (2127 ± 6.4 mW), and the LCU that emitted the lowest power was the PowerCure on the High mode (560 ± 4.2 mW).

Figure 16 shows the Spectral Radiant Power from the LCUs in each mode. The Monet Laser and SmartLite Pro delivered only one emission peak. Compared to SmarLite Pro (λ = 462 nm), the Monet Laser emitted a very narrow band of wavelengths with a single emission peak at 451 nm. The Valo Grand, PowerCure and PinkWave were multi-peak broadband LED lights. The PowerCure delivered two wavelength peaks (one in the violet region λ1 = 408 nm; and one in the blue region λ2 = 451 nm), and the Valo Grand delivered three peaks (one in the violet region λ1 = 393 nm; and two in the blue region at λ2 = 448 nm and λ3 = 461 nm). The PinkWave LCU emitted four distinct bands of wavelengths, three in the range of visible light (λ1 = 410 nm; λ2 = 471 nm, λ3 = 631 nm), and one in the near infra-red spectral range (thermal radiation) with an emission peak (λ4) at 860 nm.

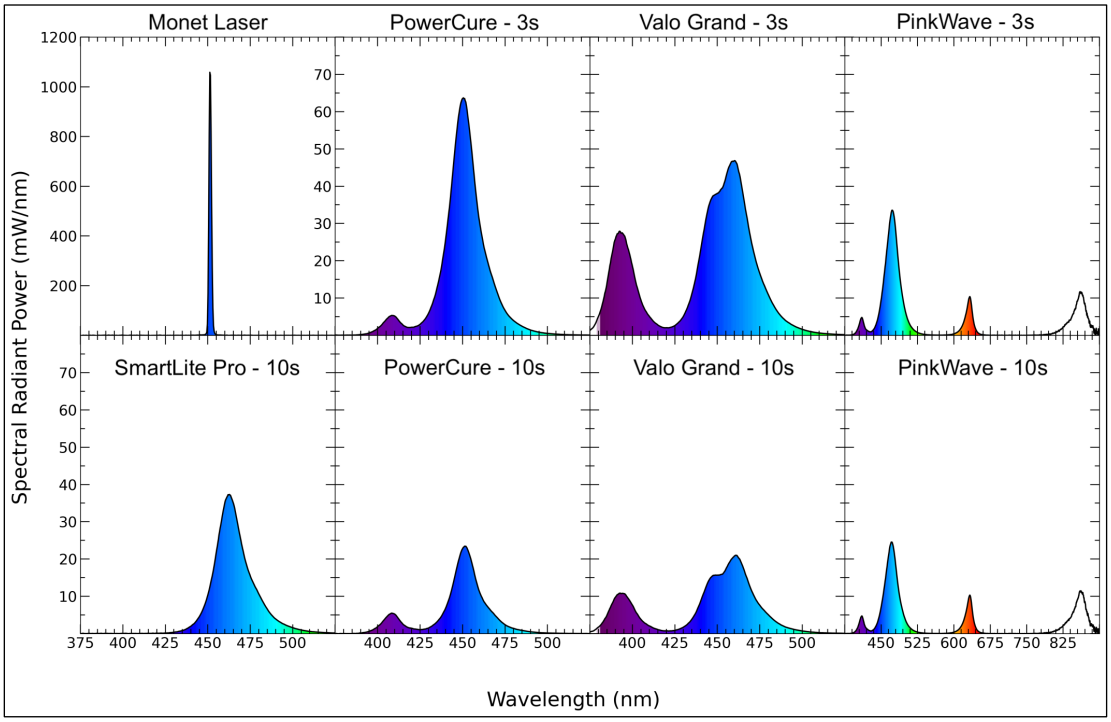

Figura 16 - Emission spectra of the six LCUs. Note that a different power scale is used for Monet because it provides sharply defined spectral emission with high irradiance. PinkWave's x-axis wavelength scale is different from other LCUs because it offers a wider range of wavelengths.

Tabela 11 – Tip Diameter, Power, Energy, Tip Irradiance (Radiant Output) and Radiant Exposure emitted for each light condition. Irradiance measured at 350 to 900 nm.

Fotopolimrizador e Tempo de Exposição	**Picos de comprimento de onda (nm)**	**Diâmetro de ponta (mm)**	**Potência (mW)**		**Energia (J)**	**Irradiância (mW/cm²)**	**Exposição Radiante (J/ cm²)**
			Média	**DP**			
Valo Grand - 3s	393, 448 e 461	11.5	2127	6.4	6.4	2047	6.1
PinkWave - 3s	410, 471, 631 e 860	11.9	1874	6.1	5.6	1685	5.1
Monet - 1s	451	12.8	1652	34.9	1.7	1284	1.3
Monet - 3s	451	12.8	1652	34.9	5.0	1284	3.9
PowerCure - 3s	408 e 451	8.3	1548	1.8	4.6	2861	8.6
PinkWave - 10s	410, 471, 631 e 860	11.9	1505	6.0	15.1	1353	13.5
SmartLite Pro - 10s	462	10.3	896	2.7	9.0	1076	10.8
Valo Grand - 10s	393, 448 e 461	11.5	868	3.2	8.7	835	8.4
PowerCure - 10s	408 e 451	8.3	560	4.2	5.6	1035	10.4

4.2.4.2 In vitro temperature measurements

One-way ANOVA showed there were no significant differences in the change in PT between the groups with and without simulated flow at the flow rate of 0.026 mL/min.

Tables 12 and 13 report the temperature rise (ΔT) for Class I and V cavities, respectively. The ΔT values were significantly affected by the “exposure modes" ($p < 0.001$). Scheffe’s post-hoc test showed that the Monet used for 3 s produced the greatest temperature rise in the empty Class I cavity. The PowerCure used for 3 s produced the greatest temperature rise in the empty Class V cavity, and the Monet used for 1s had the lowest temperature rise ($p \leq 0.05$). Overall, the cavities exposed with the light tip at the 0 mm distance had higher ΔT values than groups where the light tip was 6 mm away. Scheffe’s post-hoc test showed that increasing the distance from 0 mm to 6 mm for the Class I groups had a significant effect ($p < 0.001$). The effect of distance from the light tip was less for the Monet Laser compared to the other LCUs.

Tabela 12 - Temperature rise (ΔT) for Class I cavity.

	Aumento de temperatura (ΔT - ºC)					
	Distância de 0 mm			**Distância de 6 mm**		
	Média	**DP**		**Média**	**DP**	
Monet - 3s	2.1	0.2	Aa	2.1	0.1	Aa
PinkWave - 10s	2.1	0.1	Aa	1.8	0.2	Bb
PinkWave - 3s	1.6	0.1	Ba	1.2	0.2	Cb
Valo Grand - 10s	1.6	0.1	Ba	1.2	0.1	Cb
SmartLite Pro - 10s	1.4	0.0	BCa	1.1	0.0	CDb
PowerCure - 10s	1.2	0.0	CDa	0.7	0.1	Eb
PowerCure - 3s	1.1	0.1	Da	0.7	0.1	Eb
Valo Grand - 3s	1.1	0.1	Da	0.9	0.1	DEa
Monet - 1s	1.0	0.2	Da	0.9	0.2	DEb

Means followed by similar letters (lower case: inside the line; upper case: inside the column) are not significantly different (Scheffe post-hoc test, $p \geq 0.05$).

Tabela 13 - Temperature rise (ΔT) for Class V cavity.

	Aumento de temperatura (ΔT - ºC)					
	Distância de 0 mm			Distância de 6 mm		
	Média	DP		Média	DP	
PowerCure - 3s	4.2	0.3	Aa	2.8	0.2	Ab
PowerCure - 10s	3.6	0.2	ABa	2.5	0.1	Aa
PinkWave - 10s	3.3	0.6	ABCa	2.4	0.4	Aa
SmartLite Pro - 10s	3.1	0.2	ABCa	2.2	0.1	ABa
Valo Grand - 3s	2.6	0.3	BCa	2.5	0.2	Aa
PinkWave - 3s	2.4	0.5	BCa	1.7	0.2	ABCa
Valo Grand - 10s	2.2	0.2	Ca	2.4	0.2	Aa
Monet - 3s	1.0	0.2	Da	1.0	0.3	BCa
Monet - 1s	0.5	0.1	Da	0.6	0.1	Ca

Means followed by similar letters (lower case: inside the line; upper case: inside the column) are not significantly different (Scheffe post-hoc test, $p \geq 0.05$).

Figures 17 and 18 show the temperature profile including the peak temperature increases during light exposure from each exposure mode for Class I and Class V cavities, respectively, when they were exposed at 0 mm. The highest peak temperature for Class I cavity was when Monet was used for 3s and when PinkWave was used for 10s, while the highest peak temperature for the Class V cavity was when PowerCure was used for 3s. The lowest peak temperature rise for both cavities was when Monet was used for 1s. All the peak temperatures were below 37 º C. Overall, LCUs delivering higher irradiance values caused a PT rise with an apparently higher slope than that caused by LCUs that delivered lower irradiance values. In most groups, the PT reached the peak values when the light shut off. On the other hand, when the cavity was exposed to light emitted from the Monet, the PT reached the peak values a few seconds after light shut off.

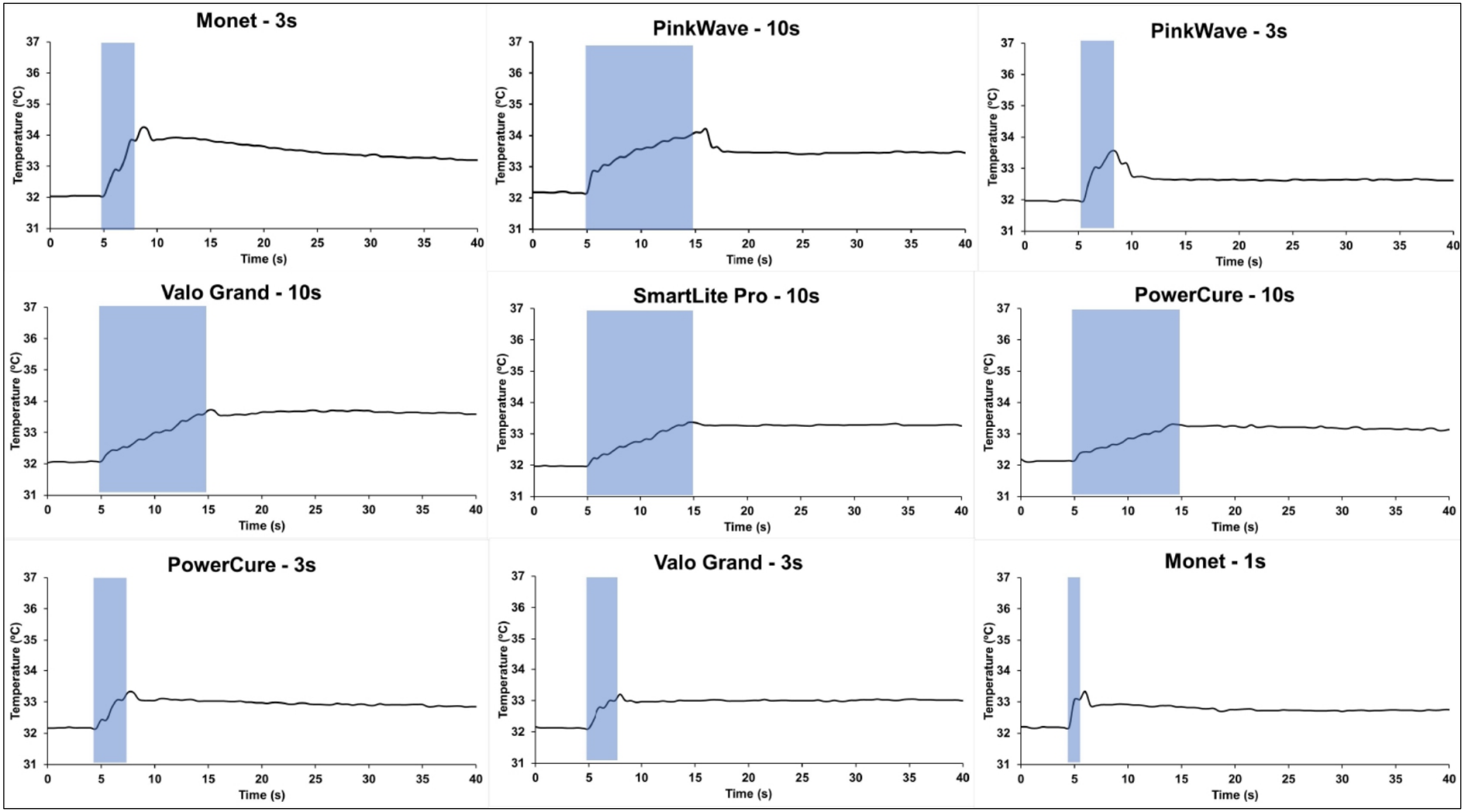

Figura 17 - The temperature profile of the Class I cavity with peak temperature rise during light exposure from each exposure mode when exposed at 0 mm..

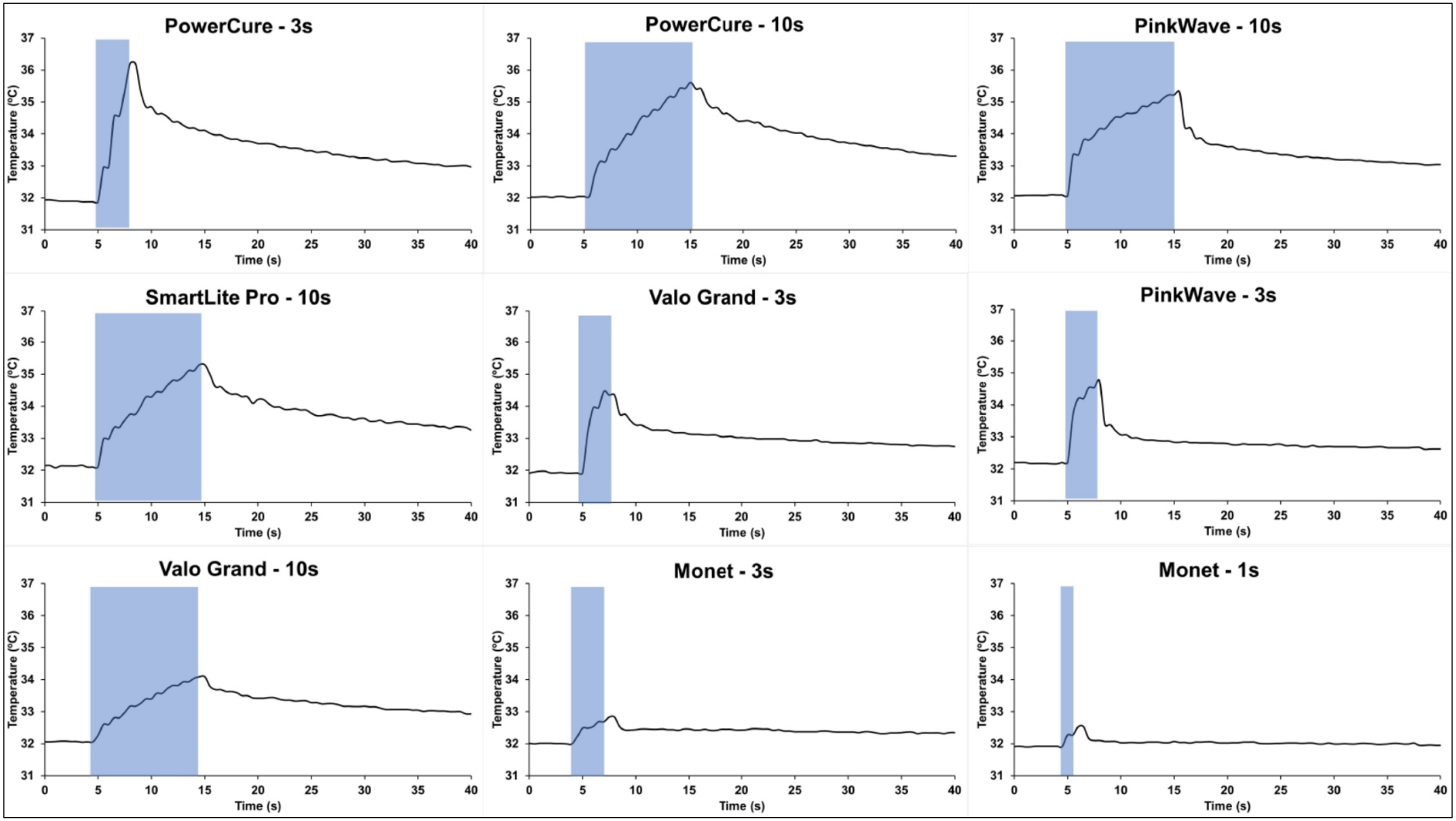

Figure 18 - The temperature profile of the Class V cavity with peak temperature rise during light exposure from each exposure mode when exposed at 0 mm..

4.2.5 Discussion

This study was designed to address the concerns that the new high-output LCUs would cause unacceptable temperature increases in the pulpal temperature. To accomplish this goal, empty cavities in the same tooth were used to simulate the condition when the bonding agent is exposed to light from the various LCUs. The way in which the tooth was mounted represented how the tooth would be isolated and how much tooth would be exposed when using a rubber dam. This study showed that the changes in the pulpal temperature values when the Class I or V cavities were exposed to light were affected by the LCU and exposure mode used. Thus, the first hypothesis was rejected. The results of this study agree with previous findings showing that LCUs that emit different emission spectra and power outputs produce different temperature changes in the pulp (MOUHAT et al., 2021). The photons from the LCU that strike the dentin floor are converted into heat (RUEGGEBERG, F., 1999) which is conducted through the remaining dentin to the pulp (LIN et al., 2010). Of the LCUs tested, the Monet - 3s and PinkWave - 10s caused the highest values when the occlusal Class I cavity was exposed to the light, regardless of the distance between the LCU tip and the tooth surface. The Monet is a Class 4 laser; thus, distance should have no effect. Furthermore, the collimated beam from this laser LCU has a narrow emission spectrum and a high irradiance (DROST et al., 2019; KOUROS et al., 2020). Therefore, distance has little effect on the irradiance (number of photons per unit area) that this laser can deliver to the pulpal floor without losing power (DROST et al., 2019). In contrast, depending on the internal optics, the irradiance delivered from conventional LCUs is greatly reduced as the distance between the LCU tip and the tooth surface increases (PIRES et al., 1993; PRICE et al., 2000). The greater photon density (irradiance) reaching the pulpal floor when the laser hits the surface (DROST et al., 2019) produces more heat at the floor of the cavity (RUEGGEBERG, F., 1999). Consequently, according to the theory of heat transfer by conduction (LIN et al., 2010), more heat is transferred through the remaining dentin to the thermocouple. The temperature changes are dependent on the characteristics of the light source (OBERHOLZER et al., 2012), and previous authors have shown that the temperature rise is closely related to the radiant exposure delivered to the tooth (RUNNACLES et al., 2015). The Monet laser used for 1s delivered the lowest radiant exposure values (1.3 J/cm^2) compared to the other LCUs (Table 11), which explains why the temperature rise from this LCU

was low when it was used for 1s, despite the apparently higher slope of the PT rise caused by the light emitted from this LCU (Figures 17 and 18).

The manufacturer of the laser LCU claims it can light cure a 2-mm depth increment in 1s, and 3s is adequate to photo-cure 5-mm increments of RBC (AMD, 2021). When the Monet was used for 3s, or the PinkWave used for 10s, this generated the highest temperature rise in the occlusal, Class I preparation, but they were all less than 5.5 °C (Table 12 and Figure 17). Interestingly, the ΔT values in these two groups were almost double those observed when the PowerCure was used for 10s. However, Table 2 shows that the irradiance and radiant exposure values delivered by PowerCure used for 10s (2861 mW/cm² and 13.5 J/cm²) were much greater than when the PinkWave used for 10s (1685 mW/cm² and 5.1 J/cm²) or the Monet used for 3s (1284 mW/cm² and 3.9 J/cm²). Although the power from the Monet was 1652 mW because the measured internal diameter of the light tip was 12.8 mm, the irradiance was lower than expected from this laser. Unlike the other multi-peak LCUs, the PinkWave has Quadwave technology that delivers four distinct wavelengths: infrared (IR), red, blue and violet light (Figure 16). The power delivered in IR (IR) band covers the wavelength range of 750 nm – 1000 nm, and the Far Infrared Radiation (FIR) transfers energy as heat that thermoreceptors can feel as radiant heat (VATANSEVER; HAMBLIN, 2012). This IR is considered thermal irradiation, which may be responsible for the greater temperature rise. Therefore, the thermal irradiation and the high-power output of 1874 mW from the PinkWave (Table 11) probably caused the greater temperature rise from this LCU.

Conversely, when the Class V preparation was exposed to the light emitted from the LCUs, the Monet caused the lowest ΔT values, regardless of the distance between the LCU tip and the tooth (Table 13 and Figure 18). On the other hand, the PowerCure caused the highest ΔT values in the Class V cavity preparation, along with the PinkWave used for 10s (Figure 18). This result is most likely due to the design of the experiment and the shape of the Monet light tip. In an attempt to simulate the clinically relevant scenario, the water bath into which the tooth was placed also simulated the presence of a clamp and a rubber dam on the tooth (Figure 4). Therefore, this arrangement and this oval-shaped Class V cavity did not permit the large diameter Valo Grand, Monet, and PinkWave light tips to be centered over the Class V cavity. Instead, the center of these light tips was close to or at the same level as the cusp tip. In contrast, the smaller diameter light tips of the PowerCure and the SmartLite Pro

could be placed directly over the Class V cavity. Consequently, both the design of the LCU tip and the light beam diameter most likely impacted the outcomes. Based on the small diameter (approximately 6 mm) of the laser beam emitted by Monet and its tip shape, it appears that the laser beam was centered more to the cusp tip above the cavity preparation rather than into the cavity. This illustrates why clinicians must establish the correct clinical conditions that will allow the light from the LCU to directly access all of the RBC in the cavity after placing the clamp, rubber dam and matrix band. To do so, they must use protective shielding so that they can watch what they are doing when using the LCU. If they are 'off-target' for even half a second in a 1s exposure, this represents a 50% reduction in the amount of energy delivered to the RBC.

In the present study, the maximum temperature increase, not how the temperature returned to baseline, was used to compare the effects of the different LCUs. There was no tongue, saliva, breath, adjacent teeth or surrounding periodontal tissue that all may affect the change in temperature back to baseline. To standardize the conditions and to better simulate the oral environment where the tooth is surrounded by soft tissues that may help to dissipate the heat (MOLNÁR et al., 2015), the simulated pulpal fluid flow rate was 0.026 mL/min (SAVAS et al., 2014; AKARSU; AKTUG KARADEMIR, 2019), and the tooth was kept in a warm water bath. The present study found no significant differences in the maximum temperature rise between groups with and without simulated flow rate ($p > 0.05$) and the second hypothesis was accepted. The blood flow through human teeth is affected by the presence of pulpal inflammation (BERGGREEN; BLETSA; HEYERAAS, 2007), tooth preparation (SUKAPATTEE et al., 2016), and the use of local anesthesia (ODOR; PITT FORD; MCDONALD, 1994; ZHENG et al., 2018; VONGSAVAN et al., 2019). The results of the present study do not agree with some previous studies reporting that the presence of a simulated pulpal fluid flow attenuated the temperature rise (KODONAS; GOGOS; TZIAFA, 2009; KODONAS; GOGOS; TZIAFAS, 2009; BRAGA et al., 2019). However, those studies used flow rates that were between 1.0 and 1.4 mL/min. This was approximately 50 times greater flow rates than the flow rate of 0.026 mL/min used in the present study. Another study evaluated the effects of flow rates of 0.0042 mL/min, 0.028 mL/min or 0.07 mL/min that were more similar to the present study on the maximum intra pulpal temperature rise (PARK; ROULET; HEINTZE, 2010). The authors (PARK; ROULET; HEINTZE, 2010) also found that these flow rates had little

effect on the maximum intra pulpal temperature increase, but the flow rate did affect the time taken for the temperature to return to the baseline temperature. Although the pulp chamber geometry is not circular, the authors referred to the Womersley equation ($\alpha = R(W/V)1/2$), where R is the vessel radius, W is the radial frequency (rad/s), and V is the kinematic viscosity (m^2/s) to explain the effect of fluid flow on the heat transfer between vessels and tissues. They suggested that the Womersley equation supports their conclusion that the rate of fluid flow through the pulp chamber in a tooth has only a very small effect on the maximum temperature rise (PARK; ROULET; HEINTZE, 2010). If these in vitro results are applied to in vivo conditions, it may be concluded that the flow rate in blood vessels in the pulp has a negligible effect on the rapid increase in the temperature in pulp during the critical phase when the curing light is activated, but it will affect how quickly the temperature returns to normal.

Overall, the light-curing the Class V preparation produced higher PT values than when the Class I cavity was exposed. The tooth anatomy and cavity design may be related to such differences. More specifically, in the current study, the Class V preparation had a thinner axial floor than the pulpal floor's thickness in the Class I preparation (approximately 2 mm). A correlation has been shown between the dentin thickness and pulp temperature rise, so the thinner the remaining dentin, the lower the dentin capacity to act as a heat insulator (MURRAY et al., 2003a; AGUIAR et al., 2006; YAZICI, A.R. et al., 2006; AKARSU; AKTUG KARADEMIR, 2019). In addition, because the buccal face was thinner than the occlusal one due to the anatomy of the lower molar, the distance between the LCU tip and the thermocouple was smaller in the Class V preparation than the distance between the LCU tip and the pulp horn in the Class I preparation. For most LCUs, there is an inverse relationship between power and distance, so the greater the distance, the lower the power, but this decrease depends on the optical design of the light source [23]. As fewer photons will hit the cavity floor (RUEGGEBERG, F., 1999), less heat will be generated in the tooth structure when the distance between the LCU tip and the tooth increases. Considering that the distance between the LCU tip and the axial wall in the Class V cavity is lower than that between the LCU tip and the Class I cavity due to the tooth anatomy, more photons will reach the floor of the cavity in the Class V preparation in comparison to the number of photons hitting the pulp floor of the Class I preparation. This also helps explain why the overall ΔT values decreased only when LED LCUs were used and

when the LCU tip was placed 6 mm away from the tooth surface. Since the Monet was a laser, and distance did not affect the ΔT values from this LCU.

In the present study, all the measurements were carried out under *in vitro* well-controlled conditions at room temperature of 20 º C using only one extracted maxillary molar. This reduced the number of variables in the study and allowed the effects of just the LCUs and the exposure times on the temperature rise to be determined. The temperature of the warm water bath was maintained so that the temperature inside the pulp chamber reached the same baseline of 32 ° C. This simulated the physiologic baseline in the pulp after a cavity preparation was performed using a high-speed diamond bur under cooling water, followed by an etch rinse bonding procedure (ZARPELLON et al., 2021). None of the evaluated experimental groups showed ΔT values higher than 5.5 º C in that condition. However, the study only analyzed the effect of the LCU itself on the temperature rise (ΔT), so the impact of heat generated from the exothermic polymerization and the insulating ability of RBCs were not considered. Further *in vitro* and *in vivo* studies are needed to better understand the contribution of the RBC to the temperature rise in the tooth.

4.2.6 Conclusions

Within the limitations of the present study, it was concluded that: (1) different LCUs produce different temperature increases inside the pulp chamber; (2) the simulated pulpal fluid of 0.026 mL/min had no significant effect on the PT rise; (3) increasing the distance between the LCU tip and the tooth surface reduces the PT for some of the LCUs used; (4) Monet Laser used for 3s and PinkWave used for 10s produced the greatest PT rise on Class I and; (5) the placement of a rubber dam for Class V restorations may prevent centering the light tip from being centered over the cavity and thus affect the rise in PT.

4.3 ARTIGO 3: IN-VITRO PULPAL TEMPERATURE INCREASES WHEN PHOTO-CURING BULK-FILL RESIN-BASED COMPOSITES USING LASER OR LIGHT-EMITTING DIODE LIGHT CURING UNITS

Cristiane Maucoski[1,2]

Richard Bengt Price[2]

Braden Sullivan[2]

Juliana Anany Gonzales Guarneri[1]
Bruno Gusso[1]
Cesar Augusto Galvão Arrais[1]

[1] Department of Restorative Dentistry, State University of Ponta Grossa, Ponta Grossa, Parana, Brazil.
[2] Department of Dental Clinical Sciences, Dalhousie University, Halifax, Nova Scotia, B3H 4R2, Canada.

Revista: Journal of Esthetic and Restorative Dentistry
Aceito: 17 de janeiro de 2023
DOI: 10.1111/jerd.13022

4.3.1 Abstract

Objective: To evaluate the in vitro pulpal temperature rise (ΔT) within the pulp chamber when low- and high-viscosity bulk-fill resin composites are photo-cured using laser or contemporary light curing units (LCUs).
Materials and Methods: The light output from five LCUs was measured. Non-retentive Class I and V cavities were prepared in one upper molar. Two T-type thermocouples were inserted into the pulp chamber. After the PT values reached 32°C under simulated pulp flow (0.026 mL/min), both cavities were restored with: Filtek One Bulk Fill (3M), Filtek Bulk Fill Flow (3M), Tetric PowerFill (Ivoclar Vivadent), or Tetric PowerFlow (Ivoclar Vivadent). The tooth was exposed as follows: Monet Laser (1s and 3s), PowerCure (3s and 20s), PinkWave (3 and 20s), Valo X (5s and 20s) and SmartLite Pro (20s). The ΔT data were subjected to one-way ANOVA followed by Scheffe's post-hoc test.
Results: Monet 1s (1.9 J) and PinkWave 20s (30.1 J) delivered the least and the highest amount of energy, respectively. Valo X and PinkWave used for 20s produced the highest ΔT values (3.4 – 4.1 ºC). Monet 1s, PinkWave 3s, PowerCure 3s (except FB-Flow) and Monet 3s for FB-One and TP-Fill produced the lowest ΔT values (0.9 – 1.7 ºC). No significant differences were found among composites.
Conclusions: Short 1- to 3-s exposures produced acceptable temperature rises, regardless of the composite.

4.3.2 Introduction

To simplify restorative procedures, manufacturers have developed restorative materials, such as bulk-fill resin-based composites (RBCs), that can be placed in thicker (4 to 5 mm) increments and may be less technique sensitive than conventional RBCs (CHESTERMAN et al., 2017). Compared to the conventional RBCs, these bulk-fill composites save clinical time, produce similar or lower levels of postoperative sensitivity (TARDEM et al., 2019), have greater depth of cure (VAN ENDE et al., 2017), and have a similar clinical performance to conventional posterior composites that are photo-cured in thinner (1.5 to 2 mm) increments (VELOSO et al., 2019; ARBILDO-VEGA et al., 2020; TIRAPELLI, 2022).

During the restorative procedure, the light from the light curing unit (LCU) and the heat released from the exothermic reaction of the RBC (BALESTRINO et al., 2016) can increase the pulp temperature (PT) (RUEGGEBERG, F. A. et al., 2017; MOUHAT et al., 2021). The PT has been reported to be affected by the output from the LCU (PARK; ROULET; HEINTZE, 2010; MOUHAT et al., 2017), and increasing the irradiance is thought to produce a greater rise in PT when photo-curing the RBC (WANG et al., 2021). The first light-emitting diode (LED) based LCUs were considered to be 'cool' because they delivered a lower irradiance (approximately 240 mW/cm²) than the quartz tungsten halogen based LCUs (approximately 450 to 1200 mW/cm²) (RUEGGEBERG, F. A. et al., 2017). Many LED lights now deliver irradiances greater than 2,000 mW/cm², and some manufacturers claim that exposure times shorter than 5 seconds may be used to reduce photo-cure RBCs and reduce clinical time (ALMEIDA et al., 2021). However, such high irradiance values have become a concern due to the potential risk to the soft tissues (MAUCOSKI et al., 2017) and the dental pulp (KIM et al., 2017; MOUHAT et al., 2017). Using monkeys, Zach and Cohen in 1965 (ZACH; COHEN, 1965) reported that an increase in PT of 5.5 °C resulted in pulpal necrosis in 15 % of the cases, and a temperature rise of 11 °C resulted in pulpal necrosis in 60 % of the cases. Therefore, many researchers have set a maximum increase of 5.5 ºC in the PT to be the acceptable limit (LEMPEL et al., 2021; MOUHAT et al., 2021).

Recently, new LCUs that emit a different emission spectra and powers than conventional LCUs have become commercially available. For example, a blue diode laser LCU that emits a high power and high irradiance (ROCHA et al., 2022) over a very narrow band of wavelengths has been introduced (Monet Laser, AMD Lasers,

West Jordan, UT, USA). This laser LCU is proposed to be an alternative to light curing using conventional LED lights (DROST et al., 2019; KOUROS et al., 2020). The Monet is a battery-operated laser that emits light with a very narrow wavelength range at a high photon density (DROST et al., 2019). The manufacturer claims (ROCHA et al., 2022) that the Monet Laser delivers an irradiance of 2,000 to 2,400 mW/cm², and it can photoactivate RBCs in 1 s exposure because it emits a collimated high irradiance beam of light (AMD, 2021). Another recently released LCU is the PinkWave (Vista Dental Products, Racine, WI, USA). The manufacturer claims that this LCU has Quadwave technology because it emits four distinct bands of wavelengths. The manufacturer claims (VISTAAPEX, 2022) that the PinkWave produces an irradiance of 1,720 mW/cm² in the 3s exposure mode, and the manufacturer claims it will reduce the shrinkage and increase the depth of cure in the RBC. The Valo X (Ultradent Products, South Jordan, UT, USA) is the third generation of the Valo LCU. This multi-peak LCU has a wider light tip than the original Valo or the Valo Grand, with 12.5 mm. The Valo X emits three bands of wavelengths, between 380 and 515 nm, and the manufacturer claims that it produces an irradiance of 1,100 for the Standard mode and 2,200 mW/cm² in the Xtra Power mode (ULTRADENT, 23 December 2022). Considering that the output from high-irradiance (MOUHAT et al., 2017) and broader emission spectrum LCUs (MOUHAT et al., 2021) may influence the increase in PT, concerns have been raised regarding the temperature increase inside the pulp chamber when the teeth are exposed to light emitted from these high-output LCUs (MAUCOSKI et al., 2022a).

The impact of photo-curing bulk-fill RBCs on the temperature within the pulp (PT) chamber has already been investigated (LEMPEL et al., 2021; WANG et al., 2021). However, these PT values are also influenced by the heat produced by the exothermic polymerization of the RBC (BALESTRINO et al., 2016), and the volume of the RBC[17]. This exotherm may be of concern when using bulk-fill RBCs because a greater volume of RBC is photocured at the same time (LEMPEL et al., 2021). Consequently, a new approach combining light curing at a high radiant emittance with a modification of the polymerization mechanism in the RBC has been proposed (ILIE; WATTS, 2020). This new generation of bulk-fill RBCs use a reversible addition-fragmentation chain transfer polymerization (RAFT) mechanism, and some manufacturers claim that these RBCs can be adequately photo-cured in only 3s. Although such short exposure times have produced similar viscoelastic behavior and

mechanical properties to those achieved when longer exposure times were used (ILIE; WATTS, 2020; ILIE; DIEGELMANN, 2021), there is no information to date regarding the effect on the PT when RAFT bulk fill RBCs are photo-cured. There is also no information currently available about the increase in temperature inside the pulp chamber when bulk-fill composite resins are photo-cured using the new diode laser or the recently introduced higher-power LCUs. Therefore, the present study evaluated the PT rise when cavity preparations were restored with low and high viscosity bulk-fill RBCs, and photo-cured with laser, Quadwave, or contemporary high-power LED LCUs. The null hypotheses were that: (1) there is no difference in the *in vitro* PT rise caused by 1, 3 or 20 s photo-curing times using laser, Quadwave, or contemporary high-power LED LCUs; (2) the differences in viscosity between bulk-fill RBCs will not affect the in-vitro PT rise regardless of LCU and exposure strategy.

4.3.3 Materials and Methods

4.3.3.1 Analysis of the light emitted by the LCUs

One laser diode, one monowave LED, and three multiple-peak high-power LED LCUs (Figure 5) were used (Table 4). The spectral radiant powers from the LCUs were measured using a fiberoptic spectroradiometer (Flame-T, Ocean Insight, Orlando, FL, USA) connected to a 6-inch diameter integrating sphere (Labsphere, North Sutton, NH, USA) that had been previously calibrated using an internal NIST referenced calibration lamp (ICS-600, Labsphere). The tip from each LCU was positioned at the entrance of the sphere to capture all the light emitted from the LCU at the 0 mm distance. The light output was recorded using OceanView software (Ocean Insight, Orlando, FL, USA), which provided the total emitted power and the spectral radiant power. The power was multiplied by the exposure time to provide the energy (J) delivered to the tooth by each LCU. To determine the radiant exitance from each LCU, the internal diameter of each LCU tip was measured using a digital caliper (Mitutoyo, Canada Inc, Mississauga, ON, Canada), and the optical emission area of the tip of each LCU was calculated. This value was divided into the power (W) to obtain the total radiant exitance (mW/cm^2) from the LCU for each exposure mode.

4.3.3.2 In vitro temperature analysis

This study was approved by the local Ethics Board (#2021-5703). The study used one healthy extracted maxillary molar from the University Tooth Bank for all the experiments. The inclusion criteria were that the molar tooth had to be intact and unrestored. An occlusal, non-retentive, Class I (3-mm wide, 4-mm deep and 5-mm long) and a buccal, non-retentive, Class V cavity (2-mm wide, 2-mm deep and 5-mm long) with divergent walls were made using a high-speed carbide bur. The cavity dimensions were verified using a William's periodontal probe. Approximately 1 mm of dentin was left on the pulpal wall of the Class I and V cavities. To verify the thickness of the remaining dentin and the position of the thermocouples, radiographs were taken and measurements were made from these radiographs (Figure 6). The Class I and V cavities in the molar tooth are shown in Figure 7. The cavity walls were polished using Enhance polisher (Dentsply Sirona) so that there was minimal mechanical retention to the cavity wall and the RBC could be easily removed. The tooth roots were sectioned 4 mm below the cement-enamel junction and were enlarged with Gates Glidden drills (Dentsply Sirona, York, PA, USA).

Two 0.011" diameter ultra-fast response T-type thermocouples (IT-23 Physitemp Instruments, Clifton, NJ, USA) were placed in the pulp chamber through the enlarged roots, one close to the pulp horn and the other close to the Class V cavity. The molar tooth was attached to an acrylic plate to simulate the effect of using a rubber dam and clamp (MAUCOSKI et al., 2022a). To simulate the conditions in the oral cavity, the tooth was inserted in a warm water bath (Isotemp 2150 Immersion Circulator, Fisher Scientific Inc., Pittsburgh, PA, USA) up to the cemento-enamel junction. Temperature measurements inside the pulp chamber were made under controlled physiological simulation at a basal pulp temperature of approximately 32° C, which is thought to simulate the baseline temperature of the tooth after etching and rinsing (ZARPELLON et al., 2021). A tube was placed into the mesial root and connected to a peristaltic pump (Peristaltic Pump P-1, Pharmacia Fine Chemicals, Uppsala, Sweden). The water flow rate through the tube into the pulp chamber was set to 0.026 mL/min (SAVAS et al., 2014; AKARSU; AKTUG KARADEMIR, 2019; MAUCOSKI et al., 2022a). A third thermocouple was placed in the water bath to measure the water temperature.

A temperature acquisition software (TCChart, Nomadics Inc., Stillwater, OK, USA) was used to record the temperature every 0.05 seconds before, during and after the restoring procedures. A schematic illustrating how the temperature was recorded is shown in Figure 8. So that the restoration could be removed after light curing, no bonding procedure was performed. Instead, a very thin coating of Vaseline (Covidien, Mansfield, MA, USA) was applied to the cavity, and a piece of dental floss was inserted into the RBC before photo-curing. After reaching the baseline temperature of 32ºC, the Class I cavity was filled up to a depth of 4 mm using one of the following RBCs (Table 2): Filtek One Bulk Fill (FB-One; Shade A2; 3M, St. Paul, MN, USA), Filtek Bulk Fill Flowable (FB-Flow; Shade A2; 3M), Tetric PowerFill (TP-Fill; Shade IVA; Ivoclar Vivadent, Schaan, Liechtenstein), or Tetric PowerFlow (TP-Flow; Shade IVA; Ivoclar Vivadent). TP-Fill and TP-Flow use the RAFT polymerization mechanism. FB-One and FB-Flow use RAFT related technology. The tip of the curing light was positioned at 0 mm from the cusp tip, and the bulk-fill RBCs were exposed to the light-curing conditions reported in Table 4. The same procedure was performed for the Class V cavity, where the LCU tip was placed on the buccal surface, except that the Class V cavity was only 2 mm deep. Figure 9 describes the design of the experiment.

4.3.3.3 Statistical analysis

Since some manufacturers market the bulk-fill RBC and LCU (Ivoclar Vivadent) as a restorative system, the factorial design of the study consisted of one independent variable (Bulk-fill RBC/LCU), and 1 dependent variable (temperature). The factorial scheme resulted in 72 experimental groups, with 5 repetitions for each (n=5). The ΔT values for Class I and Class V cavities were first subjected to a one-way analysis of variance (ANOVA) test followed by Scheffe's post-hoc tests. Statistical testing and post-hoc analyses were conducted at a preset α of 0.05. Logarithmic regression analyses were performed (Excel, Microsoft, Redmond, WA, USA) for each RBC temperature rise at the different exposure modes using the Energy (Joules) delivered from the LCUs to the RBCs.

4.3.4 Results

4.3.4.1 Analysis of the light emitted by the LCUs

Table 14 reports the tip diameter (nm), power (mW), energy (J), radiant exitance or irradiance (mW/cm²), and radiant exposure (J/cm2) emitted by each exposure condition in the wavelength range between 350 and 900 nm for PinkWave and between 350 and 550 nm for the other LCUs. The Valo X used for 5s emitted the highest power (2,579 ± 9.7 mW). The PowerCure used for 20s emitted the lowest power (572 ± 1.3 mW), but it still delivered 11.4 J in a 20 s exposure. The Monet used for 1 s delivered the least amount of energy (1.9 J), and the PinkWave used for 20s delivered the greatest amount of energy (30.1 J).

Table 14 and Figure 19 show the peak wavelengths (nm) and the spectral radiant power from the LCUs on each setting. The Monet Laser and SmartLite Pro both delivered one single emission peak. However, the Monet Laser emitted a very narrow band of wavelengths with a peak centered at 451 nm compared to SmartLite Pro that had a broader emission spectrum with a peak centered at 462 nm. The PowerCure, Valo X, and PinkWave were multi-peak broadband LED LCU lights. The PowerCure delivered two wavelength peaks, one in the violet region (λ1 = 408 nm) and one in the blue region (λ2 = 451 nm) and the Valo X (λ1 = 393 nm; λ2 = 445 nm, λ3 = 458 nm). The PinkWave LCU emitted four distinct bands of wavelengths, three in the range of visible light (λ1 = 410 nm; λ2 = 471 nm, λ3 = 631 nm), and one in the invisible near-infrared spectral range/thermal radiation (λ4 = 860 nm).

Tabela 14 – Peak wavelengths, tip diameter, tip area, power, energy delivered, radiant output (tip irradiance) and radiant exposure of the nine exposure conditions

Fotopolimerizador e tempo de exposição	Comprimentos de onda (nm)	Diâmetro de ponta (mm)	Área da ponta (cm²)	Potência (mW)		Energia (J)	Irradiância (mW/cm²)	Exposição Radiante (J/cm²)
				Média	DP			
Monet 1s	451	12.8	1.29	1933	3.7	1.9	1502	1.5
PowerCure 3s	408 and 451	8.3	0.54	1525	3.2	4.6	2818	8.5
PinkWave 3s	410, 471, 631 and 860	11.9	1.11	1874	6.1	5.6	1685	5.1
Monet 3s	451	12.8	1.29	1933	3.7	5.8	1502	4.5
PowerCure 20s	408 and 451	8.3	0.54	572	1.3	11.4	1057	21.1
Valo X 5s	393, 445 and 458	12.5	1.23	2579	9.7	12.9	2102	10.5
SmartLite Pro 20s	462	10.3	0.83	886	0.9	17.7	1064	21.3
Valo X 20s	393, 445 and 458	12.5	1.23	1277	6.5	25.5	1041	20.8
PinkWave 20s	410, 471, 631 and 860	11.9	1.11	1505	6	30.1	1353	27.1

As condições de exposição foram classificadas da menor para a maior quantidade de energia (J) entregue.

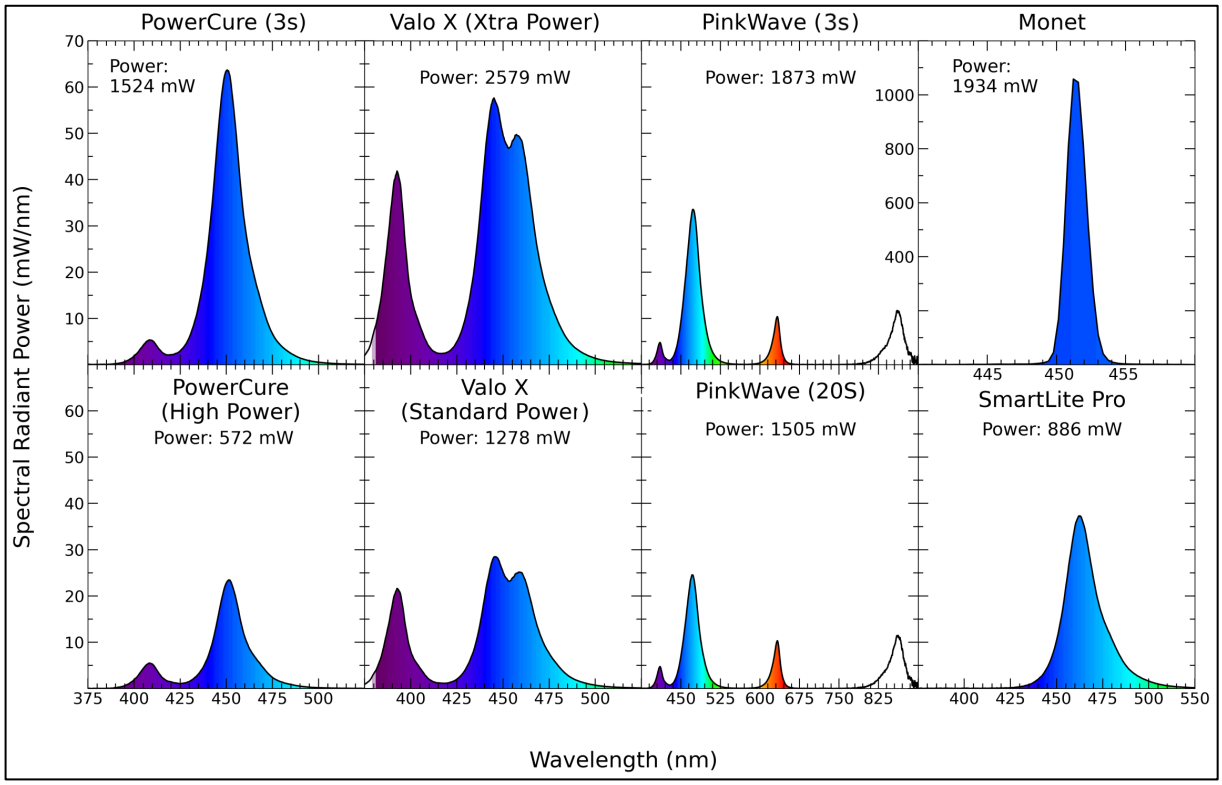

Figura 19 Emission and power spectra (mW) of LED and laser LCUs. Note the different ranges of wavelength and spectral radiant power for the Monet Laser compared to the other LCUs. The PinkWave wavelength scale is different from other LCUs because it offers a wider range of wavelengths.

4.3.4.2 In-vitro temperature analysis

Table 15 reports the temperature rise (ΔT) produced by the RBCs in the Class I cavity. The Valo X and the PinkWave used for 20s (between 3.4 – 4.1 ºC) for all the four RBCs produced the highest ΔT values. There were no significant differences between the 4 RBCs. The Monet for 1s, PinkWave for 3s, PowerCure for 3s (except when using FB-Flow) and the Monet used for 3s for FB-One and TP-Fill produced the lowest ΔT values (between 0.9 – 1.7 ºC). A similar pattern in the ΔT values was observed in both thermocouple positions. However, the rank of the ΔT values in the Class I cavity produced by the different LCU/resin composite differed from those observed in the Class V cavity.

Table 16 reports the temperature rise (ΔT) for the Class V cavity. When performing Class V restorations, the thermocouple probe that was closest to the Class V cavity reported that the PowerCure used for 20s (FB-Flow, TP-Flow and TP-Fill), the PinkWave used for 20s (FB-Flow and TP-Flow), Valo X 20s (FB-Flow) and SmartLite Pro (FB-Flow) used for 20 s produced the highest ΔT values that were between 3.3 –

4.0 ºC. However, there were no significant differences between these LCUs. The lowest ΔT values were produced by the Monet when it was used for 1s, the Monet used for 3s, and PinkWave used for 3s for all four RBCs tested (between 0.5 – 1.2 ºC). Contrary to the ΔT values reported in the Class I cavity where similar patterns in the ΔT values was observed in both thermocouple positions, in the Class V cavity, the thermocouple placed furthest from the axial wall recorded lower ΔT values than the thermocouple placed near the axial wall that was adjacent to the Class V cavity.

Figure 20 shows the results of logarithmic regression analyses of the relationship between the ΔT values (ºC) and the Energy (Joules) delivered to the tooth. For all the RBCs, there was an excellent positive correlation between the amount of energy (J) delivered from the LCU and the temperature rise inside the pulp chamber (R^2= 0.713 for FB-One, R^2 = 0.783 for FB-Flow, R^2 = 0.661 for TP-Fill and R^2 = 0.722 for TP-Flow).

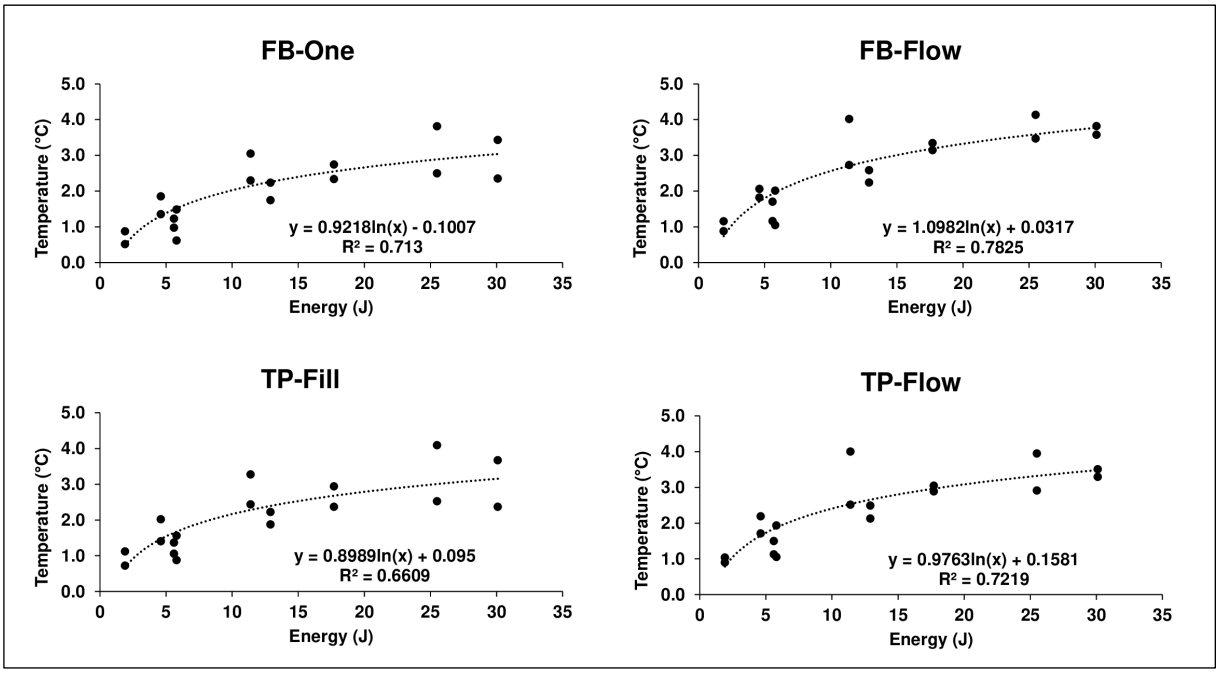

Figura 20 - Regression analyzes for temperature rise records of FB-One, FB-Flow, TP-Fill and TP-Flow RBCs for the different exposure modes by examining the relationship between the temperature rise and the total energy (J) delivered by the LCUs.

Tabela 15 – Temperature rise (ΔT) recorded for the Class I cavity ranked from highest to lowest temperature rise.

Condição de Exposição	RBC	Aumento de temperatura (ΔT - ºC)					
		Sonda na posição Classe 1			Sonda na posição Classe V		
		Média	DP		Média	DP	
Valo X 20s	**Filtek Bulk Fill Flow**	4.1	0.1	A	4.6	0.2	A
Valo X 20s	**Tetric PowerFill**	4.1	0.3	A	3.8	0.2	ABC
Valo X 20s	**Tetric PowerFlow**	3.9	0.1	AB	4.2	0.4	AB
PinkWave 20s	**Filtek Bulk Fill Flow**	3.8	0.3	AB	4.6	0.4	A
Valo X 20s	**Filtek One**	3.8	0.4	AB	3.7	0.2	ABCD
PinkWave 20s	**Tetric PowerFill**	3.7	0.5	ABC	3.7	0.5	ABCD
PinkWave 20s	**Tetric PowerFlow**	3.5	0.1	ABCD	4.2	0.2	AB
PinkWave 20s	**Filtek One**	3.4	0.4	ABCDE	3.6	0.3	ABCD
SmartLite Pro20s	**Filtek Bulk Fill Flow**	3.1	0.1	BCDEF	3.4	0.2	BCDE
SmartLite Pro20s	**Tetric PowerFill**	2.9	0.3	CDEFG	2.9	0.3	CDEFG
SmartLite Pro20s	**Tetric PowerFlow**	2.9	0.1	CDEFG	3.2	0.1	CDEF
SmartLite Pro20s	**Filtek One**	2.7	0.1	DEFGH	2.7	0.3	DEFG
PowerCure 20s	**Filtek Bulk Fill Flow**	2.7	0.0	DEFGH	2.8	0.2	DEFG
Valo X 5s	**Filtek Bulk Fill Flow**	2.6	0.2	EFGHI	2.6	0.1	EFGH
PowerCure 20s	**Tetric PowerFlow**	2.5	0.1	FGHIJ	2.5	0.2	EFGH
Valo X 5s	**Tetric PowerFlow**	2.5	0.2	FGHIJ	2.4	0.1	EFGHI
PowerCure 20s	**Tetric PowerFill**	2.4	0.3	FGHIJ	2.3	0.3	FGHIJ
PowerCure 20s	**Filtek One**	2.3	0.2	FGHIJK	2.2	0.2	FGHIJKL
Valo X 5s	**Filtek One**	2.2	0.1	GHIJKL	1.9	0.5	GHIJKLM
Valo X 5s	**Tetric PowerFill**	2.2	0.1	GHIJKL	2.2	0.1	FGHIJK

Monet 3s	**Filtek Bulk Fill Flow**	2.0	0.2	HIJKLM	2.1	0.2	GHIJKL
Monet 3s	**Tetric PowerFlow**	1.9	0.1	HIJKLMN	2.0	0.0	GHIJKLM
PowerCure 3s	**Filtek Bulk Fill Flow**	1.8	0.1	IJKLMNO	1.7	0.2	HIJKLMN
PowerCure 3s	**Tetric PowerFlow**	1.7	0.1	IJKLMNOP	1.6	0.0	HIJKLMN
PinkWave 3s	**Filtek Bulk Fill Flow**	1.7	0.1	JKLMNOP	1.7	0.1	HIJKLMN
Monet 3s	**Tetric PowerFill**	1.6	0.1	KLMNOP	1.7	0.1	HIJKLMN
PinkWave 3s	**Tetric PowerFlow**	1.5	0.1	KLMNOP	1.9	0.2	GHIJKLMN
Monet 3s	**Filtek One**	1.5	0.0	KLMNOP	1.5	0.1	IJKLMN
PowerCure 3s	**Tetric PowerFill**	1.4	0.1	LMNOP	1.4	0.1	IJKLMN
PinkWave 3s	**Tetric PowerFill**	1.4	0.0	LMNOP	1.3	0.1	JKLMN
PowerCure 3s	**Filtek One**	1.4	0.1	MNOP	1.2	0.1	KLMN
PinkWave 3s	**Filtek One**	1.2	0.2	MNOP	1.3	0.1	KLMN
Monet 1s	**Filtek Bulk Fill Flow**	1.2	0.0	MNOP	1.2	0.1	LMN
Monet 1s	**Tetric PowerFill**	1.1	0.1	NOP	1.1	0.1	MN
Monet 1s	**Tetric PowerFlow**	1.0	0.0	OP	1.1	0.1	MN
Monet 1s	**Filtek One**	0.9	0.2	P	0.9	0.2	N

Means followed by similar letters (uppercase: inside the column) are not significantly different (Scheffe post-hoc test, $p \geq 0.05$).

Tabela 16 – Temperature rise (ΔT) recorded for the Class V cavity ranked from highest to lowest temperature rise

Condição de Exposição	RBC	Aumento de temperatura (ΔT - ºC)					
		Sonda na posição Classe I			Sonda na posição Classe V		
		Mean	SD		Mean	SD	
PowerCure 20s	**Filtek Bulk Fill Flow**	0.9	0.1	ABCD	4.0	0.3	A
PowerCure 20s	**Tetric PowerFlow**	1.0	0.0	ABCD	4.0	0.4	A
PinkWave 20s	**Filtek Bulk Fill Flow**	1.0	0.1	ABC	3.6	0.2	AB
Valo X 20s	**Filtek Bulk Fill Flow**	1.1	0.1	A	3.5	0.1	ABC
SmartLite Pro 20s	**Filtek Bulk Fill Flow**	0.9	0.1	ABCDE	3.3	0.1	ABCD
PinkWave 20s	**Tetric PowerFlow**	0.9	0.1	ABCD	3.3	0.3	ABCDE
PowerCure 20s	**Tetric PowerFill**	0.9	0.0	ABCDE	3.3	0.2	ABCDEF
SmartLite Pro 20s	**Tetric PowerFlow**	0.9	0.1	ABCDE	3.1	0.2	BCDEFG
PowerCure 20s	**Filtek One**	0.9	0.1	ABCDE	3.0	0.1	BCDEFG
Valo X 20s	**Tetric PowerFlow**	1.0	0.0	AB	2.9	0.2	BCDEFGH
Valo X 20s	**Tetric PowerFill**	1.1	0.1	A	2.5	0.3	CDEFGHI
Valo X 20s	**Filtek One**	1.1	0.1	AB	2.5	0.3	DEFGHI
SmartLite Pro 20s	**Tetric PowerFill**	0.9	0.1	ABCDE	2.4	0.1	EFGHI
PinkWave 20s	**Tetric PowerFill**	0.7	0.1	BCDEFGH	2.4	0.1	EFGHI
PinkWave 20s	**Filtek One**	0.8	0.1	BCDEF	2.4	0.2	FGHI
SmartLite Pro 20s	**Filtek One**	0.8	0.1	ABCDE	2.3	0.2	GHI
Valo X 5s	**Filtek Bulk Fill Flow**	0.8	0.0	BCDEFG	2.2	0.2	GHI
PowerCure 3s	**Tetric PowerFlow**	0.7	0.1	CDEFGHIJK	2.2	0.2	GHI
Valo X 5s	**Tetric PowerFlow**	0.7	0.1	BCDEFG	2.1	0.2	GHI
PowerCure 3s	**Filtek Bulk Fill Flow**	0.7	0.1	CDEFGHI	2.1	0.2	HIJ
PowerCure 3s	**Tetric PowerFill**	0.6	0.1	EFGHIJKLM	2.0	0.1	HIJ
Valo X 5s	**Tetric PowerFill**	0.6	0.1	DEFGIJKL	1.9	0.2	IJK

PowerCure 3s	**Filtek One**	0.7	0.0	CDEFGHI	1.9	0.2	IJK
Valo X 5s	**Filtek One**	0.7	0.1	CDEFGHIJ	1.7	0.1	IJKL
PinkWave 3s	**Filtek Bulk Fill Flow**	0.4	0.1	HIJKLM	1.2	0.3	JKLM
PinkWave 3s	**Tetric PowerFlow**	0.3	0.0	IJKLM	1.1	0.1	JKLM
PinkWave 3s	**Tetric PowerFill**	0.3	0.1	IJKLM	1.1	0.2	KLM
Monet 3s	**Tetric PowerFlow**	0.4	0.1	HIJKLM	1.1	0.2	KLM
Monet 3s	**Filtek Bulk Fill Flow**	0.4	0.1	GHIJKLM	1.0	0.3	KLM
PinkWave 3s	**Filtek One**	0.3	0.1	KLM	1.0	0.0	KLM
Monet 1s	**Tetric PowerFlow**	0.3	0.1	LM	0.9	0.1	LM
Monet 3s	**Tetric PowerFill**	0.4	0.1	FGHIJKLM	0.9	0.1	LM
Monet 1s	**Filtek Bulk Fill Flow**	0.3	0.1	M	0.9	0.1	LM
Monet 1s	**Tetric PowerFill**	0.2	0.1	M	0.7	0.2	M
Monet 3s	**Filtek One**	0.3	0.1	JKLM	0.6	0.0	M
Monet 1s	**Filtek One**	0.2	0.1	M	0.5	0.0	M

Means followed by similar letters (uppercase: inside the column) are not significantly different (Scheffe post-hoc test, $p \geq 0.05$).

4.3.5 Discussion

This study evaluated the PT changes when low and high viscosity bulk-fill RBCs, both having a form of RAFT technology (3M, 23 December 2022; ILIE; WATTS, 2020) were photo-cured in Class I and Class V cavities using laser, Quadwave and contemporary LED LCUs. Most exposure conditions that used longer exposures (up to 20 s) at a lower radiant exitance value caused higher ΔT values inside the pulp chamber than shorter exposures at higher radiant exitance values because less energy was delivered. More specifically, when the Valo X LCU and PinkWave were used for 20s (the longer exposure times) in the Class I cavity produced the highest ΔT values, while the groups that were exposed for 1 or 3 s had the lowest values (Table 15). Therefore, the first hypothesis that there is no difference in the *in vitro* PT rise caused by 1, 3 or 20 s photo-curing times using laser, Quadwave, or contemporary high-power LED LCUs was rejected. LCUs that emit a wider spectrum of light may produce a greater rise in temperature when compared to narrow-spectrum LED-LCUs (MOUHAT et al., 2017). This occurs because photons in the violet range are at shorter wavelengths, and they deliver more energy (HARLOW et al., 2016). The impact of the photo-curing on the PT rise is greater at longer exposures (ARMELLIN et al., 2016) because the increase in temperature is closely related to the radiant exposure values delivered to the tooth (RUNNACLES et al., 2015). Therefore, the Valo X (delivering 1277 mW and 1,041 mW/cm^2) used for 20s delivered approximately 25.5 J and 20.8 J/cm^2. While the higher output mode from this LCU delivered 2,102 mW/cm^2, when used for 5 s, it only delivered approximately 12.9 J and 10.5 J/cm^2 (Table 3). This difference in the energy delivered to the tooth explains the higher ΔT values in the groups with the longer exposures than those observed during the shorter exposure times, despite delivering 1933 mW. Although the Monet is a high-powered Class 4 laser, it emits a very narrow wavelength range (Figure 19 and Table 14), and when used for 1s, it delivered the least amount of energy (1.9 J). Consequently, it produced the lowest ΔT values. Such findings reinforce the previous reports that the PT rise is more closely related to the radiant exposure values (J/cm^2) received rather than the irradiance values from the LCU (RUNNACLES et al., 2015; ZARPELLON et al., 2021).

Of note, the rank of LCUs/RBCs based on the descending order of ΔT values in the Class I cavity (Table 15) differed from that observed from the Class V cavity (Table 16). The highest ΔT values in Class I restorations were observed during the 20 s

exposure to the Valo X and Pinkwave (Table 4), while PowerCure combined with FB-Flow and TP-Flow caused the highest ΔT values in the Class V restoration. As described in the Methods section, to simulate a clinical Class V restoration scenario where a rubber dam is used, the molar tooth was fixed in an acrylic plate so that only the crown above the cemento-enamel junction was exposed. This arrangement did not allow some LCUs with larger tip diameters, such as the Valo X (tip diameter of 12.5 mm) and PinkWave (tip diameter of 11.9 mm), to be centered directly over the Class V cavity. Thus, the PowerCure, which has a smaller diameter than the other LCUs used in this study (Table 14), could be positioned directly over the Class V cavity, and the tip could cover the entire restoration. This position of the LCU tip allowed more direct illumination and a better transfer of light and energy to the restoration (RUEGGEBERG, F. A. et al., 2017). This allowed a greater heat transfer through the RBC and remaining dentin floor to the pulp and resulted in the highest ΔT values. In contrast, much of the light from the Valo X and PinkWave was directed over the cusp tip.

Previous studies have reported that low viscosity composites cause a higher PT increase than high viscosity RBCs because they contain lower filler contents and more resin. This increase in the resin content produces more exothermic heat (MASUTANI et al., 1988; AL-QUDAH et al., 2005; BAROUDI; SILIKAS; WATTS, 2009; LEMPEL et al., 2021). Although the FB-Flow and TP-Flow caused the highest PT rise (ΔT) used in the Class V cavity (Table 16), overall, there was no significant difference, and the second hypothesis that the differences in viscosity between bulk-fill RBCs will not affect the in-vitro PT rise regardless of LCU and exposure strategy was accepted for these 4 RAFT associated RBCs. In the present study, the Class I and Class V cavities had approximately 1mm of dentin on the pulpal wall between the bottom of the cavity and the pulp chamber. Some studies have shown that dentin has an excellent insulation capacity because of its low thermal diffusivity (≈$1.87 \times 10^{-3} cm^2/s$) (CHIANG et al., 2008). Therefore, when there is thicker dentin remaining on the cavity floor, a lower PT increase will occur (MURRAY et al., 2003b; AGUIAR et al., 2006; YAZICI, A. R. et al., 2006; JAKUBINEK et al., 2008). Consequently, when the heat released by the exothermic reaction reached the surface, the remaining dentin on both pulpal and axial walls might have been capable of absorbing that heat and transferring it to the surrounding structure slowly. Thus, any differences in the heat released between the low viscosity and high viscosity RBCs were not detected by the thermocouple after the

heat had passed through the remaining dentin. Of note, some studies have noticed that the heat produced during photo-curing is more influenced by the choice of LCU rather than by the exothermic reaction of the RBC (BALESTRINO et al., 2016; NILSEN et al., 2020). These two factors could explain why, overall, there were no significant differences in the PT increase in the low viscosity and high viscosity RBCs.

The 20-s exposure using PinkWave caused the highest PT rise (ΔT) in the Class I restorations (Table 15) and when FB-Flow and TP-Flow were used in the Class V cavity (Table 16). The PinkWave is a multi-peak LED LCU that delivers infra-red (IR) and red wavelengths of light as well as blue and violet light. The Far Infrared Radiation (FIR) is a subdivision of the IR band that transfers energy as heat that thermoreceptors can feel as radiant heat (VATANSEVER; HAMBLIN, 2012). Thus, the thermal irradiation from PinkWave, in addition to the relatively high-power output from this LCU (1,874 mW), helps to explain why the PinkWave LCU caused one of the highest PT rise values among all groups.

In the present study, the two thermocouples placed inside the pulp chamber of a maxillary molar simultaneously recorded the temperature changes in the pulpal chamber of the Class I and the axial floor of the Class V cavities. The results reported some differences in PT increase when the values recorded by both thermocouples were compared for each cavity and within each exposure condition and RBC. As the light emitted from the LCU hits the surface, part of the light is reflected, part is transmitted, part is scattered, and part is converted into heat (DEDERICH, 1993). This heat is transferred to and absorbed by the surrounding structures (JAKUBINEK et al., 2008), and a temperature gradient is created in the surrounding structure and pulp tissue (JAKUBINEK et al., 2008). Consequently, when the RBC was placed and photo-cured within the Class V cavity, the temperature values recorded by the thermocouple placed near the axial floor were higher than those recorded by the thermocouple that was located further away from RBC and the axial floor.

The Logarithmic regression (Figure 20) examining the effect of the Energy (J) on the temperature rise, shows that there was a significant positive correlation between the Energy (J) delivered and the PT (R^2= 0.713 for FB-One, R^2 = 0.783 for FB-Flow, R^2 = 0.661 for TP-Fill and R^2 = 0.722 for TP-Flow). Despite the fact that different LCUs were used, the lower the amount of energy delivered, the lower the temperature rise inside the tooth. This agrees with a previous study that showed that the temperature rise was mainly determined by the radiant exposure (PAR et al., 2019). The clinician

should also be aware that delivering a low radiant exposure will compromise the mechanical properties of the restorations (ILIE et al., 2021; GRAZIOLI et al., 2022), and can increase the material's toxicity (ILIE et al., 2021).

For this in vitro study, the fluid flow through the pulp was adjusted to a flow rate of 0.026 mL/min based on previous studies (SAVAS et al., 2014; AKARSU; AKTUG KARADEMIR, 2019; MAUCOSKI et al., 2022a). After comparing *in vitro* and *in vivo* models regarding pulp temperature rise, a previous study found that PT rise in the *in vitro* model was close to those exhibited by the *in vivo* model (RUNNACLES et al., 2019). The pulp fluid flow can significantly reduce the PT increase (KODONAS; GOGOS; TZIAFA, 2009; KODONAS; GOGOS; TZIAFAS, 2009), which is also influenced by the pulp flow rate (KODONAS; GOGOS; TZIAFA, 2009). Therefore, the impact of the evaluated LCUs, radiant exitance (irradiance), exposure time, and resin composites on the PT rise may be different if the pulp flow rate changes. However, when evaluating the effects of low flow rates of 0.0042 mL/min, 0.028 mL/min or 0.07 mL/min, which were close to the one used in the study, a previous in vitro study found little effect on pulp temperature (PARK; ROULET; HEINTZE, 2010). Thus, it is reasonable to expect such LCUs and RBCs would cause temperature rise values similar to those observed in the current study.

Although significant increases in the PT values were noticed, all exposure modes produced acceptable temperature rises within the pulp chamber of this *in vitro* tooth because the PT rise values were lower than the threshold of 5.5 °C (ZACH; COHEN, 1965). The extent of the rise in PT was related to the energy delivered and not to the radiant exitance (irradiance) values delivered by the LCUs. An *in vivo* study performed in humans reported that short-exposures delivering 10,000 mW/cm^2, caused an increased expression of some precursors of the inflammatory response, such as Interleukin-1β, in the pulp tissue, compared to the expression of this marker when lower radiant exitance values that were below 24.6 J/cm^2 were delivered for a longer time. However, when 73.8 J/cm^2 was delivered in 60 s at 1,231 mW/cm^2 the blood vessels were dilated and congested (GROSS et al., 2020). The authors attributed the outcomes to the higher rate of temperature rise observed when 10,000 mW/cm^2 was delivered for 1 or 2 seconds (GROSS et al., 2020). This radiant exitance and the radiant exposure values were 3 to 10 times greater than the maximum radiant exitance (2,818 mW/cm^2) and radiant exposure values (27.1 J/cm^2) used in the present study (Table 14) and highlight why it is important to report the radiant exitance and

energy delivered, rather than uses ill-defined terms such as ‘high irradiance, or a high power LCU’.

The Class I and V restorations were made in only one maxillary molar. Therefore, the current temperature increases should not be expected in teeth with smaller crown volumes, such as premolars and incisors or when using more RBC in a larger cavity. But the observation that the more energy that is delivered, the greater the temperature rise should still be valid (Figure 20). The Class I and V cavity preparations left approximately 1 mm of dentin at the floor of the cavity, if there is a thinner amount of dentin on the cavity floor, this may result in different increases in PT. Furthermore, the study was designed to only examine RAFT modified bulk-fill RBCs, that were photo-cured in one 2 or 4-mm thick increments. Therefore, the current finding should not be expected when a cavity preparation is restored with conventional RBCs using the incremental technique.

4.3.6 Conclusions

Within the limitations of this in vitro study, it was concluded that:

(1) Fast photo-polymerization in 1 to 3 s using radiant exitances that were below 3,000 mW/cm^2 did not produce unacceptable temperature rises within the pulp chamber because amount of energy delivered to the tooth in 1 to 3 s was less than 6J.

(2) The in-vitro PT rise is related to the amount of energy delivered to the tooth.

5 DISCUSSÃO

Os três experimentos do presente trabalho seguem uma sequência lógica para avaliação do aumento de temperatura pulpar in vitro por fotopolimerizadores LED contemporâneos e fotopolimerizador laser. O primeiro experimento avaliou a temperatura em tempo real na base de RCs quando fotopolimerizadas usando diferentes quantidades de luz bem definidas de diferentes fotopolimerizadores. O segundo e terceiro experimentos avaliaram o aumento de TP in vitro em molar superior com preparos cavitários Classe I e V quando expostos a diferentes condições de exposição e tempos de exposição. O segundo experimento utilizou de cavidades vazias no mesmo dente para simular a condição em que o agente adesivo é exposto à luz. A maneira que o dente foi montado representou como o dente estaria isolado. O terceiro estudo avaliou as mudanças de TP quando RCs *bulk-fill* de baixa e alta viscosidade, ambas com tecnologia RAFT, foram fotopolimerizadas em preparos de cavidades Classe I e V utilizando diferentes fotopolimerizadores.

O efeito combinado do fotopolimerizador com os fotopolimerizadores não produzem o mesmo aumento de temperatura. A Figura 1 e a Tabela 8 mostram que a reação de fotopolimerização é dependente da RBC utilizada (NILSEN et al., 2020). Portanto, o aumento de temperatura é um resultado cumulativo da reação exotérmica e da exposição à luz do fotopolimerizador. Em contraste, para as RBCs totalmente polimerizadas (T3 na Figura 1 e Tabela 8), o aumento da temperatura foi apenas o resultado do efeito da luz oriunda do fotopolimerizador (NILSEN et al., 2020). Com exceção dos grupos em que Transcend UB, Filtek Universal A2, Tetric Evoceram A2 foram fotoativadas utilizando o fotopolimerizador Monet por 1 s, e Tetric Evoceram A2 fotoativada por 10s utilizando Power Cure (Experimento 01), todas as outras combinações de RC/fotopolimerizador produziram aumentos de temperatura maiores que 5,5 °C na base da resina composta (Figura 14). O aumento foi maior que 5,5 °C porque o a temperatura basal era baixa. A Tabela 8 mostra que a escolha da RC afeta o aumento de temperatura e diferentes tipos de RBC produzem diferentes na contribuição da reação exotérmica. Embora alguns estudos mostrem que as partículas de carga das RBCs são quimicamente inertes e não afetam o aumento de temperatura (AKARSU; AKTUG KARADEMIR, 2019) e que há uma alta correlação da proporção de matriz e o aumento de temperatura (HORI et al., 2020), a resina experimental Transcend (Ultradent Products) exibiu o maior aumento de temperatura pulpar

independentemente do modo de exposição utilizado, mesmo com informações do fabricante relatando possuir a maior quantidade de carga dentre as RCs analisadas (77,5% por peso – Tabela 1). Isto pode ser explicado pela sua alta translucidez (Tabela 6), que permitiu que uma maior quantidade de luz atravessasse o compósito, causando um maior aumento de temperatura (LEMPEL et al., 2021) na base do mesmo (Tabela 8), e promovendo uma polimerização eficiente na base da RC, conforme observado nos valores de dureza no tope e base da resina (Tabela 10).

Transcend foi a resina mais transparente utilizada no Experimento 01 (Tabela 6), e não foi encontrada diferenças significantes de VH entre as superfícies de topo e base (Tabela 10). A relação topo/base da resina Transcend após as três repetições foi de 0,90 para quatro dos cinco fotopolimerizadores utilizados. Entretanto, quando o Monet foi utilizado, por um total de 9s, a razão foi de 0,84 e quando foi utilizado por três repetições de 1s, o valor da razão foi de 0,65. Isso ocorre porque a extensão da polimerização possui uma relação exponencial com a quantidade de luz recebida pela RC (PAR et al., 2018). Quando analisando apenas os fotopolimerizadores, independentemente da RBC utilizada, o Monet Laser obteve os menores valores de VH (Figura 15 e Tabela 10). Embora emitisse uma alta irradiância de 5441 mW/cm^2, a exposição radiante entregue às RCs foi de apenas 5,4 J/cm^2. O incremento de 2 mm de RBC deve receber uma exposição radiante de aproximadamente 16 J/cm^2 (ANUSAVICE et al., 2013), por isso os valores de VH foram baixos.

Quando se leva em conta a viscosidade da RC, alguns estudos prévios reportaram que RCs de baixa viscosidade podem causar um maior aumento da TP do que RCs de viscosidade regular por possuírem um menor conteúdo de carga e conterem um maior conteúdo de resina. Este aumento na quantidade de resina produz um maior aumento da exotermia (MASUTANI et al., 1988; AL-QUDAH et al., 2005; BAROUDI; SILIKAS; WATTS, 2009; LEMPEL et al., 2021). Embora no Experimento 03 as RCs FB-Flow e TP-Flow causaram o maior aumento de PT (ΔT) no preparo de Classe V (Tabela 16), não houve diferença significante. Portanto, as diferenças de viscosidade de RCs *bulk-fill* não afetaram o aumento da TP *in vitro*, independentemente do fotopolimerizador e do modo de exposição utilizado. No Experimento 03, os preparos cavitários de Classe I e Classe V tinham aproximadamente 1 mm de espessura de dentina remanescente na parede de fundo entre a base da cavidade e a câmara pulpar. A dentina possui uma excelente capacidade isolante devido sua baixa difusividade térmica ($\approx$ 1,87 x 10^{-3} cm^2/s)

(CHIANG et al., 2008), logo quando há uma espessura remanescente de dentina maior, um baixo aumento PT irá ocorrer (MURRAY et al., 2003a; AGUIAR et al., 2006; YAZICI, A. R. et al., 2006; JAKUBINEK et al., 2008). Consequentemente, quando o calor é liberado pela reação exotérmica, a dentina remanescente nas paredes pulpar e axial podem ter sido capazes de absorver o calor e transferi-lo para a estrutura ao redor. Assim, as diferenças no calor liberado pelas RCs de viscosidade baixa e regular não foram detectadas pela sonda termopar depois do calor ter passado pela dentina remanescente. Além disso, alguns estudos observaram que o calor produzido durante a fotopolimerização é mais influenciado pela luz do fotopolimerizador do que pela reação exotérmica da RC (BALESTRINO et al., 2016; NILSEN et al., 2020)

No presente estudo, foram utilizados diferentes tipos de fotopolimerizadores. Portanto, não era esperado que os fotopolimerizadores emitissem irradiâncias e exposições radiantes similares. Porém, a magnitude das diferenças não era esperada. No Experimento 01 pode se observar uma grande diferença na potência (de 408 a 1538 mW) e na exposição radiante emitida (de 5,4 a 31 J/cm^2) quando os cinco fotopolimerizadores foram utilizados (Figura 10 e Tabela 7). Os fotopolimerizadores não emitem a mesma quantidade de energia (Joules) durante a fotopolimerização e muitos cirurgiões dentistas não reconhecem o quão grande estas diferenças são, e por esse motivo muitos utilizam o mesmo tempo de exposição para fotopolimerizar diversos compósitos (ERNST et al., 2018; WATTS et al., 2019; FRAZIER et al., 2020). Também no Experimento 01 foi possível observar que o PinkWave utilizado por 10s levou a um aumento significante de temperatura na base das RCs (Figura 12). No Experimento 03, esse mesmo fotopolimerizador causou o maior aumento de TP nas restaurações de Classe I (Tabela 15) e quando os compósitos FB-Flow e TP-Flow foram utilizados na cavidade de Classe V (Tabela 16). Este aumento de temperatura significativo pode ser atribuído à grande quantidade de energia emitida e aos diferentes comprimentos de onda emitidos por este fotopolimerizador (Figura 12). Fotopolimerizadores que emitem diferentes espectros e potências produzem diferentes alterações na temperatura pulpar (MOUHAT et al., 2021), já que a emissão espectral e as características dos fótons destes fotopolimerizadores (LIN et al., 2010) que atingem a dentina são convertidos em calor (RUEGGEBERG, F., 1999) que é conduzido através da dentina remanescente para a polpa. Fotopolimerizadores que emitem um espectro mais amplo de luz podem produzir um maior aumento de temperatura quando comparado a fotopolimerizadores que emitem um espectro mais

estreito (MOUHAT et al., 2017). A análise espectral (Figuras 10, 16 e 19) mostra que o fotopolimerizador PinkWave emite quatro bandas de comprimento de onda, que além da luz azul e violeta, tem a capacidade de emitir comprimentos de onda na faixa vermelha e infravermelha. A radiação infravermelha distante (*Far Infrared Radiation*) é uma subdivisão da banda infravermelha capaz de transferir energia como calor que termoreceptores podem interpretar como calor radiante (VATANSEVER; HAMBLIN, 2012). Assim, a irradiação térmica do PinkWave, com a saída de alta potência deste fotopolimerizador (1874 mW), corrobora para explicar o grande aumento de PT dentre os grupos. Quando observado o espectro de transmissão (mW/nm) dos fotopolimerizadores PinkWave e Valo Grand através de moldes Delrin vazios e preenchidos (Figura 11), a maior parte da luz vermelha e infravermelha penetrou através do compósito, ao contrário da luz azul e violeta, ajudando a explicar o aumento de temperatura observado quando este fotopolimerizador foi utilizado.

A energia radiante (J) é o fator que mais influencia no aumento de temperatura e não a irradiância (PAR et al., 2019). Quanto maior a quantidade de energia liberada, maior será o aumento de temperatura. Quando observamos a regressão logarítmica para o aumento de temperatura das RCs (Figura 13 e Figura 20), apenas a Energia (Joules) obteve uma correlação positiva. Nenhuma correlação foi encontrada para Potência (Watts) e temperatura (°C). Portanto, mesmo emitindo a maior potência (1538 mW) e a maior irradiância (5441 mW/cm^2) para as resinas (Tabela 7), o Monet Laser produziu os menores aumentos de temperatura no Experimento 01. A exposição de 1s emitiu o menor valor de exposição radiante (5,4 J/cm^2). Importante salientar que quando o Monet foi utilizado nas RCs (Figura 14), a contribuição exotérmica foi também baixa, indicando uma polimerização menos efetiva das RBCs. Desta forma, fotopolimerizar RCs em exposições de 1 ou 3s não é aconselhado, visto que uma menor energia do fotopolimerizador é liberada e as contrações de polimerização podem desenvolver mais rapidamente (PAR et al., 2020). Isto pode levar a um comprometimento de propriedades mecânicas e longevidade das RCs. A toxicidade do material também pode ser aumentada com uma baixa exposição radiante devido à maior liberação de monômeros residuais no meio oral (ILIE et al., 2021). Portanto, cirurgiões dentistas devem apenas utilizar um protocolo de fotopolimerização rápida com RCs que foram especificamente designadas para serem fotopolimerizadas em 1 ou 3s (GAROUSHI; LASSILA; VALLITTU, 2021; ROCHA et al., 2022).

Se um tempo mais longo de exposição conforme recomendam os fabricantes de RCs for utilizado, o fotopolimerizador que emite uma maior irradiância depositará uma quantidade de energia maior. Consequentemente, poderá levar a uma maior transferência térmica e aumentar o risco de dano pulpar (KIM et al., 2017). Deste modo, se reduzirmos o tempo de exposição ou a irradiância, o risco de dano pulpar será menor, pois menor será a energia depositada. Entretanto, as Tabelas 6 e 10 mostram que isto pode afetar de maneira negativa as propriedades mecânicas da RC (MOUHAT et al., 2017). Portanto, é preferível a utilização de um tempo de exposição de 10s de um fotopolimerizador convencional que libere uma quantidade adequada de energia, produza uma restauração adequadamente polimerizada e que produza um aumento de temperatura tolerável para o tecido pulpar (PAR et al., 2019).

No Experimento 02, quando o Monet foi utilizado por 3 s, ou o PinkWave foi utilizado por 10s, isto levou ao maior aumento de temperatura na cavidade de Classe I, porém menor que 5,5 °C (Tabela 12 e Figura 17). No Experimento 03, quando o Valo X e o PinkWave foram utilizados por 20s (tempos de exposição maiores) na cavidade Classe I, maiores foram os valores de ΔT (Tabela 15). Isto mostra o impacto da fotopolimerização no aumento de TP, que foi maior quando exposições mais longas foram utilizadas (ARMELLIN et al., 2016). O fotopolimerizador LED Valo X usado por 20 s com irradiância de 1041 mW/cm^2 depositou aproximadamente 20,8 J/cm^2, enquanto o modo de exposição de 5s emitiu 2102 mW/cm^2 e depositou 10,5 J/cm^2 (Tabela 14). Embora o laser Monet seja um laser de alta potência Classe 4, quando utilizado por 1s, emitiu a menor quantidade de energia, causando consequentemente os menores valores de aumento de TP.

Por outro lado, quando a Classe V foi exposta à luz dos fotopolimerizadores tanto no Experimento 02 quanto no Experimento 03, a ordem decrescente de valores de ΔT foi diferente. No Experimento 02, o Monet causou os menores valores de ΔT. Já o fotopolimerizador PowerCure obteve os maiores valores de ΔT junto com o PinkWave utilizado por 10s (Figura 18). No Experimento 03, PowerCure combinado com FB-Flow e TP-Flow obteve os maiores valores de ΔT para a Classe V. Isto está relacionado ao modelo experimental. De maneira a simular um cenário clínico relevante em que há um fluxo de fluido no interior da polpa, a fixação do dente em uma placa acrílica necessária para o funcionamento do sistema simulou a presença de grampo e dique de borracha (Figura 4). Portanto esta disposição não permitiu

fotopolimerizadores com diâmetro de ponta maior (Monet, Valo Grand, PinkWave, Valo X) que fossem centralizados na no preparo Classe V. Ao invés disso, o centro destas pontas estava próximo ou ao mesmo nível da ponta de cúspide. Fotopolimerizadores de ponta menor (PowerCure, SmartLite Pro) puderam ser posicionados centralmente à cavidade Classe V, permitindo uma melhor iluminação direta e melhor transferência de luz e energia (RUEGGEBERG et al., 2017). Consequentemente, o design da ponta do fotopolimerizador teve um impacto nos resultados. Isso reforça a importância de cirurgiões dentistas estabelecerem condições clínicas corretas que permitem a luz do fotopolimerizador acessar diretamente a RC na cavidade após isolamento absoluto. Para isso, o uso de óculos protetor laranja é indispensável para estarem certos do que estão fazendo quando utilizando o fotopolimerizador.

Nos Experimentos 02 e 03, para melhor simular o ambiente oral onde o dente está envolto por tecidos moles que ajudam a dissipar o calor (MOLNÁR et al., 2015), um fluxo pulpar simulado foi estabelecido em 0,026 mL/min (SAVAS et al., 2014; AKARSU; AKTUG KARADEMIR, 2019) e foi mantido em banho aquecido. No Experimento 02, nenhuma diferença no aumento de TP foi encontrada entre grupos com e sem fluxo pulpar simulado ($p > 0,05$). O fluxo sanguíneo através do dente humano é afetado pela presença de inflamação pulpar (BERGGREEN; BLETSA; HEYERAAS, 2007), preparo cavitário (SUKAPATTEE et al., 2016) e uso de anestesia local (ODOR; PITT FORD; MCDONALD, 1994; ZHENG et al., 2018; VONGSAVAN et al., 2019). Os resultados do presente estudo não estão de acordo com estudos prévios onde a presença de fluxo pulpar atenuou o aumento de temperatura (KODONAS; GOGOS; TZIAFA, 2009; BRAGA et al., 2019). Entretanto, estes estudos utilizaram taxas de fluxo entre 1,0 e 1,4 mL/min. Isto é aproximadamente 50 vezes maior que o fluxo de 0,026 mL/min usado no presente estudo. Outro estudo avaliou os efeitos de fluxos de 0,0042, 0,028 e de 0,07 mL/min (PARK; ROULET; HEINTZE, 2010), que foram mais similares ao valor utilizado no presente estudo. Os autores observaram que estes fluxos possuíam pouco efeito no aumento máximo de TP. Embora a geometria da câmara pulpar não seja circular, os autores citaram a Equação Womerslay ($\alpha = R(W/V)1/2$), onde R é o raio do vaso, W é a frequência radial (rad/s), e V é a viscosidade cinemática (m^2/s) para explicar o efeito do fluxo na transferência de energia entre vasos e tecidos. Eles sugeriram que esta equação suporta a conclusão de que a taxa de fluxo pulpar através da câmara pulpar em um dente tem

apenas um pequeno efeito no aumento de temperatura máximo. Se estes resultados in vitro forem aplicados para condições in vivo, pode-se concluir que a taxa de fluxo nos vasos sanguíneos da polpa possui um efeito insignificante no rápido aumento de PT durante a fase crítica quando o fotopolimerizador é ativado, mas irá afetar quão rápido a temperatura retorna ao normal. No entanto, tais observações foram aplicadas para pequenas variações no fluxo pulpar. É possível que maiores variações tenham impacto no aumento da temperatura pulpar.

Para a maioria dos fotopolimerizadores, há uma relação inversa entre potência e distância, então quanto maior a distância, menor a potência, mas isso depende do design óptico da fonte de luz (OBERHOLZER et al., 2012). Como menos fótons irão atingir a estrutura do dente quando a distância dente e ponta do fotopolimerizador aumenta, menor calor será gerado na estrutura do dente (RUEGGEBERG, F., 1999). No Experimento 02, considerando que a distância entre a ponta do fotopolimerizador e a parede axial no preparo Classe V é menor do que a distância no preparo Classe I devido à anatomia do dente, mais fótons irão atingir o assoalho do preparo Classe V em comparação ao número de fótons atingindo a parede pulpar da Classe I. Isso ajudar explicar porque de uma maneira geral os valores de ΔT diminuíram apenas quando fotopolimerizadores LED foram usados e quando a ponta do fotopolimerizador foi posicionada à 6 mm da superfície do dente. Entretanto, como Monet é um laser, a distância não afetou os valores de ΔT deste fotopolimerizador.

Os cirurgiões dentistas devem estar cientes de que a escolha do fotopolimerizador e da resina podem afetar o aumento de temperatura na base das restaurações devido a energia liberada do fotopolimerizador e da contribuição exotérmica da resina. Isso se faz importante quando restaurações são realizadas em cavidades profundas, já que a transferência térmica é afetada pela espessura de dentina remanescente (ARMELLIN et al., 2016). O primeiro experimento avaliou a propriedade mecânica de dureza, porém o impacto de outros fotopolimerizadores e tempos de exposição em outras propriedades mecânicas de outros tipos de RCs devem ser estudados e analisados.

O motivo de utilizar apenas um molar, nos Experimentos 02 e 03, foi com o intuito de reduzir o número de variáveis do estudo e permitiu que apenas os efeitos dos fotopolimerizadores e dos tempos de exposição no aumento de temperatura fossem determinados. Nos experimentos onde a TP foi analisada in vitro sob

condições simuladas no molar, nenhum grupo experimental obteve valores de ΔT maiores que 5,5 °C (ZACH; COHEN, 1965). As análises in vitro foram realizadas em um molar superior. Portanto, os aumentos de temperatura encontrados não devem ser esperados em dentes de tamanho de coroa menor, como incisivos ou pré-molares, ou quando utilizados preparos cavitários de dimensões maiores. O terceiro experimento avaliou apenas RCs do tipo *bulk-fill* com modificação RAFT, que foram fotopolimerizadas em incrementos de 2 ou 4 mm, portanto os presentes achados não devem ser esperados quando uma cavidade é restaurada com RCs convencionais usando a técnica incremental.

6 CONCLUSÃO

Dentre os limites do presente estudo, pode-se concluir que: (1) as energias emitidas pelos diferentes fotopolimerizadores não são as mesmas e diferentes fotopolimerizadores produzem diferentes mudanças de temperatura quando a RC é fotoativada; (2) a translucidez das RCs afetam o aumento de temperatura e dureza (VH); (3) o fluxo pulpar simulado de 0.026 mL/min não tem efeito significante no aumento de TP; (4) o aumento da distância entre ponta de fotopolimerizador e superfície do dente reduziu o aumento de temperatura para a maioria dos fotopolimerizadores; (5) o aumento de temperatura é relacionado à quantidade de energia entregue ao dente e à habilidade do fotopolimerizador de ser posicionado diretamente sobre a restauração; e (6) a fotopolimerização com modos de exposição curtos de 1 e 3s não produzem aumentos de temperatura inaceitáveis dentro da câmara pulpar porque a quantidade de energia liberada é pequena.

REFERÊNCIAS

AGUIAR, F. H.*, et al.* Effect of composite resin polymerization modes on temperature rise in human dentin of different thicknesses: an in vitro study. **Biomed Mater**, v. 1, n. 3, p. 140-143, 2006.

AKARSU, S.; AKTUG KARADEMIR, S. Influence of Bulk-Fill Composites, Polimerization Modes, and Remaining Dentin Thickness on Intrapulpal Temperature Rise. **Biomed Res Int**, v. 2019, n., p. 4250284, 2019.

AL-QUDAH, A. A.*, et al.* Thermographic investigation of contemporary resin-containing dental materials. **J Dent**, v. 33, n. 7, p. 593-602, 2005.

ALGAMAIAH, H.; SILIKAS, N.; WATTS, D. C. Polymerization shrinkage and shrinkage stress development in ultra-rapid photo-polymerized bulk fill resin composites. **Dent Mater**, v. 37, n. 4, p. 559-567, 2021.

ALMEIDA, R.*, et al.* High-Power LED Units Currently Available for Dental Resin-Based Materials-A Review. **Polymers (Basel)**, v. 13, n. 13, p., 2021.

ANUSAVICE, K. J.*, et al.* **Phillips' science of dental materials**. St. Louis, Mo.: Elsevier/Saunders, 2013;Page 290, v.Page 290. xiii, 571 p. p.
APEX, V. **Pinkwave**: secondary title.

ARBILDO-VEGA, H. I.*, et al.* Clinical Effectiveness of Bulk-Fill and Conventional Resin Composite Restorations: Systematic Review and Meta-Analysis. **Polymers (Basel)**, v. 12, n. 8, p., 2020.

ARMELLIN, E.*, et al.* LED Curing Lights and Temperature Changes in Different Tooth Sites. **Biomed Res Int**, v. 2016, n., p. 1894672, 2016.

BALESTRINO, A.*, et al.* Heat generated during light-curing of restorative composites: Effect of curing light, exotherm, and experiment substrate. **Am J Dent**, v. 29, n. 4, p. 234-2240, 2016.

BAROUDI, K.; SILIKAS, N.; WATTS, D. C. In vitro pulp chamber temperature rise from irradiation and exotherm of flowable composites. **Int J Paediatr Dent**, v. 19, n. 1, p. 48-54, 2009.

BERGGREEN, E.; BLETSA, A.; HEYERAAS, K. J. Circulation in normal and inflamed dental pulp. **Endodontic Topics**, v. 17, n. 1, p. 2-11, 2007.

BLUEPHASE PowerCure. **Ivoclar Vivadent**, 2023. Disponível em: <https://www.ivoclar.com/en_li/products/equipment/bluephase-powercure>. Acesso em: 18 de abril de 2023.

BRAGA, S.*, et al.* Effect of Simulated Pulpal Microcirculation on Temperature When Light Curing Bulk Fill Composites. **Oper Dent**, v. 44, n. 3, p. 289-301, 2019.

CHESTERMAN, J.*, et al.* Bulk-fill resin-based composite restorative materials: a review. **Br Dent J**, v. 222, n. 5, p. 337-344, 2017.

CHIANG, Y. C.*, et al.* Microstructural changes of enamel, dentin-enamel junction, and dentin induced by irradiating outer enamel surfaces with CO2 laser. **Lasers Med Sci**, v. 23, n. 1, p. 41-48, 2008.

CMS. **FlashMax2 Product description**: secondary title. Copenhagen, Denmark: CMS Dental, 2016.

DEDERICH, D. N. Laser/tissue interaction: what happens to laser light when it strikes tissue? **J Am Dent Assoc**, v. 124, n. 2, p. 57-61, 1993.

DROST, T.*, et al.* Effectiveness of photopolymerization in composite resins using a novel 445-nm diode laser in comparison to LED and halogen bulb technology. **Lasers Med Sci**, v. 34, n. 4, p. 729-736, 2019.

ELIPAR DeepCure Technical Product Profile. **3M**. Disponível em: <https://multimedia.3m.com/mws/media/1138935O/3m-elipar-deepcure-s-led-curinglight- technical-product-profile.pdf>. Acesso em: 18 de abril de 2023.

ERNST, C. P.*, et al.* Visible Light Curing Devices - Irradiance and Use in 302 German Dental Offices. **J Adhes Dent**, v. 20, n. 1, p. 41-55, 2018.

FILTEK One Bulk Fill. **3M**. Disponível em: <https://multimedia.3m.com/mws/media/1509317O/filtek-one-bulk-fill-technicalprofile.pdf>. Acesso em: 18 de abril de 2023.

FRAZIER, K.*, et al.* Dental light-curing units: An American Dental Association Clinical Evaluators Panel survey. **J Am Dent Assoc**, v. 151, n. 7, p. 544-545 e542, 2020.

GAROUSHI, S.; LASSILA, L.; VALLITTU, P. K. Impact of Fast High-Intensity versus Conventional Light-Curing Protocol on Selected Properties of Dental Composites. **Materials (Basel)**, v. 14, n. 6, p., 2021.

GRAZIOLI, G.*, et al.* Evaluation of irradiance and radiant exposure on the polymerization and mechanical properties of a resin composite. **Braz Oral Res**, v. 36, n., p. e082, 2022.

GROSS, D. J.*, et al.* In vivo temperature rise and acute inflammatory response in anesthetized human pulp tissue of premolars having Class V preparations after exposure to Polywave(R) LED light curing units. **Dent Mater**, v. 36, n. 9, p. 1201-1213, 2020.

HARLOW, J. E.*, et al.* Transmission of violet and blue light through conventional (layered) and bulk cured resin-based composites. **J Dent**, v. 53, n., p. 44-50, 2016.

HORI, M.*, et al.* Development of image analysis using Python: Relationship between matrix ratio of composite resin and curing temperature. **Dent Mater J**, v. 39, n. 4, p. 648-656, 2020.

ILIE, N.; WATTS, D. C. Outcomes of ultra-fast (3 s) photo-cure in a RAFT-modified resin-composite. **Dent Mater**, v. 36, n. 4, p. 570-579, 2020.

ILIE, N.*, et al.* Correlation of the mechanical and biological response in light-cured RBCs to receiving a range of radiant exposures: Effect of violet light. **J Dent**, v. 105, n., p. 103568, 2021.

ILIE, N.; DIEGELMANN, J. Impact of ultra-fast (3 s) light-cure on cell toxicity and viscoelastic behavior in a dental resin-based composite with RAFT-mediated polymerization. **J Mech Behav Biomed Mater**, v. 124, n., p. 104810, 2021.

JAKUBINEK, M. B.*, et al.* Temperature excursions at the pulp-dentin junction during the curing of light-activated dental restorations. **Dent Mater**, v. 24, n. 11, p. 1468-1476, 2008.

JANDT, K. D.; MILLS, R. W. A brief history of LED photopolymerization. **Dent Mater**, v. 29, n. 6, p. 605-617, 2013.

KAISER, C.; PRICE, R. B. Effect of time on the post-irradiation curing of six resin-based composites. **Dent Mater**, v. 36, n. 8, p. 1019-1027, 2020.

KIM, M. J.*, et al.* Thermographic analysis of the effect of composite type, layering method, and curing light on the temperature rise of photo-cured composites in tooth cavities. **Dent Mater**, v. 33, n. 10, p. e373-e383, 2017.

KNEZEVIC, A.*, et al.* Composite photopolymerization with diode laser. **Oper Dent**, v. 32, n. 3, p. 279-284, 2007.

KODONAS, K.; GOGOS, C.; TZIAFAS, D. Effect of simulated pulpal microcirculation on intrapulpal temperature changes following application of heat on tooth surfaces. **Int Endod J**, v. 42, n. 3, p. 247-252, 2009.

KODONAS, K.; GOGOS, C.; TZIAFA, C. Effect of simulated pulpal microcirculation on intrachamber temperature changes following application of various curing units on tooth surface. **J Dent**, v. 37, n. 6, p. 485-490, 2009.

KOUROS, P.*, et al.* Evaluation of photopolymerization efficacy and temperature rise of a composite resin using a blue diode laser (445 nm). **Eur J Oral Sci**, v. 128, n. 6, p. 535-541, 2020.

LAKHANI, J.*, et al.* Pulpal Temperature Rise: Evaluation after Light Activation of Newer Pulp-Capping Materials and Resin Composite. **Contemp Clin Dent**, v. 9, n. 4, p. 644-648, 2018.

LEE, C.-H.; LEE, I.-B. Effects of wall compliance and light-curing protocol on wall deflection of simulated cavities in bulk-fill composite restoration. **Journal of Dental Sciences**, v., n., p., 2021.

LEMPEL, E.*, et al.* Degree of conversion and in vitro temperature rise of pulp chamber during polymerization of flowable and sculptable conventional, bulk-fill and short-fibre reinforced resin composites. **Dent Mater**, v. 37, n. 6, p. 983-997, 2021.

LIN, M.*, et al.* A review of heat transfer in human tooth--experimental characterization and mathematical modeling. **Dent Mater**, v. 26, n. 6, p. 501-513, 2010.

LIPSKI, M.*, et al.* In Vitro Infrared Thermographic Assessment of Temperature Change in the Pulp Chamber during Provisionalization: Effect of Remaining Dentin Thickness. **J Healthc Eng**, v. 2020, n., p. 8838329, 2020.

LYNCH, C. D.*, et al.* An ex-vivo model to determine dental pulp responses to heat and light-curing of dental restorative materials. **J Dent**, v. 79, n., p. 11-18, 2018.

MASUTANI, S.*, et al.* Temperature rise during polymerization of visible light-activated composite resins. **Dent Mater**, v. 4, n. 4, p. 174-178, 1988.

MAUCOSKI, C.*, et al.* Analysis of temperature increase in swine gingiva after exposure to a Polywave((R)) LED light curing unit. **Dent Mater**, v. 33, n. 11, p. 1266-1273, 2017.

MAUCOSKI, C.*, et al.* In vitro temperature changes in the pulp chamber caused by laser and Quadwave LED-light curing units. **Odontology**, v., n., p., 2022a.

MAUCOSKI, C.*, et al.* Power output from 12 brands of contemporary LED light-curing units measured using 2 brands of radiometers. **PLoS One**, v. 17, n. 7, p. e0267359, 2022b.

MILLY, H.; BANERJEE, A. Evaluating the Clinical Use of Light-emitting Diode vs Halogen Photocuring Units. **Oral Health Prev Dent**, v. 16, n. 1, p. 21-25, 2018.

MOLNÁR, E.*, et al.* Assessment of heat provocation tests on the human gingiva: the effect of periodontal disease and smoking. **Acta Physiol Hung**, v. 102, n. 2, p. 176-188, 2015.

MONET Curing Light. **AMD Lasers**, 2022. Disponível em: <https://www.amdlasers.com/products/monet-laser-curing-light>. Acesso em: 18 de abril de 2023.

MOUHAT, M.*, et al.* Light-curing units used in dentistry: factors associated with heat development-potential risk for patients. **Clin Oral Investig**, v. 21, n. 5, p. 1687-1696, 2017.

MOUHAT, M.*, et al.* Light-curing units used in dentistry: Effect of their characteristics on temperature development in teeth. **Dent Mater J**, v., n., p., 2021.

MURRAY, P. E.*, et al.* Remaining dentine thickness and human pulp responses. **Int Endod J**, v. 36, n., p. 33-43, 2003a.

MURRAY, P. E.*, et al.* Remaining dentine thickness and human pulp responses. **Int Endod J**, v. 36, n. 1, p. 33-43, 2003b.

NILSEN, B. W.*, et al.* Heat Development in the Pulp Chamber During Curing Process of Resin-Based Composite Using Multi-Wave LED Light Curing Unit. **Clin Cosmet Investig Dent**, v. 12, n., p. 271-280, 2020.

OBERHOLZER, T. G.*, et al.* Modern high powered led curing lights and their effect on pulp chamber temperature of bulk and incrementally cured composite resin. **Eur J Prosthodont Restor Dent**, v. 20, n. 2, p. 50-55, 2012.

ODOR, T. M.; PITT FORD, T. R.; MCDONALD, F. Adrenaline in local anaesthesia: the effect of concentration on dental pulpal circulation and anaesthesia. **Endod Dent Traumatol**, v. 10, n. 4, p. 167-173, 1994.

OLIVEIRA, D.; ROCHA, M. G. Dental Light-Curing-Assessing the Blue-Light Hazard. **Dent Clin North Am**, v. 66, n. 4, p. 537-550, 2022.

PAR, M.*, et al.* Real-time Light Transmittance Monitoring for Determining Polymerization Completeness of Conventional and Bulk Fill Dental Composites. **Oper Dent**, v. 43, n. 1, p. E19-E31, 2018.

PAR, M.*, et al.* The effects of extended curing time and radiant energy on microhardness and temperature rise of conventional and bulk-fill resin composites. **Clin Oral Investig**, v. 23, n. 10, p. 3777-3788, 2019.

PAR, M.*, et al.* Effect of rapid high-intensity light-curing on polymerization shrinkage properties of conventional and bulk-fill composites. **J Dent**, v. 101, n., p. 103448, 2020.

PARK, S. H.; ROULET, J. F.; HEINTZE, S. D. Parameters influencing increase in pulp chamber temperature with light-curing devices: curing lights and pulpal flow rates. **Oper Dent**, v. 35, n. 3, p. 353-361, 2010.

PINKWAVE. **Vista Apex**. Disponível em: <https://vistaapex.com/wpcontent/uploads/2021/03/91037-I-AP-ENG5.pdf>. Acesso em: 18 de abril de 2023.

PIRES, J. A.*, et al.* Effects of curing tip distance on light intensity and composite resin microhardness. **Quintessence Int**, v. 24, n. 7, p. 517-521, 1993.

PRICE, R. B.*, et al.* Effect of distance on the power density from two light guides. **J Esthet Dent**, v. 12, n. 6, p. 320-327, 2000.

PRICE, R. B.; FERRACANE, J. L.; SHORTALL, A. C. Light-Curing Units: A Review of What We Need to Know. **J Dent Res**, v. 94, n. 9, p. 1179-1186, 2015.

PRICE, R. B.*, et al.* The light-curing unit: An essential piece of dental equipment. **Int Dent J**, v. 70, n. 6, p. 407-417, 2020.

ROCHA, M. G.*, et al.* Depth of cure of 10 resin-based composites light-activated using a laser diode, multi-peak, and single-peak light-emitting diode curing lights. **J Dent**, v., n., p. 104141, 2022.

RUEGGEBERG, F. Contemporary issues in photocuring. **Compend Contin Educ Dent Suppl**, v., n. 25, p. S4-15; quiz S73, 1999.

RUEGGEBERG, F. A. State-of-the-art: dental photocuring--a review. **Dent Mater**, v. 27, n. 1, p. 39-52, 2011.

RUEGGEBERG, F. A.*, et al.* Light curing in dentistry and clinical implications: a literature review. **Braz Oral Res**, v. 31, n. suppl 1, p. e61, 2017.

RUNNACLES, P.*, et al.* In vivo temperature rise in anesthetized human pulp during exposure to a polywave LED light curing unit. **Dent Mater**, v. 31, n. 5, p. 505-513, 2015.

RUNNACLES, P.*, et al.* Comparison of in vivo and in vitro models to evaluate pulp temperature rise during exposure to a Polywave(R) LED light curing unit. **J Appl Oral Sci**, v. 27, n., p. e20180480, 2019.

SAVAS, S.*, et al.* Evaluation of temperature changes in the pulp chamber during polymerization of light-cured pulp-capping materials by using a VALO LED light curing unit at different curing distances. **Dent Mater J**, v. 33, n. 6, p. 764-769, 2014.

SPANOVIC, N.*, et al.* Real-time Temperature Monitoring During Light-Curing of Experimental Composites. **Acta Stomatol Croat**, v. 52, n. 2, p. 87-96, 2018.

SPRANLEY, T. J.*, et al.* Curing light burns. **Gen Dent**, v. 60, n. 4, p. e210-214, 2012.

SUKAPATTEE, M.*, et al.* Effect of full crown preparation on pulpal blood flow in man. **Arch Oral Biol**, v. 70, n., p. 111-116, 2016.

TARDEM, C.*, et al.* Clinical time and postoperative sensitivity after use of bulk-fill (syringe and capsule) vs. incremental filling composites: a randomized clinical trial. **Braz Oral Res**, v. 33, n. 0, p. e089, 2019.

TIRAPELLI, C. Is the clinical performance of incremental and bulk-fill resin composite different? **Evid Based Dent**, v. 23, n. 2, p. 84, 2022.

VALO Grand Cordless. **Ultradent**, 2023. Disponível em: <https://www.ultradent.com.br/products/categories/equipment/curing lights/valograndd>. Acesso em: 18 de abril de 2023.

VALO X LED Curing Light. **Ultradent**, 2023. Disponível em: <https://www.ultradent.com/products/categories/equipment/curing-lights/valox?sku=5973->. Acesso em: 18 de abril de 2023.

VAN ENDE, A.*, et al.* Bulk-Fill Composites: A Review of the Current Literature. **J Adhes Dent**, v. 19, n. 2, p. 95-109, 2017.

VATANSEVER, F.; HAMBLIN, M. R. Far infrared radiation (FIR): its biological effects and medical applications. **Photonics Lasers Med**, v. 4, n., p. 255-266, 2012.

VELOSO, S. R. M.*, et al.* Clinical performance of bulk-fill and conventional resin composite restorations in posterior teeth: a systematic review and meta-analysis. **Clin Oral Investig**, v. 23, n. 1, p. 221-233, 2019.

VINALL, C. V.*, et al.* Intrapulpal Temperature Rise During Light Activation of Restorative Composites in a Primary Molar. **Pediatr Dent**, v. 39, n. 3, p. 125-130, 2017.

VONGSAVAN, K.*, et al.* The effect of intraosseous local anesthesia of 4% articaine with 1:100,000 epinephrine on pulpal blood flow and pulpal anesthesia of mandibular molars and canines. **Clin Oral Investig**, v. 23, n. 2, p. 673-680, 2019.

WAHBI, M. A.*, et al.* Characterization of heat emission of light-curing units. **Saudi Dent J**, v. 24, n. 2, p. 91-98, 2012.

WANG, W. J.*, et al.* The effect of light curing intensity on bulk-fill composite resins: heat generation and chemomechanical properties. **Biomater Investig Dent**, v. 8, n. 1, p. 137-151, 2021.

WATTS, D. C.*, et al.* Reporting of light irradiation conditions in 300 laboratory studies of resin-composites. **Dent Mater**, v. 35, n. 3, p. 414-421, 2019.

YANG, J.; ALGAMAIAH, H.; WATTS, D. C. Spatio-temporal temperature fields generated coronally with bulk-fill resin composites: A thermography study. **Dent Mater**, v. 37, n. 8, p. 1237-1247, 2021.

YAZICI, A. R.*, et al.* Comparison of temperature changes in the pulp chamber induced by various light curing units, in vitro. **Oper Dent**, v. 31, n. 2, p. 261-265, 2006.

YAZICI, A. R.*, et al.* Comparison of temperature changes in the pulp chamber induced by various light curing units, in vitro. **Operative Dentistry**, v. 31, n., p. 261-265, 2006.

ZACH, L.; COHEN, G. Pulp Response to Externally Applied Heat. **Oral Surg Oral Med Oral Pathol**, v. 19, n. 4, p. 515-530, 1965.

ZARPELLON, D. C.*, et al.* Influence of Class V preparation on in vivo temperature rise in anesthetized human pulp during exposure to a Polywave((R)) LED light curing unit. **Dent Mater**, v. 34, n. 6, p. 901-909, 2018.

ZARPELLON, D. C.*, et al.* Controlling In Vivo, Human Pulp Temperature Rise Caused by LED Curing Light Exposure. **Oper Dent**, v. 44, n. 3, p. 235-241, 2019.

ZARPELLON, D. C.*, et al.* In Vivo Pulp Temperature Changes During Class V Cavity Preparation and Resin Composite Restoration in Premolars. **Oper Dent**, v., n., p., 2021.

ZHENG, Q. H.*, et al.* A Clinical Study on the Effect of Injection Sites on Efficacy of Anesthesia and Pulpal Blood Flow in Carious Teeth. **Oper Dent**, v. 43, n. 1, p. 22-30, 2018.

ANEXO A – APROVAÇÃO DO COMITÊ DE ÉTICA

DALHOUSIE UNIVERSITY
Research Services

Health Sciences Research Ethics Board
Letter of Approval

July 19, 2021

Richard Price
Dentistry\Dental Clinical Sciences

Dear Richard,

REB #: 2021-5703
Project Title: The in-vitro effects of high irradiance delivered by laser and polywave light-curing units on the simulated pulp temperature rise

Effective Date: July 19, 2021
Expiry Date: July 19, 2022

The Health Sciences Research Ethics Board has reviewed your application for research involving humans and found the proposed research to be in accordance with the Tri-Council Policy Statement on *Ethical Conduct for Research Involving Humans*. This approval will be in effect for 12 months as indicated above. This approval is subject to the conditions listed below which constitute your on-going responsibilities with respect to the ethical conduct of this research.

Effective March 16, 2020: Notwithstanding this approval, any research conducted during the COVID-19 public health emergency must comply with federal and provincial public health advice as well as directives from Dalhousie University (and/or other facilities or jurisdictions where the research will occur) regarding preventing the spread of COVID-19.

Sincerely,

Lori Weeks

Dr. Lori Weeks, Chair